The Sedimentology, Stratigraphy and Reservoir Characteristics of the Montney D1 and D2 Horizons, Greater Pouce Coupe Area, Alberta and British Columbia

by

Donald Prenoslo

A thesis submitted in partial fulfillment of the requirements for the degree of

Master of Science

Department of Earth and Atmospheric Sciences
University of Alberta

ABSTRACT

The Middle Montney D1 and D2 Horizons in the Greater Pouce Coupe Area are important exploration targets. These moderate porosity and low permeability siltstone units have been referred to as distal shelf deposits in the past, based primarily on their restricted grain size. The D1 and D2 Horizons host a considerable volume of liquids rich natural gas. Considering this, a refined and robust interpretation of the paleodepositional setting and stratigraphic architecture of these units is crucial to facilitate exploration success. To achieve this objective, detailed sedimentological and ichnological data was recorded from 31 cores within an area of approximately 3200 km^2. Geophysical logs from 1000 wells were analyzed to correlate important surfaces and to understand the distribution of the D1 and D2 Horizons throughout the study area. Additionally, XRF derived elemental compositions were used to confirm and refine sequence stratigraphic interpretations and were used as proxies to infer changes in D1 and D2 Horizons depositional processes. Eight distinct lithofacies are identified from the dataset. Lithofacies analyses indicate that the studied strata represent distal offshore to offshore-transition sedimentary environments. Linear sourced turbidity currents are thought to be the most important mechanism for sediment deposition. An arid coastline with numerous ephemeral river systems transported large volumes of sediment to the coast during storms. This may have created an over steepened shoreface / wave-dominated delta profile, which was prone to mass wasting events. Additionally, the study area was in a structurally complex setting, and as a result syn-depositional structural reactivations

would have been equally likely to trigger mass wasting events. The D1-D2 transition is characterized by the presence of silty shale beds. The presence of appreciable amounts of clay in the Montney is rare except for a few areas. These areas are interpreted to have been deposited under the influence of perennial deltaic systems. During the D1-D2 transition silty shale beds indicate that there was a perennial river system running through the Hines Creek Graben sourcing clay. This work has contributed to the understanding of the sedimentology and the stratigraphic architecture of the Montney Formation in the Greater Pouce Coupe Area that will help decrease exploration risk. Ideally, the integration of detailed sedimentologic observations with regional mapping and geochemistry shown within this work will aid in other studies of the Montney Formation as well as in other unconventional plays around the world.

“Through chances various, through all vicissitudes, we make our way…”

Aeneid

ACKNOWLEDGEMENTS

The opportunity to pursue my masters at the U of A has been one of great enjoyment and fulfilment. There are many people responsible for helping me to get here and making it such an enjoyable experience. First and foremost, I have to thank my family for their constant love, encouragement and support. Especially my parents, Terry and Angela, without them none of this would have been possible.

Thanks to both of my supervisors, Dr. Murray Gingras and Dr. JP Zonneveld. They set me up with a project that was both challenging and extremely worthwhile. Their doors were always open and were always there to lend a helping hand. I will be eternally thankful for the amount of knowledge they passed onto me in a short time. Thanks to Dr. Jeff Kavanaugh and Dr. S. George Pemberton for sitting on my committee.

My time at the U of A has without a doubt been some of the most enjoyable years of my life, largely because of the people I was surrounded with in the EAS department. Thanks to everyone in the Ichnology Research Group for making it such an enjoyable time; playing frisbee in quad and our summer lab trips to Hornby Island, Pine Point and Willapa Bay were the highlights of my masters. Big thanks to my office mates Eric Timmer, David Herbers, Aimee Gegolick and Derek Hayes for always making the office a fun place to be… if not a productive one. Thanks to Dr. Ryan King and Scott Botterill who were always there to give good advice even after they had moved on. Thanks to my Barrel teammates Martin Schwangler, Olga Kovalchuk, Tyson Epp and Olivia Henderson who somehow made pulling all nighters looking at seismic fun! Ta'ing the Jasper field school was definitely one of the highlights of my 3 years here, thanks to Martin, Morgan Snyder, Dr. Murray Gingras and Dr. Sarah Gleeson for making that such a fun experience and making me realize that structural geology isn't so bad. Thanks to Tiffany Playter and Hillary Corbett at the Alberta Geologic Survey for their help with chemostratigraphy, and to Brette Harris for the many hours she spent supervising me on the XRF machine. Thanks to all the summer assistants that helped wash my core, digitize logs and take photos, your help was much appreciated.

Thanks to all the members of the Montney Consortium: Birchcliff Energy, Canbriam Energy, Progress, TAQA North, SASOL, and Shell Canada whose funding made this project possible. Thanks to the other students in the Montney Consortium: Carolyn Furlong, Tiffany Playter, Aimee Gegolick, Shelby Sanders, and Patricia Gonzales, I was always able to count on you guys for help when needed. A big thanks to Laura Ferguson and Bruce Palmer at Birchcliff Energy for their help. The project gained a lot with your involvement and I was fortunate to learn from your exceptional mentorship.

TABLE OF CONTENTS

LIST OF FIGURES

CHAPTER 1

CHAPTER 2

CHAPTER 3

LIST OF TABLES

CHAPTER 2

CHAPTER 3

CHAPTER 1: INTRODUCTION

The Lower Triassic Montney Formation is a complex accumulation dominantly comprised of siltstone and sandstone with shale and bioclastic packstone/grainstone occurring in some areas and intervals (Davies, 1997; Zonneveld et al., 2010). It is estimated that the Montney Formation contains 447 TCF of natural gas, 14 500 mmbbl of natural gas liquids and 1125 mmbbl of oil (NEB, 2013; ERCB, 2012; CUR, 2010). As such it is clearly one of Canada's premier unconventional hydrocarbon plays.

Hydrocarbons were first discovered in 1951 along the Montney eastern subcrop edge in west-central Alberta, although inconsistent distribution of conventional reservoir facies and problems with seismic resolution hindered the development of these plays (Bird, 1994). Conventional hydrocarbon development in the Montney Formation focused on two primary play types: 1) turbidite deep-water sandstone plays; and 2) Shoreface clastic and bioclastic plays along the eastern edge of the basin (Bird, 1994; Moslow, 2000).

With advances in horizontal drilling and multi-stage hydraulic fracturing in the last decade the thick siltstone intervals within the Montney have become the focus of industry exploration. However even with the increased importance of these intervals, existing publications deal predominantly with conventional reservoir units within the Montney.

In order for an unconventional play to be successful economics dictate the plays must be aerially extensive and the reservoir geometries must be well understood (Wood, 2012). The detailed stratigraphy of the full Montney and the nature and distribution of porosity and permeability throughout the thick siltstone intervals remains poorly understood. This thesis focuses on these attributes in the greater Pouce Coupe area.

Geologic Setting

The Montney Formation was deposited in the Early Triassic in an arcuate shaped extensional basin along the northwestern margin of Pangaea (Davies, 1997). The thickest accumulations occur in the area of the Peace River Embayment (Barclay et al. 1990; Davies 1997). This area, which had been a topographic high pre-Devonian time (Peace River Arch), was actively subsiding during the early Triassic (Davies, 1997). Continued subsidence resulted in the formation of a system of grabens referred to as the Dawson Creek Graben Complex (Mei, 2009). This graben complex consisted of the primary Fort St. John Graben and the satellite Hines Creek and Cindy Grabens (Barclay, 1990). Episodic reactivation of these basement faults had major effects on sediment distribution throughout the Triassic in the Western Canadian Sedimentary Basin (Davies, 1997; Mei, 2009). Originally thought to have been a passive margin during Montney Deposition (Davies 1997; Moslow 2000), recent work has suggested that terrane collisions on the western margin of North America may have commenced in the Early to Middle Triassic (Beranek and Mortensen, 2006; 2007; Ferri and Zonneveld, 2008).

During the Early Triassic the western margin of North America was situated in a midlatitudinal position and paleogeographic reconstructions show it was rotated 30 degrees clockwise relative to its current position (Davies, 1997). Desert and semiarid conditions are thought to have existed on land with ephemeral rivers episodically bringing sediment into the basin (Sellwood and Valdez, 2006; Zonneveld et al 2010; Playter, 2013). Aeolian transport and deposition is commonly postulated as being the dominant mechanism of sand and silt delivery to the coast (Davies et al. 1997, Davies 1997); although it is certainly a contributor ephemeral

fluvial transport was the more important process in the Montney Formation, as it is in most modern desert depositional systems (Zonneveld et al., 2010).

The Early Triassic was a time of biologic recovery as it immediately follows the End-Permian extinction, the most severe biologic perturbation in history (Raup, 1979; Erwin 2006; Zonneveld et al., 2010). Regionally extensive shallow water anoxia/dysoxia in conjunction with increased oceanic acidity are thought to have played a major roll in the extinction (Woods et al., 2007; Zonneveld, 2010b; Playter, 2013). These conditions are assumed to have continued into the Early Triassic based on the lack of preserved carbonate fossils and the diminished levels of bioturbation observed in the Montney Formation (Zonneveld 2010b; Playter, 2013).

Objectives

This research was undertaken to enhance the understanding of the sedimentology, stratigraphy and reservoir characteristics of the Middle Montney D1 and D2 horizons (Figure 1) in the Greater Pouce Coupe Area (Figure 2). The D1 and D2 horizons are characterized by liquids rich natural gas. Four hundred and ninety-one wells have produced from the D1 Horizon and 4 wells have produced from the D2 horizon. Detailed sedimentological and ichnological analysis of 31 drill cores has allowed for the recognition of 8 distinct lithofacies in the study area. Additional analysis of 1000 petrophysical wireline logs enabled the detailed mapping of the different stratigraphic packages throughout the area.

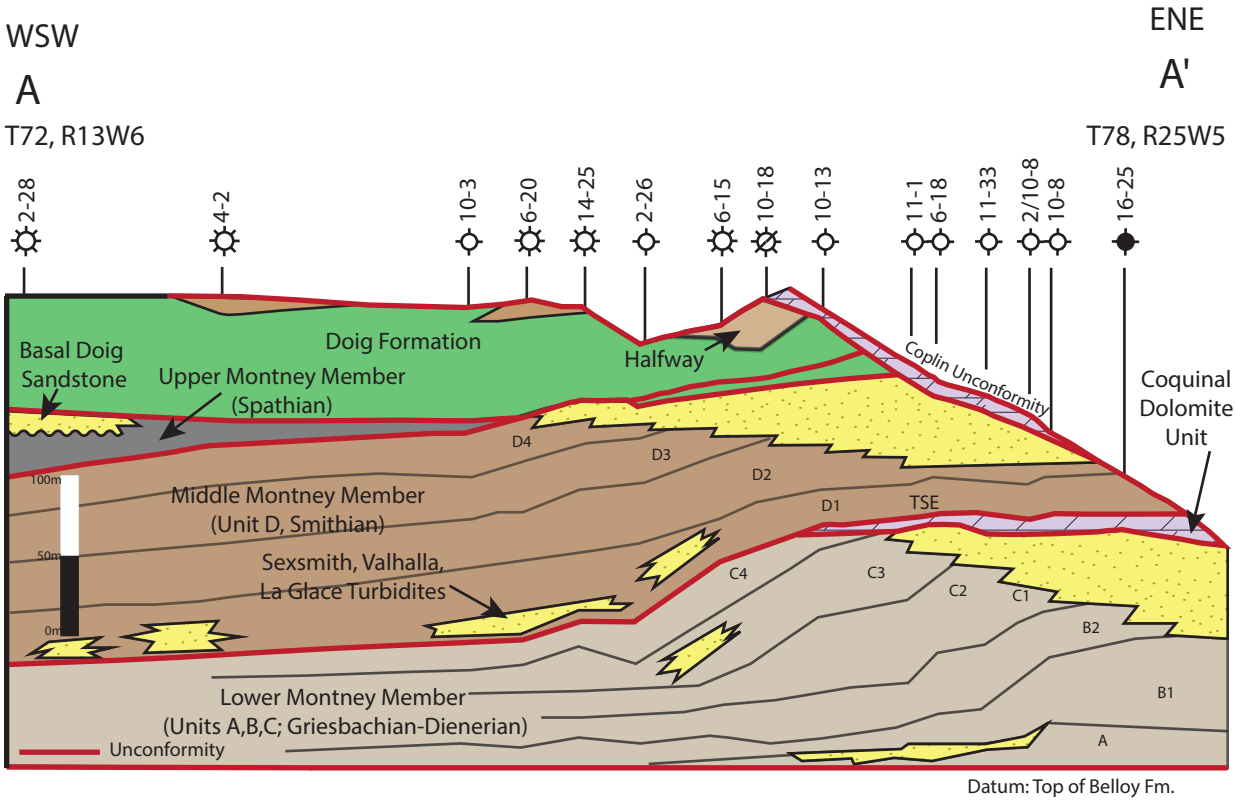

Figure 1.1– Early to Middle Triassic regional schematic stratigraphy oriented parallel to depositional dip. Datum is the top of the Belloy Formation. Modified from Moslow and Davies, 1997; Davies and Hume, 2016

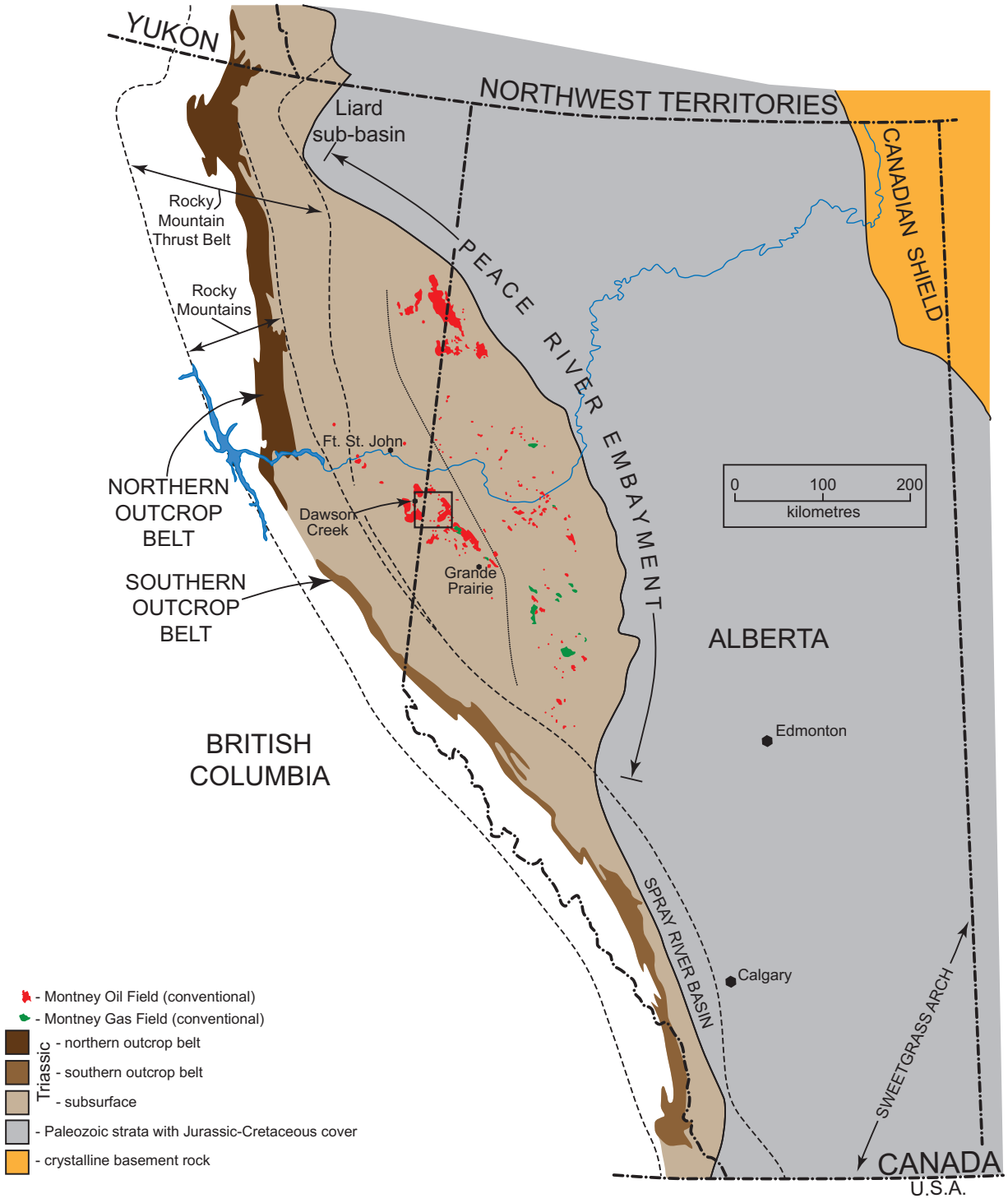

Figure 1.2–Distribution of Triassic Strata in the Western Canada Sedimentary Basin (after Zonneveld et al., 2011). Location of study area outlined in black.

Chapter 2 focuses on the sedimentology and stratigraphy of the area with lithofacies analyses indicating deposition took place in a distal offshore to offshore transition environment. Linear sourced turbidity currents are thought to have been the most important mechanism for sediment deposition. An arid coastline with numerous ephemeral river systems that transported large volumes of sediment to the coast during storms, created an over steepened shoreface / wave-dominated delta profile, which was prone to mass wasting events. The D1-D2 transition is characterized by the presence of silty shale beds. The presence of appreciable amounts of clay in the Montney is rare except for a few areas, these areas are interpreted to have been deposited under the influence of perennial deltaic systems. During the D1-D2 transition silty shale beds indicate that there was a perennial river system running through the Hines Creek Graben sourcing the clays.

Chapter 3 consists of a chemostratigraphic study of the area. Chemostratigraphy has become a widely-used tool in mudrock plays where perceived macro-scale homogeneity has prevented the use of more traditional methods of sedimentologic and stratigraphic analysis (Pearce et al., 2005; Ratcliffe et al., 2012; Sano et al., 2013). Energy-Dispersive X-Ray Fluorescence measurements of three cores in the area compliment detailed sedimentologic descriptions. Geochemical data enabled the definition of 7 distinct chemofacies and allowed for the refinement of the internal stratigraphy of the D1 and D2 horizons. In addition variations in selected elemental ratios and elemental concentrations were used as proxies for processes occurring during deposition.

In summary, this thesis aims to better understand the architecture, paleodepositional setting, and evolution of the Montney Formation within project limits. This work will contribute to the current knowledge of the Montney Formation by providing in-depth facies analysis, high-

resolution mapping and will ideally aid in the refinement of exploration activity, especially in the lithologically complex-less targeted D2 horizon. Additionally, it is hoped that the patterns recognized within this dataset will assist with facies analysis in other areas of the Montney Formation as well as in other mudstone deposits around the world.

CHAPTER 2: THE SEDIMENTOLOGY, STRATIGRAPHY AND RESERVOIR CHARACTERISTICS OF THE MONTNEY D1 AND D2 HORIZONS IN THE GREATER POUCE COUPE AREA

Introduction

The Montney Formation in the greater Pouce Coupe Area is characterized by liquids rich natural gas. Situated along the Alberta-British Columbia Border, 150 km north west of Grand Prairie (Fig. 2.1), this area has been an important region of Montney exploration for over 25 years. Overlying the southeastern extension of the Ft. St. John Graben Complex, this area is positioned in a complex tectonic setting. In 1993 hydrocarbons, hosted within turbidite channels and lobes, were discovered in this area. Turbidite deposition is associated with syn-sedimentary tectonism and occurred along fault-controlled ramp breaks (Moslow, 2000).

Technological innovations over the last 15 years, including horizontal drilling and hydraulic fracturing technology, have rendered the moderate porosity and low permeability Middle Montney D1 and D2 horizons economic. Deposited immediately following the Montney Turbidite Zone, these fine to coarse-grained siltstone and subordinate silty shale units have porosities ranging from 2-9%. To date, 491 wells have produced from the D1 horizon and 4 wells have produced from the less understood and more lithologically complex D2 horizon. Despite its important economic potential, there has been no published research focusing on the sedimentology and stratigraphy of the D1 and D2 horizons.

Therefore, the objectives of this study are threefold: 1) to provide a detailed facies framework and depositional system interpretation for the Montney D1 and D2 horizons in the greater Pouce Coupe area, 2) to establish robust and practical lithostratigraphic correlations for

the Montney Formation in the subsurface of the greater Pouce Coupe Area and 3) to investigate the reservoir quality of the different facies within the D1 and D2 horizons and speculate on prospective intervals. Relating the sedimentary facies to reservoir characteristics along with regional mapping allows for the delineation of areas with superior reservoir quality.

Geological Setting

The Montney Formation was deposited in the Early Triassic along the northwestern margin of Pangaea (Gibson and Barclay, 1988; Edwards et al., 1994; Davies, 1997). The thickest accumulations occur in the area of the Peace River Embayment (Barclay et al. 1990; Davies, 1997). This area, which had been a topographic high prior to the Devonian (Peace River Arch), subsided actively during the early Triassic (Davies, 1997). Continued tectonic inversion resulted in the formation of a system of grabens referred to as the Dawson Creek Graben Complex (Mei, 2009; Davies, 1997; Barclay et al., 1990). This graben complex consisted of the primary Fort St. John Graben and the satellite Hines Creek and Cindy grabens (Fig. 2.1; Barclay et al., 1990). Episodic reactivation of these basement faults had major effects on sediment distribution throughout the Triassic in the Western Canadian Sedimentary Basin (Davies, 1997; Mei, 2009).

Figure 2.1 (next page)- Regional facies associations of the Lower Triassic Montney Formation with major structural elements of the Dawson Creek Graben Complex shown; Study area outlined in red. Map compiled and modified from Barclay et al, 1990; Panek, 2000; Zonneveld et al, 2010a; Zonneveld et al, 2010b; Zonneveld and Moslow, 2014; and Zonneveld, pers. comm.

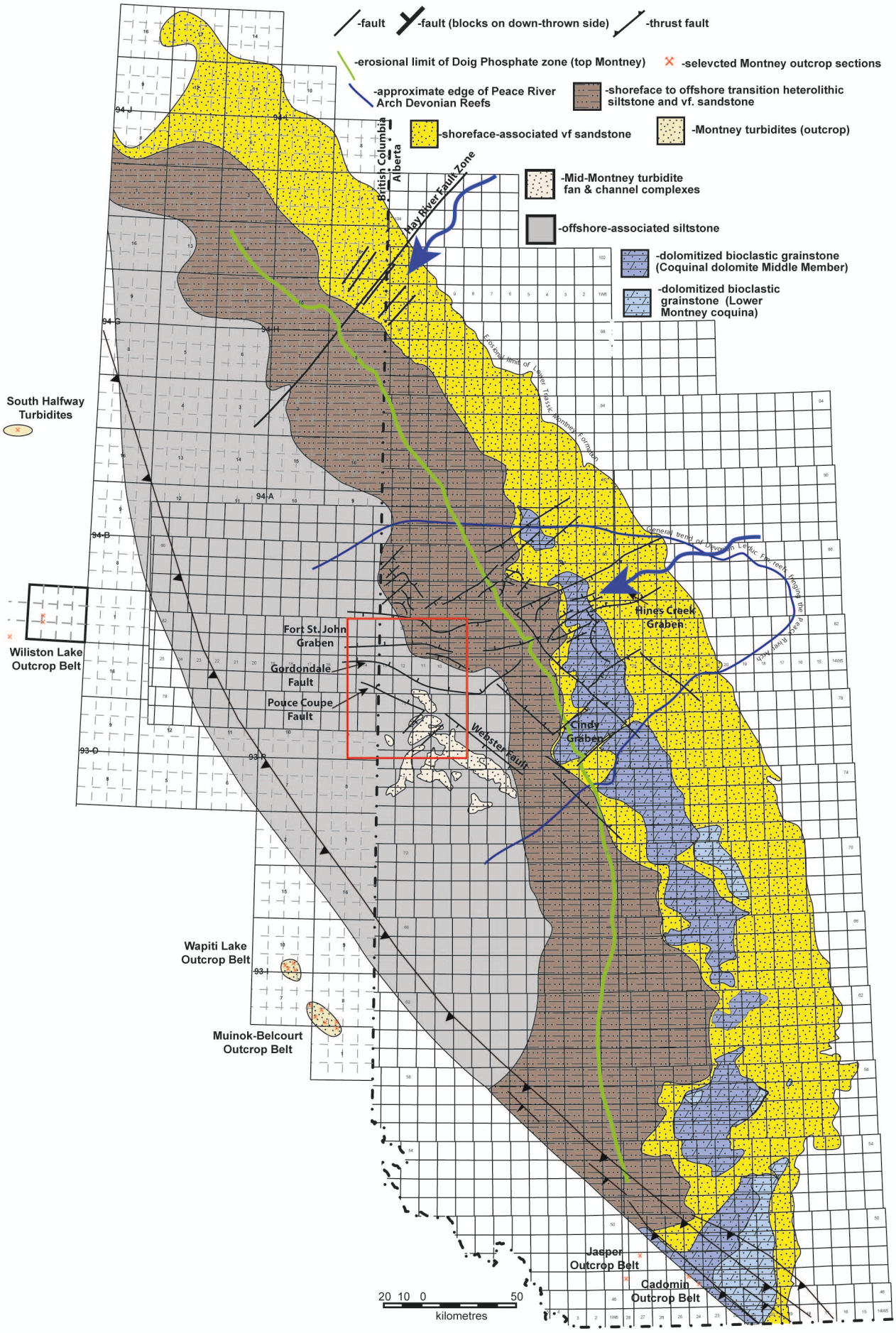
-fault
-fault (blocks on down-thrust side)
-thrust fault
-erosional limit of Doig Phosphate zone (top Montney)
-selevcted Montney outcrop sections
-approximate edge of Peace River Arch Devonian Reefs
-shoreface to offshore transition heterolithic siltstone and vf. sandstone
-shoreface-associated vf sandstone
-Montney turbidites (outcrop)
-Mid-Montney turbidite fan & channel complexes
-offshore-associated siltstone
-dolomitized bioclastic grainstone (Coquinal dolomite Middle Member)
-dolomitized bioclastic grainstone (Lower Montney coquina)
British Columbia
Alberta
Hay River Fault Zone
South Halfway Turbidites
Wiliston Lake Outcrop Belt
Fort St. John Graben
Gordondale Fault
Pouce Coupe Fault
Webster Fault
Hines Creek Graben
Cindy Graben
Wapiti Lake Outcrop Belt
Muinok-Belcourt Outcrop Belt
Jasper Outcrop Belt
Cadomin Outcrop Belt
94-J
94-I
94-G
94-H
94-A
94-B
93-O
93-P
93-I
20 10 0 50
kilometres

Deposition of the Montney Formation took place in a continental-ramp basinal setting (Davies, 1997; Moslow, 2000). It was originally thought that the northwestern margin of Pangea was tectonically stable and inactive during this time (Davies, 1997; Moslow, 2000). However, recent work has suggested that terrane collisions on the western margin of North America may have occurred as early as the Early to Middle Triassic (Beranek and Mortensen, 2006; 2007; Ferri and Zonneveld, 2008). This tectonic activity may have contributed to sedimentation in the study area by reactivating faults in the Dawson Creek Graben Complex (Davies, 1997; Zonneveld, 2010; Playter, 2013).

Desert and semiarid conditions are thought to have existed on land and aeolian transport and deposition is commonly postulated as being the dominant mechanism of sand and silt delivery to the coast (Davies et al. 1997, Davies 1997; Sellwood and Valdez, 2006). Although it is certainly a contributor, ephemeral fluvial transport was the more important process (Zonneveld et al., 2010). The Montney coastline would have been characterized by few perennial rivers with abundant seasonal river systems that would only deliver sand and silt to the coast during major storms (Zonneveld et al., 2010). Arid conditions on land are reflected by the paucity of clay minerals that occur in the Montney Formation in most areas. Significant clay formation, resulting from mica and feldspar hydrolysis, was inhibited by the lack of time sediments spent subaqueously submerged in fluvial feeder channels (Velbel, 1990; Zonneveld and Moslow, 2014). However, large amounts of clays have been reported in two locations: the Pedigree-Ring area along the Alberta-British-Columbia border and the Dixonville area in west-central Alberta (Zonneveld 2010). Cores in these areas are characterized by abundant soft sediment deformation and elevated levels of bioturbation (Zonneveld 2010). These areas were interpreted to have

accumulated under the influence of rare Montney perennial deltas (Zonneveld and Moslow, 2014; 2017; Zonneveld et al., 2010).

Montney Stratigraphic Framework

A wide range of stratigraphic nomenclatures exist for the Montney Formation in the subsurface. Company specific nomenclatures and contrasting names for identical stratigraphic surfaces in Alberta and British Columbia have added to the confusion. The two informal naming schemes that have been proposed by Davies (1997) and Dixon (2000) were constructed when the main focus of Montney exploration was on the conventional strata along the eastern subcrop edge. As such they do not incorporate the necessary detail for the western, more basinward part of the Montney Formation. Stratigraphic nomenclature used in this paper has been modified and is based off the stratigraphic scheme proposed by Davies (1997) and incorporates updated nomenclature devised by Davies and Hume (2016) (Fig. 2.2).

The Montney Formation in the study area lies unconformably on the Permian Belloy Formation and is erosively overlain by the Doig Phosphate Zone. Deposition of the Montney Formation took place during a major global transgression and consists of three third-order depositional sequences. A well-developed sequence boundary separates the Lower and Middle Montney members. In the east it is marked by the development of a subaerial unconformity and occurs adjacent to the Coquinal Dolomite Member. In the west the sharp base of the turbidite zone marks the sequence boundary (Davies et al., 1997). The Middle Montney Member was deposited during the Smithian stage (Markhasin, 1994; Davies et al., 1997; Kendall, 1999; Panek, 2000). The D1 and D2 horizons that are the focus of this study are part of this member.

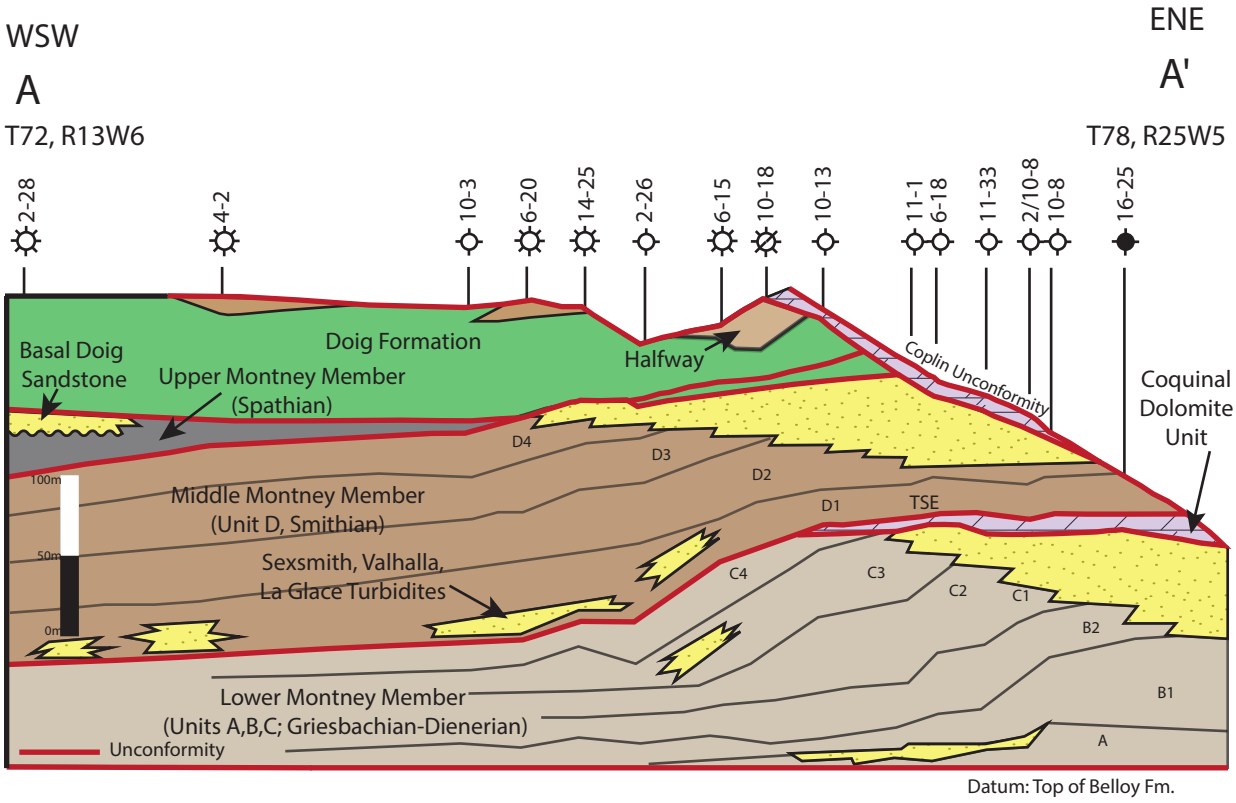

Figure 2.2– Early to Middle Triassic regional schematic stratigraphy oriented parallel to depositional dip. Datum is the top of the Belloy Formation. Modified from Moslow and Davies, 1997; Davies and Hume, 2016.

Study Area and Methods

This investigation focuses on the Middle Montney D1 and D2 horizons in the subsurface between Townships 75 to 82 and Ranges 10W6 to 15W6 (Fig. 2.3). As a result of legacy exploration in the prolific Montney Turbidite play, there is dense well coverage in the area. There are 2150 vertical wells penetrating the top of the Montney Formation with 1000 of those wells spanning the entire Montney Formation in the study area.

The Montney D1 and D2 horizons directly overlie the Montney Turbidite interval and, although stratigraphically equivalent successions are dry in surrounding areas, this area is characterized by liquids rich natural gas. There are 491 wells that have produced from the D1 horizon, whereas only 4 producing wells have targeted the D2 horizon. Thirty-one wells have been cored in the D1 and D2 horizons, sedimentological and ichnological descriptions of these core form the basis for the interpretations presented within this paper. Lithofacies were identified based on lithology, primary physical and biogenic sedimentary structures, bioturbation intensity and fossil composition. Grain size follows the Wentworth-Udden grain size classification (Uden, 1914; Wentworth, 1922). Overall intensity of bioturbation was assessed using the ichnofabric indices following the semi-quantitative methodology described by Bottjer and Droser (1991). Thin section and scanning electron microscopy (SEM) images were studied for each facies, to determine grain size, mineralogy, cement types, presence of clays, and porosity characteristics. Thin sections were cut 22 microns thick, impregnated with blue epoxy or rhodamine-b epoxy and stained to allow for the rapid identification of minerals. To distinguish calcite and dolomite grains, the thin sections were stained with Alizarin-Red S and Potassium Ferrocyanide; to identify feldspar grains, thin sections were stained with Sodium Cobaltinitrite. SEM images were

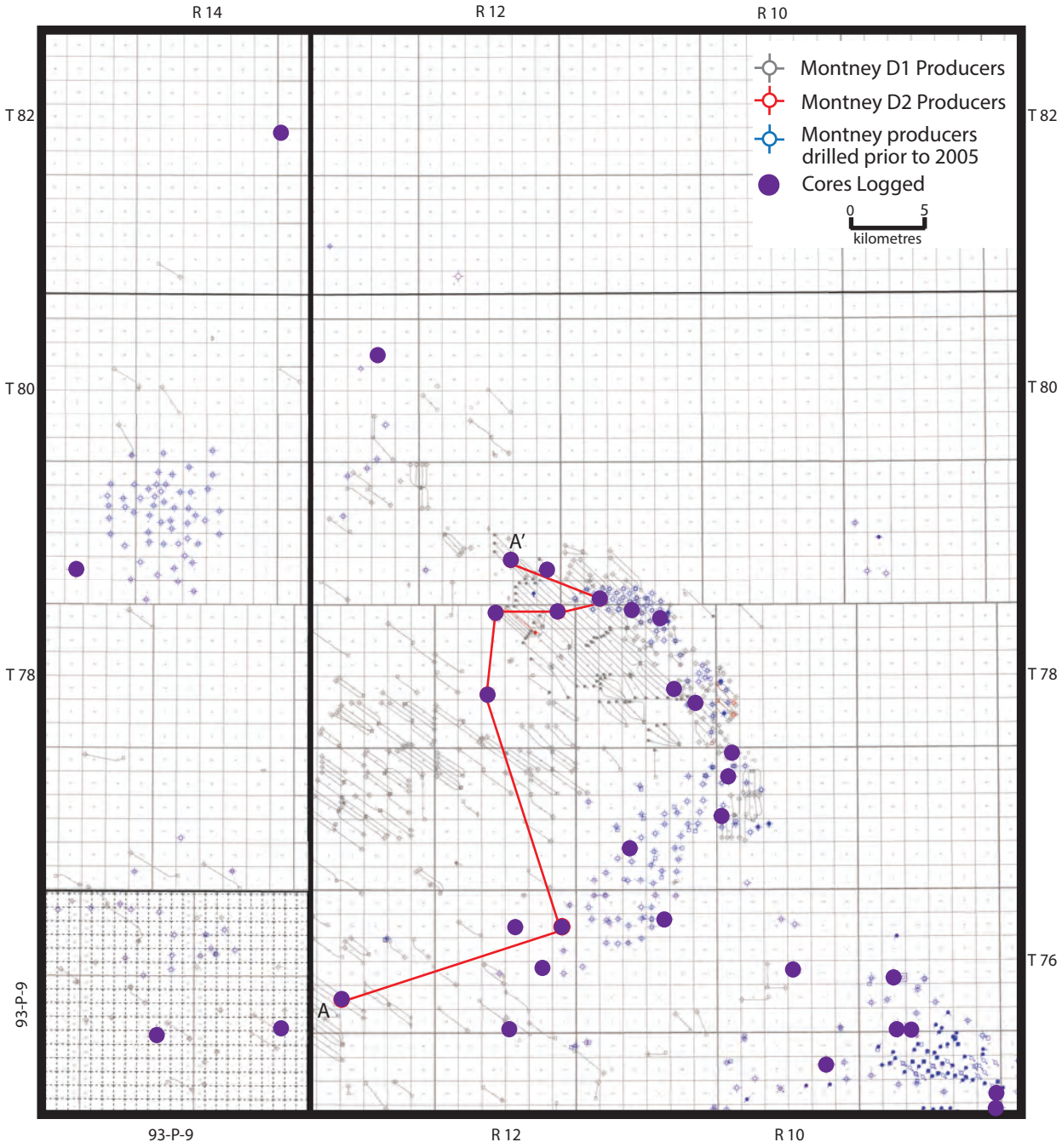

Figure 2.3- Map of the study area. Wells in purple denote cores that have been logged for the study. Location of cross section A-A' shown.

acquired from The University of Alberta Earth and Atmospheric Sciences SEM Lab with a Zeiss Sigma 300 VP-FESEM instrument.

Following the identification of important surfaces in core, surfaces were extrapolated to non-cored wells and were picked, using geoSCOUT, on the 1000 vertical wells that penetrate the entire Montney Formation within this area. Using Surfer 10, isopach maps were then generated to understand the distribution of different units throughout the study area.

Lithofacies Descriptions and Interpretations

Based on core examination in the greater Pouce-Coupe Area, eight lithofacies were identified within the lower to middle Montney Formation. These lithofacies are discussed below and summarized in figures 2.4 and 2.5 and table 2.1.

Lithofacies 1

Description:

Lithofacies 1 consists of finely laminated medium-grained siltstone interbedded with sharp-based, highly bioturbated coarse siltstone beds (Fig. 4A). The medium-grained siltstone beds are dominantly planar laminated with isolated starved ripples. Ammonoid impressions and Ganoid fish scales are common on bedding planes. Carbonaceous debris is occasionally observed, most commonly at the base of coarse-siltstone beds. The coarse-siltstone beds gradually fine upwards. Thin (<5cm) coarse-grained siltstone interbeds have been highly bioturbated (BI-6) obscuring any sedimentary structures. Traces observed include *Phycosiphon*, *Skolithos* and *Teichichnus*. Few to no traces are observed within the medium grained siltstone (BI<1).

Lithofacies	Descriptions	Interpretations
1 Interbedded parallel laminated and burrowed siltstones	•Planar laminated fine siltstone interbedded with highly bioturbated coarse siltstone beds •Carbonaceous debris found throughout •Ammonoid impressions and Ganoid fish scales found on bedding planes •Thin (<5cm) coarse siltstone interbeds have been highly bioturbated (BI-6) traces include *phycosiphon, skolithos and teichichnus*.	•Deposited in a distal ramp/ offshore position •Coarser beds are deposited by turbidity flows •Burrowed beds represent doomed pioneer assembledge
2 Interbedded sandstone and siltstone with abundant soft sediment deformation	•Interbedded very-fine sandstone, siltstone and shale. •Beds commonly erosively based with phosphatic grains and rip up clasts at base •Abundant soft sediment deformation, dewatering structures, climbing ripples, and planar laminations •Well developed Bouma Sequences in some cores. •No bioturbation observed	•Deposited by point-sourced turbidity flows •Major accumulations controlled by syn-sedimentary tectonism •Thick accumulations are not found throughout study area indicating inter channel or channel levee deposition
3 *Claria* Shell Beds	•Finely laminated fine-coarse siltstone with low relief planar wavy bedding •Abundant disarticulated and fragmented small (<3mm long) dolomitized Claraia shells oriented roughly parallel to bedding	•Following turbidite deposition the ensuing transgression caused erosion and redeposition of fragmented Claraia shells from the further up-dip Coquinal Dolomite Member •Deposited as transgressive lag
4 Massive Brown Dolostone	•Massive brown finely crystaline dolostone •Abundant small (<5 micron) pyrite framboids •Often has sub-vertical calcite filled fractures cutting through the beds.	•Deposited in distal ramp/offshore position •Deposited when sea level was at its highest, there was no sediment input into this part of the basin and anoxic conditions developed
5 WavyPlanar Laminated Siltstone	•Planar to wavy parallel laminated fine-coarse siltstone •Starved ripples, erosionally scoured beds, minor soft sediment deformation . •Low contrast between fine and coarse siltstone laminae •Low calcite cementation. •Low bioturbation (BI-1) consisting of isolated *nereites, planolites*.	•Deposited in proximal offshore position •Deposited by linear sourced turbidity currents
6 Pinstripe Laminated Siltstone	•Thin (<5cm) dark black beds of silty shale interbedded with fine to coarse siltstone. •Wavy parallel bedding is common, starved ripples and soft sediment deformation occur. • The coarser siltstone laminae are often highly cemented by both calcite and dolomite	•deposited in proximal offfshore position •Dark black silty shale beds are deposited by hyperpycnal flows •Interbedded siltstone beds are deposited by linear sourced turbidity currents
7 Lenticular Bedded Siltstones	•Lenticular bedded coarse to fine siltstone interbedded with silty shale beds •Abundant asymmetric and climbing ripples •Sediment loading and flame structures are common. •Coarser siltstone beds are cemented by calcite and dolomite.	•Deposited in the distal offshore transition to proximal offshore position •Interbedded hyperpycnal flows and linear sourced turbidity currents
8 Planar Laminated Bituminous Siltstone	•Planar laminated fine-medium siltstone •Rare pyritized starved ripples •Calcisphere beds are common	•Deposited in the distal offshore setting •Calcisphere beds associated with organisms that inhabited an unstable eutrophic environment

Table 3.1 - Summary of sedimentary lithofacies characteristics in the D1 and D2 Horizons in the Greater Pouce Coupe Area, Alberta and British Columbia

Interpretation:

Lithofacies 1 is interpreted to represent deposition in a distal offshore/ramp setting with low frequency turbidites depositing the highly bioturbated coarse-siltstone beds. The absence of wave-generated structures implies that this facies was deposited below storm wave base. The sharp-based coarse siltstone beds are examples of event beds that formed by rapid and episodic deposition. Such features have been attributed to numerous phenomena, such as seismic shock, turbidites, tempestites, and flooding deposits (Seilacher 1969; Reineck and Singh 1972; Pemberton and MacEachern 1997). Turbidites are the mechanism of deposition favored herein, as no wave generated or combined flow ripples are observed at the base of beds and a fining upwards sequence was observed within the coarse-siltstone beds (Pemberton et al., 1992).

The lack of bioturbation in the medium grained siltstone suggests that there is an environmental stress that prevented a diverse and abundant infauna. Previous authors have attributed this stress to a deficiency in oxygen, and potentially oceanic acidity, which precluded infaunal populations from thriving (Hayes et al. 2007; Zonneveld et al. 2010b). In contrast, the low diversity but high intensity trace fossil suite observed in the coarser beds likely represents a 'doomed pioneer' ichnological assemblage (sensu Föllmi and Grimm, 1990). In the doomed pioneer concept fauna are transported basinward by sediment gravity flows and deposited within the coarser-grained beds that they subsequently colonize (Föllmi and Grimm, 1990; Zonneveld et al. 2010a). It has been postulated that oxygen transported out into dysaerobic environments by turbidity currents may persist for more than one month (Sholkovitz and Soutar, 1975). Relatively rapid return to dysoxic conditions limits the time the fauna can survive, does not allow larval recruitment and prevents colonization of the surrounding finer grained beds (Folmmi & Grimm, 1990; Zonneveld et al. 2010b).

Lithofacies 2:
Description:

Lithofacies 2 comprises a heterolithic succession of interbedded very fine-grained sandstone, siltstone and silty shale. Decimeter-scale interbedding is characteristic of this facies, although sandstone beds greater than 1 meter thick are observed in some areas. Beds are sharp based and commonly marked by the presence of rip up clasts. An overall fining upwards trend was observed in this lithofacies. A wide range of physical sedimentary structures was observed and includes massive bedding, planar parallel bedding, climbing ripples (Fig. 2.4E) and abundant synsedimentary deformation structures. Complete (Ta-Te) and incomplete Bouma sequences are common. In the well-sorted sandstone beds water escape structures are limited to dish and pillar structures. Where siltstone and silty shale interbeds are present, convolute bedding, flame structures, and ball and pillow structures are common. Observed in both thin section and core the coarser grained beds are typically highly cemented by calcite cement. Bioturbation is not observed in this facies (BI-0).

Figure 2.4 (Next Page) - Core photographs of lithofacies from the Montney Formation in the greater Pouce-Coupe Area. **A.** Coarse-grained siltstone beds are highly bioturbated by *Phycosiphon* (Ph), white arrow points to carbonaceous fragment*;* Lithofacies 1; 15-31-77-10w6; 2233.75m. **B**. Parallel laminated siltstone with disarticulated and fragmented *Claria* shells aligned approximately parallel to bedding; Lithofacies 3; 15-31-77-10w6; 2224.65m. **C.** Massive brown finely crystalline dolostone with calcite filled vertical fracture; Lithofacies 4; 14-36-78-12w6; 2115.72m. **D.** Ganoid fish scales on bedding plane; Lithofacies 8; a-063-A/94-P-09; 2286.18m. **E.** Climbing ripples with phosphatic grain at base of bed; Lithofacies 2; 8-3-75-8w6; 2152.04m. **F.** Combined flow ripple; Lithofacies 7; 14-36-78-12w6; 2050.80m. **G.** Pyritized starved ripple; Lithofacies 8; 5-9-76-13w6 2638.82m.

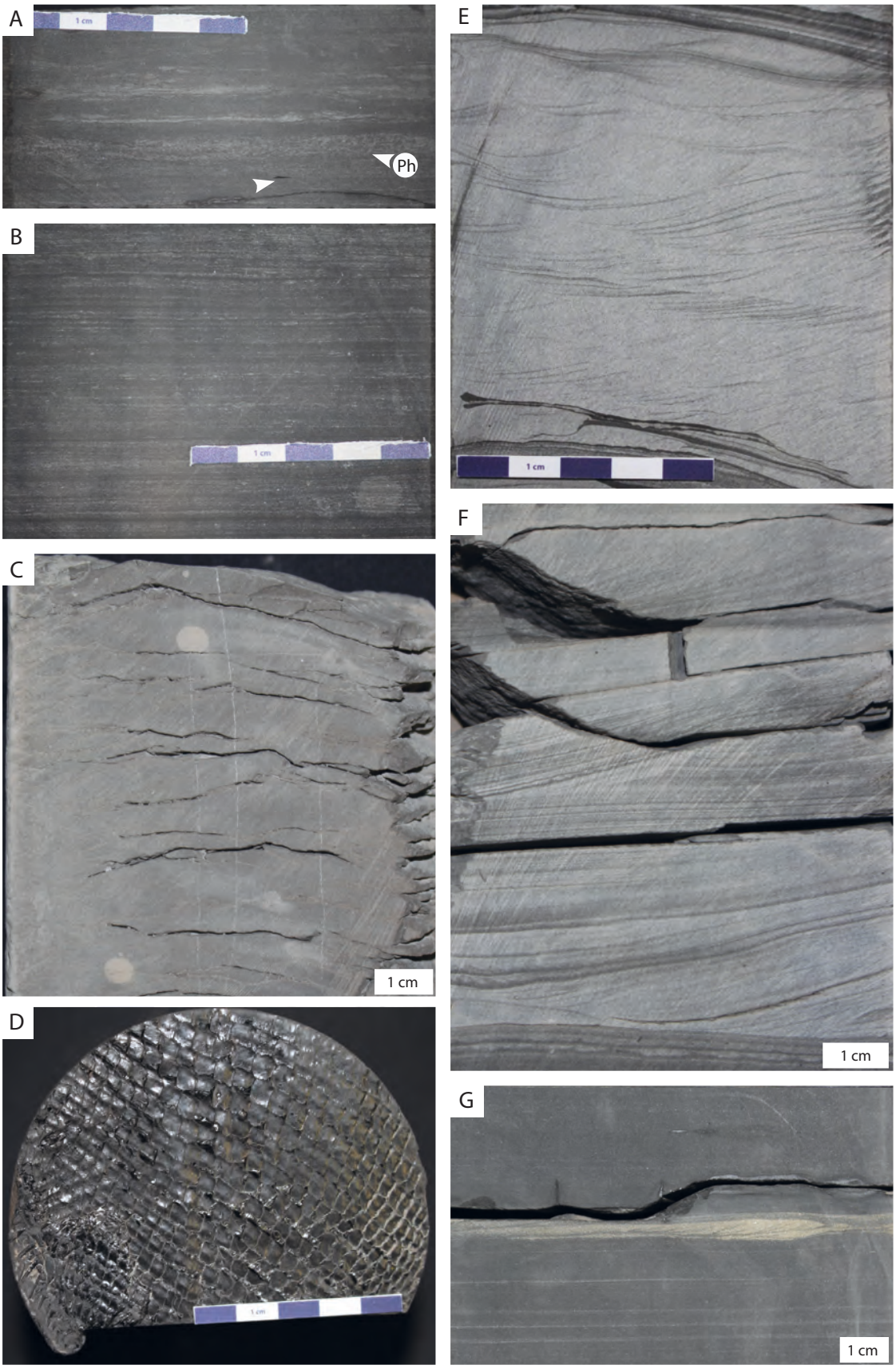
A
1 cm
Ph
B
1 cm
C
1 cm
D
1 cm
E
1 cm
F
1 cm
G
1 cm

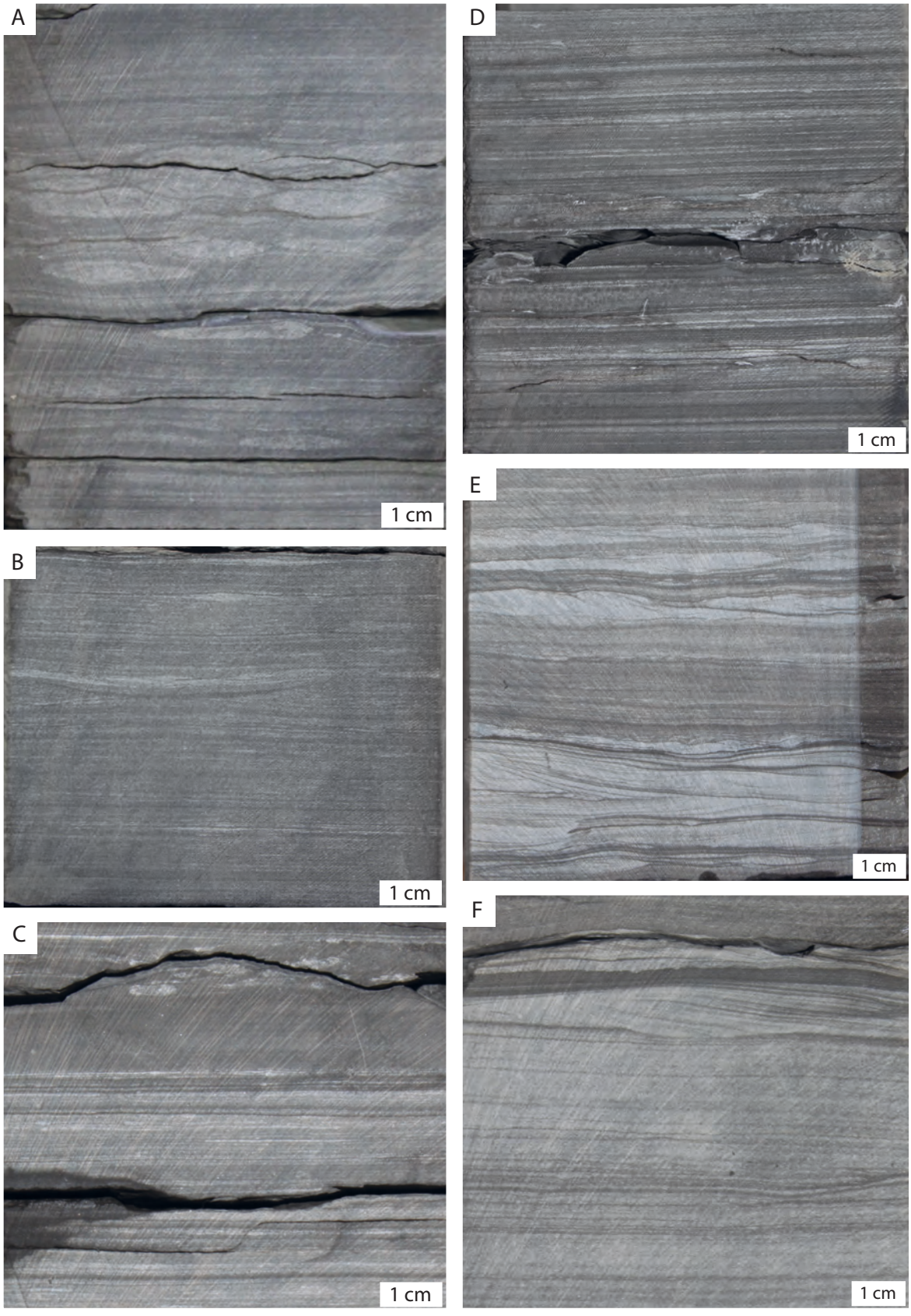
A
1 cm
B
1 cm
C
1 cm
D
1 cm
E
1 cm
F
1 cm

Figure 2.5 (Previous Page) - Core photographs of lithofacies 5-7 from the middle Montney Formation, greater Pouce-Coupe Area. **A.** Starved ripples and ball and pillow structures; Lithofacies 5; 14-36-78-12w6; 2119.21m. **B.** Scour and fill structure and starved asymmetric ripple at top of photo; Lithofacies 5; 4-16-78-12w6; 2277.5m. **C.** Dark black silty shale bed that has small scale ball and pillow structures at top of bed; Lithofacies 6; 4-16-78-12w6; 2061.75m. **D**. Pinstripe bedding; Lithofacies 6; 4-16-78-12w6; 2258.78m. **E.** Lenticular bedding; Lithofacies 7; 2-5-79-11w6; 2045.77. **F.** Tb –Td beds of bouma sequence; Lithofacies 7; 2-5-79-11w6; 2045.77m.

Interpretation:

Lithofacies 2 is interpreted to record deposition by turbidity currents and mass wasting processes. Supporting this interpretation is the presence of Bouma sequences and an overall fining upward trend that represents a waning flow typical of sediment gravity flows (Walker, 1967). The thickest sands represent turbidite channel axis or turbidite lobe deposits. The location of these accumulations was controlled by syn-sedimentary tectonism (Moslow and Davies, 1997, Moslow 2000). Walker (1985) interpreted co-occurring climbing ripples, convolute bedding and intraclast lags as CCC turbidites and interpreted them to record deposition with turbidite channel margin / inter channel areas. The common co-occurrence of climbing ripples and convolute bedding is consistent with this interpretation. The areas underlying the main D1 fairway is noticeably lacking in thick-massive sandstone accumulations, indicating that most of the study area is located off the main turbidite trend and occurs within an interchannel area (Waker, 1985). Lateral to the study area, thick accumulations of well-sorted sandstone comprise the Montney Turbidite Zone, a Montney legacy play pursued in the 1990s through vertical drilling. The Montney Turbidites were described in detail by several previous authors (Moslow and Davies, 1997; Moslow, 2000; Kendall, 1999).

Lithofacies 3:

Description

Lithofacies 3 consists of finely laminated medium grained siltstone with low relief wavy parallel bedding. Abundant fragmented small (<0.3cm long) dolomitized *Claria* shells occur, oriented approximately parallel to bedding (Figs. 2.4B and 2.6A-B). No bioturbation was observed in these beds (BI-0). Individual bed thicknesses range from 10 – 150 cm thick. Lithofacies 3 occurs stratigraphically above, and in contact with, Lithofacies 2 in all wells and separates the turbidite deposits from the overlying lithofacies.

Interpretation

Lithofacies 3 is interpreted to consist of a series of bioclastic lags that were transported basinward due to storm processes. The coquinal dolomite member (CDM) occurs eastwards (landwards) of the study area and is dominated by bioclastic packstone and grainstone consisting of densely packed bivalve (*Claraia, Unionites, etc…*), gastropod and lingulide brachiopod shells (Mederos, 1995; Markhasin, 1997; Davies et al., 1997). The CDM has been interpreted to represent deposition in a shallow marine, wave-reworked shoreface setting (Mederos, 1995; Markhasin, 1997; McCormick et al., 2016) analogous to the coquinal accumulations at Shell Beach, Sharks Bay, Australia (Johert et al., 2012). At the onset of relative sea level rise, wave action eroded sediment from these shoreline deposits and redistributed it further basinward (Posmentier and Allen, 1993). The shells in lithofacies 3 have clearly experienced significant reworking, as the shells are all fragmentary and commonly rounded.

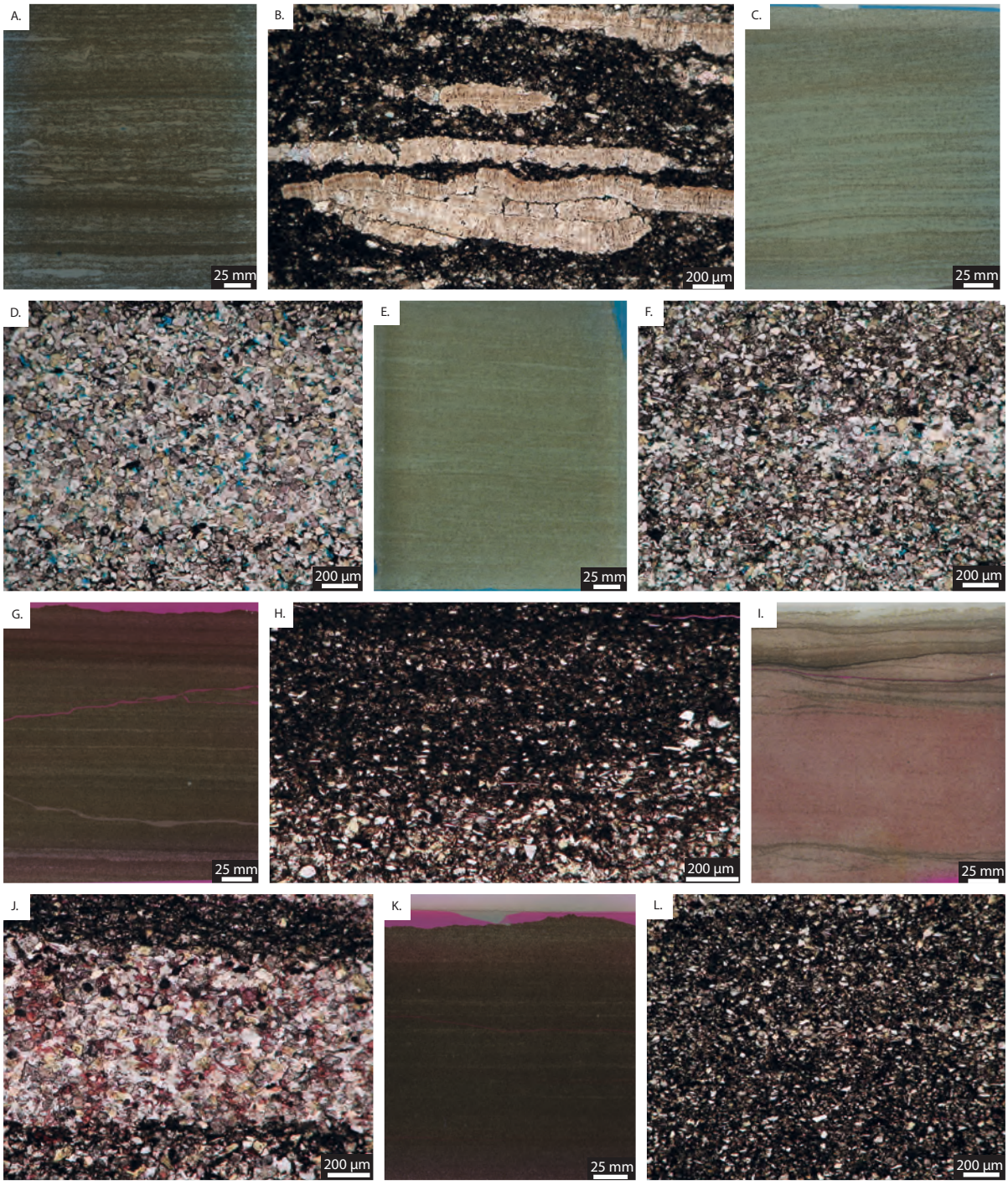

Fig 2.6- Scanned images of thin sections and thin section photomicrographs of each facies. All think section photomicrograph photos are in PPL and 20X magnification, thin sections have been double carbonate stained and feldspar stained. **A-B.** Fragmented Claraia shells in Lithofacies 3; 15-31-77-10; 2224.65m. **C-D.** Coarser bed in Lithofacies 5, note lack of calcite cement; 14-33-78-11w6; 2106.25m. **E-F.**Lithofacies 5; 14-33-78-11w6; 2109.75m. **G-H.** Lithofacies 6; interbedded silty shale and siltstone beds; 4-16-78-12w6; 2262.06m. **I-J.** Lithofacies 7; lenticular bedded siltstone, note intensive calcite cementation throughout coarse lense; 2-5-79-11w6; 2045.82m. **K-L.** Lithofacies 8; fine bituminous siltstone; 4-16-78-12w6; 2264.31m.

Lithofacies 4:

Description

Lithofacies 4 consists of massive brown, finely-crystalline dolostone with small (2-6 micron) pyrite framboids distributed throughout the interval (Figs. 2.4C, 7A and 2.8A). Sub vertical calcite filled fractures commonly cut through this facies. Intervals of this facies are thin (<30cm) but laterally continuous and occur at the same stratigraphic interval throughout the area. No bioturbation was observed in Lithofacies 4.

Interpretation

Lithofacies 4 is interpreted to represent deposition in an offshore anoxic setting below storm wave base. Similar fine-grained dolomite has been reported in multiple settings within both the modern and rock record (Pisccioto, 1981;Lumsden, 2003; Kelts and McKensie, 1984). In these occurrences the dolomite is formed due to organogenesis, which involves bacterial sulfate reduction in anoxic and organic rich sediments (Mazzullo, 2002). Pyrite framboid sizes have been used to define redox conditions with a continuum existing between euxinic and dysoxic conditions (Bond and Wignall, 2010). Under euxinic conditions, framboids form in the water column but fall below the iron reduction zone relatively quickly, limiting the time they have to grow and restricting their sizes to diameters of around 5-6 μm (Wilkin et al. 1996). In dysoxic environments the sea floor is weakly oxygenated and framboids form on surficial sediment where size is governed by the local availability of reactants, as a result framboid size is more variable and generally larger (Bond and Wignall, 2010). SEM analysis of Lithofacies 4 has shown a restricted size range of pyrite framboids with diameters less than 7-8 μ (Fig. 2.7A). Pyrite distribution and the absence of bioturbation suggests Lithofacies 4 was deposited in an anoxic setting where there was no oxygen in bottom waters for long periods of time. Lithofacies

would have been deposited at a time when there was extremely limited sediment input into this part of the basin and the area was fully anoxic.

Lithofacies 5:

Description

Lithofacies 5 is a dull gray siltstone and is notable for its lack of definition between laminae (Figs. 2.5A,B and 2.8B-D). Millimeter scale, fine-medium and coarse-grained siltstone laminae are present. The coarse-grained siltstone laminae are slightly lighter colored, but unlike in other lithofacies, the coarse-grained laminae are rarely cemented by calcite resulting in minimal color contrast between laminae (Fig. 2.6C-F). The coarse-grained siltstone laminae have been partially cemented by dolomite. Sedimentary structures consist primarily of wavy parallel bedding with occasional laterally restricted starved ripples (<1 cm in height). Erosionally scoured beds and scour and fill structures are found through out. Small-scale penecontemporaneous deformation structures (micro flame structures and low relief convolute bedding) are common. Sparsely bioturbated (BI-1), traces include isolated *Planolites* and *Nereites. Listracanthus* spines were observed on some bedding planes.

Lithofacies 5 has been subdivided into Lithofacies 5a (L5a) and Lithofacies 5b (L5b) based on the proportion of coarse-grained siltstone. The physical sedimentary features are the same in both subfacies but L5a has <50% coarse-grained siltstone and L5b has >50% coarse-grained siltstone. Based on their respective sedimentary textures, L5a and L5b have different reservoir characteristics, which will be further discussed in the reservoir lithologies section.

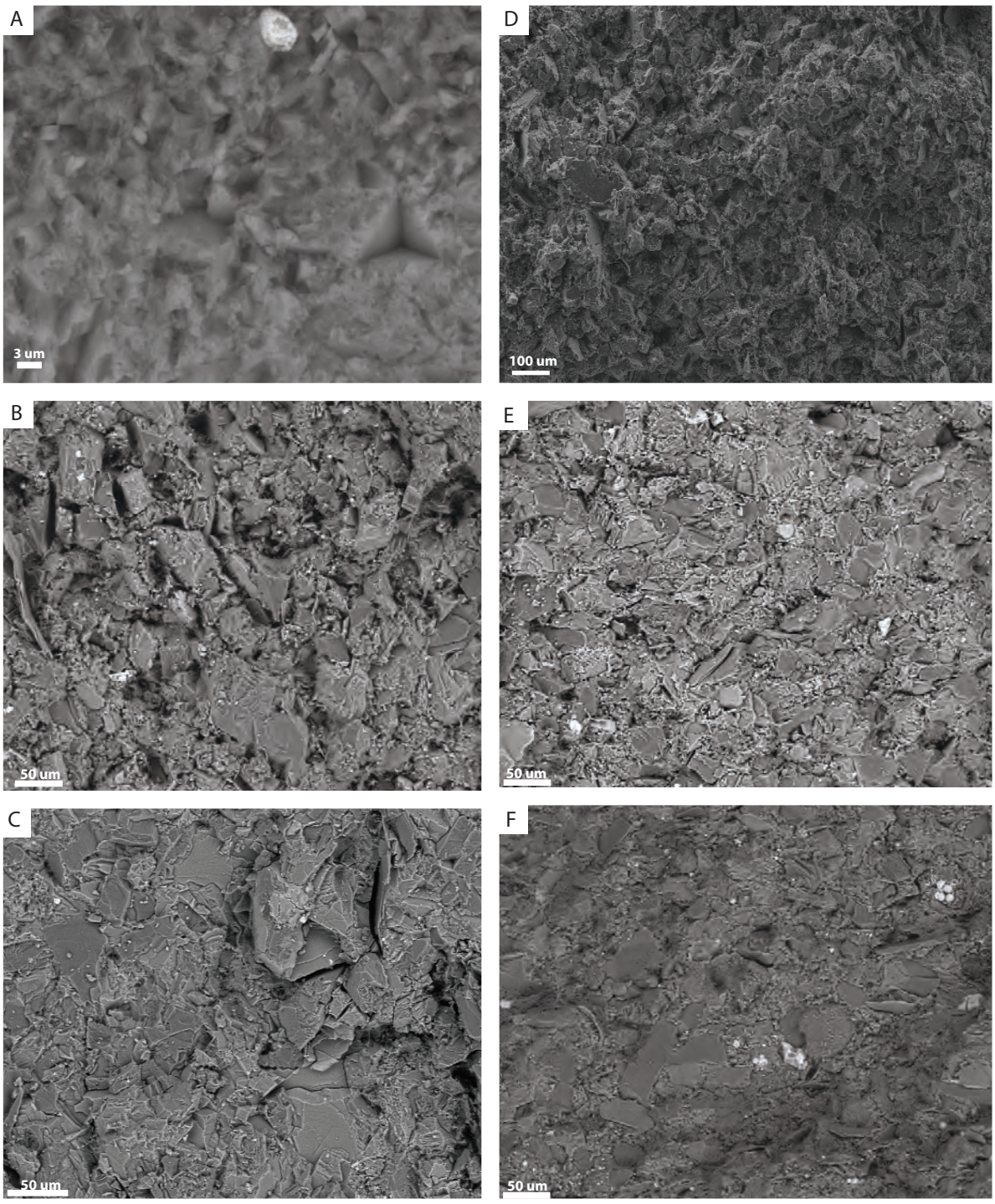

Fig 2.7- A. SEM image of Lithofacies 4 showing fine grained dolomite with small pyrite framboid at top of image; 1560 X magnification **B.** BSE SEM image of Lithofacies 5 showing high intragranular porosity; 150X Magnification **C.** BSE SEM image of Lithofacies 7, note larger grains and limited porosity; 150 X Magnification **D.** SEM image of Lithofacies 5; 41X Magnification **E.** BSE SEM image of Lithofacies 6; 150X Magnification **F.** BSE SEM image of Lithofacies 8; 150X Magnification.

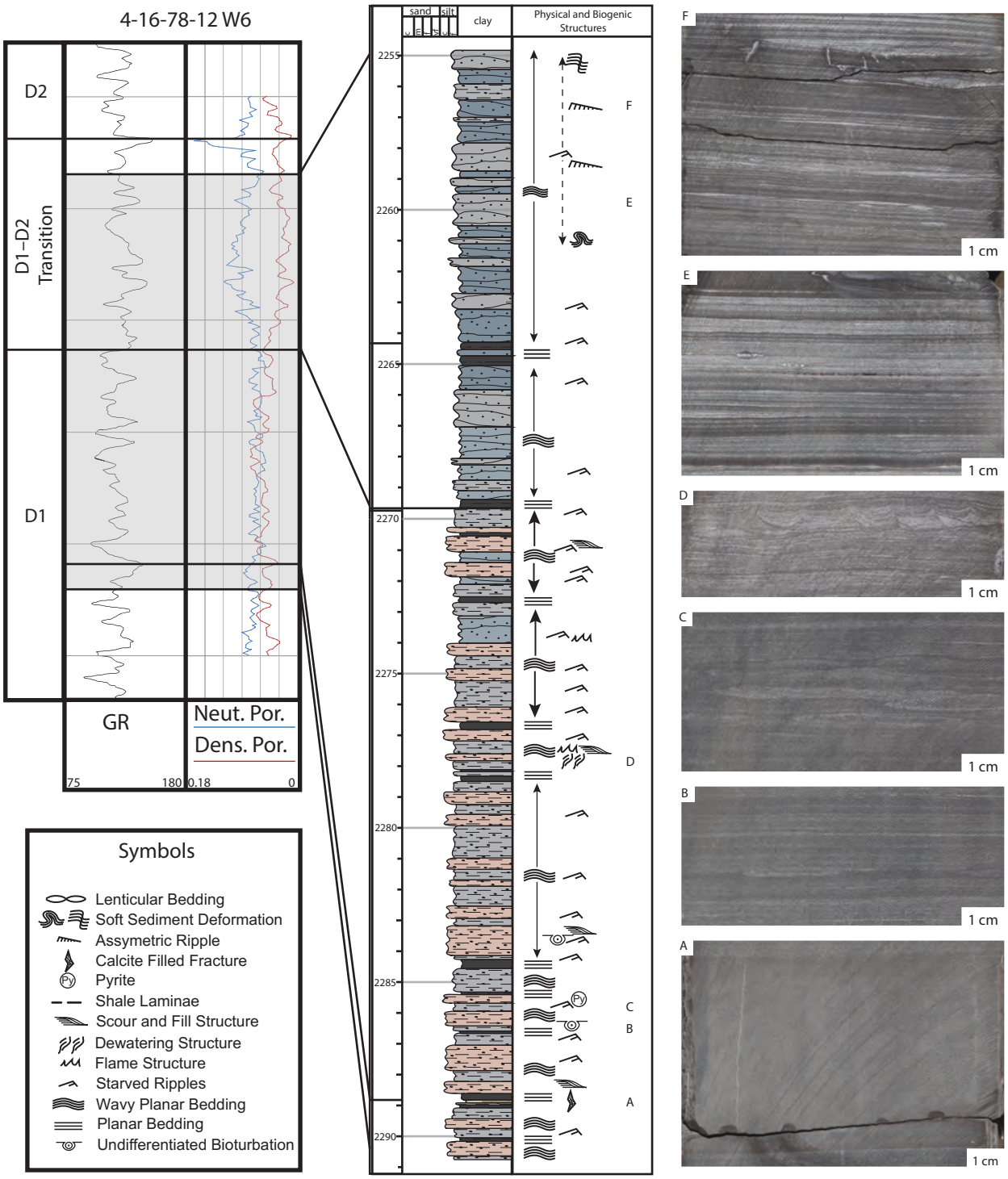

Figure 2.8- Cored interval in well 4-16-78-11w6 (2254.91-2290.40m TVD) showing the contact between the D1 horizon and the D1-D2 transition. For Lithofacies coloration refer to Figure 10. Note in the D1-D2 transition the Neutron-Density curves diverge due to the presence of clay. Photographs representative of facies throughout the core. **A.** Massive brown dolostone with vertical calcite filled fracture; Lithofacies 4; 2288.96m. **B.** Nereites burrow; Lithofacies 5a; 2286.36m. **C.** Starved ripples; Lithofacies 5a; 2285.82m.

Fig 2.8 (Continued)- D. Dewatering structures; Lithofacies 5b; 2277.75m. **E.** Pinstripe bedding, white crystals forming in core induced fractures are gypsum that is precipitated during the core washing process; Lithofacies 6; 2259.87m. **F.** Pinstripe bedding with starved ripples; Lithofacies 6; 2256.61m.

Interpretation

Lithofacies 5 is interpreted to represent deposition by turbidity currents in a proximal offshore setting. Erosionally scoured beds, asymmetric starved ripples and abundant minor soft sediment deformation structures indicate rapid deposition by a unidirectional current on top of an unconsolidated, sometimes soupy substrate (Muti, 1997; Dzulynski and Kotlarcczyk, 1962; Van Loon and Wiggers, 1976). The turbidity currents responsible for the deposition of Lithofacies 5 were not fed by a single channel; instead mass wasting events at multiple sites along the ramp generated linear sourced turbidity currents (Reading and Richards, 1994; Zaragozi et al., 2001; Martison et al., 2005). The rapid deposition of sediment caused fluid escape (dewatering), which prevented the development of well-defined coarser and finer laminae. It is likely that this made post-depositional fluid movement inefficient through this unit and greatly inhibited cementation. L5a and L5b are both interpreted to have been deposited by linear sourced turbidity currents but in more distal and proximal locations respectively (or lateral/ central to individual flow events).

Trace fossils within this lithofacies are not readily assigned to a traditional ichnofacies due to low resident ichnofaunal diversity. The paucity of trace fossils is attributed to a lack of oxygen at the sea floor, scarcity of food, and periodic disruption by turbidity currents (Ekdale and Mason, 1988; MacEachern et al. 2007). *Planolites* are interpreted to be traces constructed by infaunal deposit feeders (Seilacher and Hemleben, 1969). *Nereites*, which are meandering, horizontal traces consisting of a medial back-filled tunnel enveloped by an even to lobate zone of

reworked sediment, represent grazing behaviors by deposit feeders (Wetzel & Uchman, 1998). *Nereites* are most commonly reported in turbidite sequences and occur post-depositionally (Wetzel, 2002). The *Listracanthus* spines that occur on some bedding planes are the remains of enigmatic chondrichthyans that ranged from the Carboniferous to their final disappearance during the Lower Triassic (Mutter and Neumann, 2006). *Listracanthus pectenatus* occurs in the outcrop belt in British Columbia, west of the present study area, and is common in offshore depositional settings in the Montney Formation and equivalent outcrop units (Mutter and Neumann, 2006; Orchard and Zonneveld, 2009). In western Canada they are most common in Dienerian and Smithian strata (Mutter and Neumann, 2006; Orchard and Zonneveld, 2009).

Lithofacies 6:

Description

Lithofacies 6 comprises interbedded fine-grained to coarse-grained siltstone and silty shale. Individual lithologies occur in variably thick beds (0.2 to 5cm). Silty shale beds are commonly sharp based and occasionally appear to have scoured bases. The silty shale beds often show coring induced fractures that are roughly parallel to bedding. When washed the silty shale beds often precipitate gypsum on the surface of the core (Fig. 2.8E,F). The coarse-grained beds are commonly calcite cemented, which causes a large color contrast between the white coarser beds and black silty shale beds, this gives the facies its diagnostic pinstripe appearance.

Physical sedimentary structures consist primarily of wavy parallel bedding with common erosional scour surfaces, occasional starved ripples, climbing ripples and a variety of penecontemporaneous deformation structures (Figs. 2.5C,D and 2.8E,F). Deformation structures include small-scale ball and pillow structures, loaded ripples, small-scale convolute bedding and micro flame structures. Bioturbation is not observed in Lithofacies 6 (BI -0).

Interpretation

Lithofacies 6 is interpreted to have been deposited by an alternation of linear sourced turbidity currents and hyperpycnal flows. The erosionally scoured beds, asymmetric starved ripples and abundant soft sediment deformation structures are indicative of deposition by a fast unidirectional current on top of an unconsolidated, sometimes soupy substrate (Dzulynski and Kotlarcczyk, 1962; Bhattacharya and MacEachern, 2009). The black silty shale beds are interpreted to have been deposited by hyperpycnal density flows. Hyperpycnal conditions develop at marine deltas when sediment concentrations are high, especially during exceptional river floods (Bhattacharya and MacEachern, 2009; Mulder and Syvitsky, 1995). These turbid, heavily sediment-laden plumes have been observed to travel long distances. Nakijima (2006) reported hyperpycnal deposits as far as 700 km from the river mouth in the Central Japan Sea. Cyclical fluctuations result in the interbedding of hyperpycnal flow deposits, formed at times of seasonally high fluvial discharge, and linear sourced turbidity current deposits.

Lithofacies 7:
Description

Lithofacies 7 consists of a heterolithic succession of interlaminated very fine-grained sandstone, siltstone and silty shale beds. Individual lithologies are thinly bedded (0.1- 10cm). This lithofacies is characterized by lenticular bedding (Fig. 2.5E). The coarse-grained lenses range from 0.1 cm- 10 cm in thickness but are generally less than 2 cm thick. The coarse-grained lenses are highly cemented by calcite and dolomite. Coarse-grained lenses often have calcite filled sub-vertical fractures running through them. The silty shale beds occur regularly, are sharp based, and have a consistent thickness of 0.5 cm to 2 cm.

Wavy parallel bedding and asymmetric ripples are commonly observed. Coarse-grained beds are sharp-based, with tool structures occurring at bases, climbing ripples are abundant with Bouma sequences (Ta-Td subdivisions) occasionally being observed (Fig. 2.5F). Soft sediment deformation structures are common, laterally restricted starved ripples occur throughout the interval and combined flow ripples are rarely observed (Fig. 2.4F). Penecontemporaneous deformation structures include microflame structures, small scale convolute bedding, syn-sedimentary faults, loaded ripples and water escape structures. Bioturbation is extremely rare with isolated *Planolites* and *Skolithos* (BI-1).

Interpretation

Lithofacies 7 is interpreted to have been deposited by linear sourced turbidity currents in the distal offshore transition to proximal offshore area. Based on the abundance of coarse-grained siltstone lenses and the increase in the proportion of coarse-grained siltstone relative to fine-grained siltstone, it is interpreted that Lithofacies 7 was deposited in an area proximal to the site of mass wasting. The presence of loaded ripples, flame structures and syn-sedimentary faults indicate rapid sedimentation over a hydroplastic mud layer, resulting in penecontemporaneous deformation (Dzulynski and Kotlarcczyk, 1962; Van Loon and Wiggers, 1976). Combined flow ripples are interpreted to form from a combination of waves, and in this case, unidirectional currents generated by turbidity currents, insinuating that this lithofacies was deposited above storm wave base in the offshore transition (Myrow et al., 2002). The presence of thin silty shale beds shows that there was still deltaic activity capable of periodically generating hyperpycnal flows.

Lithofacies 8:

Description

Lithofacies 8 comprises finely bedded, bituminous, fine-grained to medium-grained siltstone with thin laminae of coarse-grained siltstone found throughout (Fig. 2.4G). Occasional thin (10-50cm thick) calcisphere-dominated beds occur. Lithofacies 8 is conspicuous in its dark black color. Physical sedimentary structures consist primarily of plane parallel laminae with pyritized laterally restricted starved ripples occurring occasionally. Carbonaceous debris is found throughout and ammonoid impressions, ganoid fish scales (Fig. 2.4D) and *Listracanthus* impressions are found on bedding planes. Bioturbation was not observed in this facies (BI-0).

Interpretation

Lithofacies 8 in interpreted to represent deposition in a distal offshore setting. This is supported by the absence of wave generated sedimentary structures. The laminated fine-grained to medium-grained siltstone beds are the product of deposition from suspension. The disseminated coarse silt grains in this facies may have been transported by offshore-directed winds (Windom and Chamberlain, 1978; Davies et al. 1997), although transport could not have been very far as coarse silt can only be transported in suspension in air for short distances under very high wind velocities (Nickling and Neumann, 2009). The rare asymmetric ripples represent distal low-density turbidity flows. Calcispheres have been associated with anoxic events and are interpreted to be the product of organisms that inhabited a eutrophic but unstable environment (Drzewiecki and Simo, 1997; Playter 2013). Wind-blown silt is commonly associated with phytoplankton blooms offshore of the Namibian desert (NASA, 2008), and thus the co-occurrence of floating silt grains with calcisphere-enriched beds may support the aeolian source of some of this silt. The common occurrence of pyrite further substantiates that this lithofacies

was deposited in anoxic/dysoxic conditions and the paucity of trace fossils observed in this facies may also be explained by oxygen stress (Ekdale, 1985; Wilkin et al. 1996).

Discussion

During the Early Smithian stage, the greater Pouce Coupe Area was situated in a distal ramp/offshore setting, mainly below storm wave base. During this period, the dominant mechanism for sedimentation was subaqueous density flows. Subaqueous density flows are classified based on the rheology of the flow and the sediment concentration, separating into cohesive flows, hyperconcentrated flows, concentrated flows and turbidity currents (Mulder and Alexander, 2001). The majority of the deposits analyzed in this study are interpreted to have been deposited by turbidity currents, in the sense that the main particle support mechanism was fluid turbulence (Mulder and Alexander, 2001; Arnott, 2010).

The variability in turbidity current deposits is enormous and is controlled by numerous factors including relative sea level, number and nature of sediment entry points into the basin, and grain size (Reading and Richards, 1994; Arnott, 2010). When turbidity currents are fed by a point source they develop the depositional elements often thought of as essential to every turbidite system (e.g. channel, levees, crevasse splay and depositional lobes) (Arnott, 2010). But density flows sourced from multiple locations are common in the rock record and do not form large channel deposits but instead are deposited by sheet-like flows (Fig. 2.9; Mulder and Alexander, 2010; Reading and Richards, 1994) with small scale channels in some areas.

The present day Skeleton Coast of Namibia, which is considered a likely modern analogue for the arid Montney coast, is characterized by numerous ephemeral rivers (Smith et al., 1993; Krapf et al., 2003; Botes et al., 2003; Svendsen et al., 2003; Zonneveld and Moslow,

2014). The Skeleton Coast Erg separates the rivers from the Atlantic Ocean and dams river flow. Only during major storms is the water discharge high enough to break through the dune belt and reach the ocean (Smith et al., 1993; Krapf et al., 2003; Botes et al., 2003; Svendsen et al., 2003). During these storms, run-off is intense and carries atypically high sediment loads, due in part to the lack of vegetation in sediment source areas (Zonneveld et al., 2010b; Krapf et al., 2003; Stollhoven et al., 2014). During catastrophic rainfall events multiple rivers carry sediment into the Atlantic Ocean, resulting in multiple sites of fluvial input along the coast (Krapf et al., 2003; Stollhoven et al., 2014). Rapidly deposited sediments are prone to over steepening and susceptible to mass wasting events (Zonneveld and Moslow, 2014). During Montney deposition there would have been rapidly deposited unstable beds all along the ramp, producing linearly sourced turbidity currents. In addition, the study area is situated in the south-eastern extension of the Fort St. John Graben Complex, thus syn-depositional structural movements would also have been likely to generate mass wasting events.

Regional Sequence Stratigraphy

The Montney D1 and D2 horizons are composed of multicyclic coarsening upwards successions of siltstone with occasional shale beds. The cycles are easily recognizable and mappable in the northeastern part of the study area, but become difficult to correlate downdip to the southwest as the units pinch out (Fig. 2.10). The study area is situated in a structurally complex area with the Fort St John Graben and other structural lineaments playing a major roll in sedimentation through out the area (Fig. 2.11). A regional cross section running from the Montney subcrop edge through the study area then southwest into British Columbia shows that the distribution of the D1 and D2 horizons is largely fault controlled (Fig. 2.12). The northeast

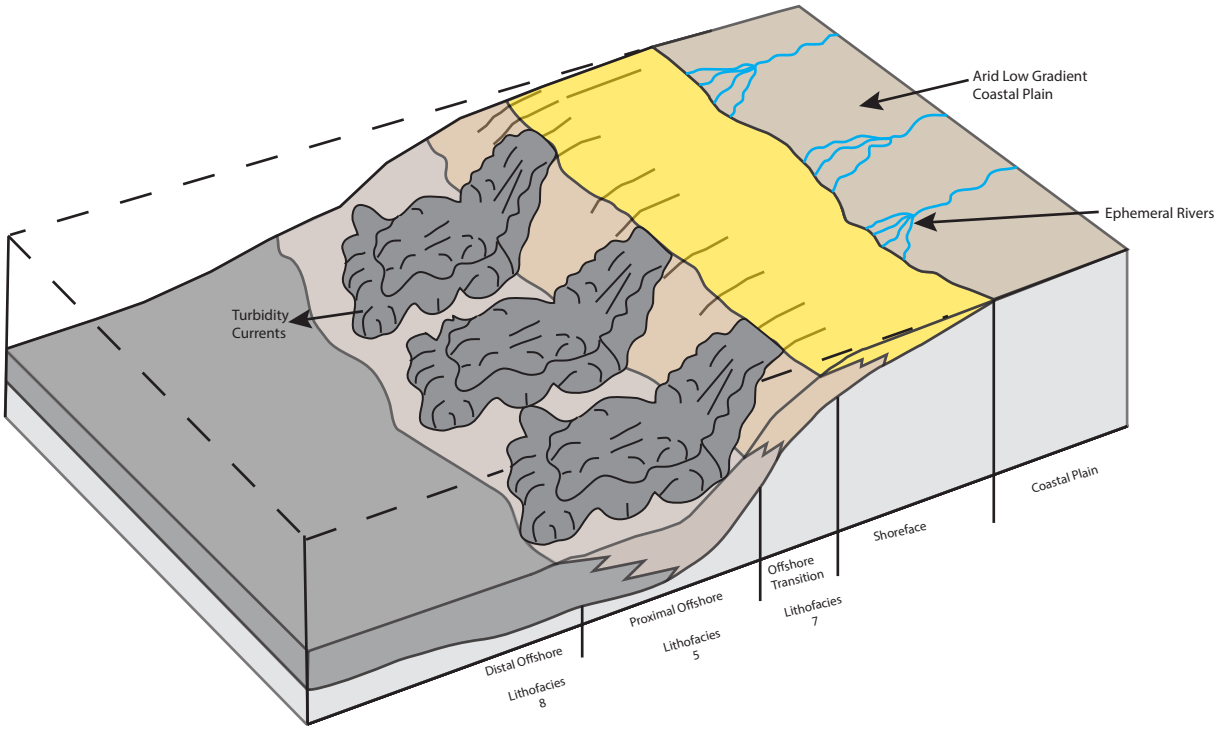

Figure 2.9- Depositional model for linear sourced turbidity currents. During major storms ephemeral rivers deposit large amounts of sediment rapidly, producing an oversteepened shoreface/ wave dominated delta profile. Sediment loading or tectonites produce mass wasting events. The offshore transition is close to the site of the mass wasting event and is characterized by coarser-grained sediment (Lithofacies 7). As distance from the mass wasting event increases less coarse-grained siltstone is deposited, this is the proximal offshore area (Lithofacies 5). The distal offshore is rarely affected by turbidite currents and deposition from suspension is the main process occurring (Lithofacies 8). Modified from Reading and Richards (1994).

extent of the D1 and D2 horizons is controlled by the Dunvegan fault, and it thins dramatically southwest of the Pouce Coupe Fault. In the study area the Middle Montney has been broken up into 4 main units, the Montney Turbidite Zone, the D1 horizon, the D1-D2 Transition and the D2 Horizon.

In the study area, the Montney Turbidite Zone is represented by turbidite channel and lobe sandstone beds and their associated interchannel deposits (Lithofacies 2). The Dienerian-Smithian boundary, which is marked by the development of the coquinal dolomite in the east, represents a fall in sea level and led to the shoreline advancing westward (Davies et al., 1997). Sand bypassed the shoreface and was brought to the outer ramp. Faulting along the Cindy Graben formed a conduit for this sediment to be transported (Moslow, 2000). As a result, subaqueous density flows with a single point source were developed. These deposits occurred along fault-controlled ramp breaks and major accumulations were controlled by localized syn-sedimentary tectonism (Moslow and Davies, 1997; Playter, 2013).

The occurrence of a bioclastic lag, diagnostic of Lithofacies 3, marks the onset of transgression. Relative sea level rise continued and its maximum extent is marked by the occurrence of the brown finely crystalline dolostone (Lithofacies 4) signifying a time with restricted sediment input and pervasive anoxia. The top of Lithofacies 4 marks the maximum flooding surface and is used as the datum for the cross section (Fig. 2.10).

The majority of the D1 horizon was deposited during the subsequent highstand system tract. At this time the study area was situated in a proximal offshore setting and deposition was dominated by subaqueous density flows (Lithofacies 5) that prograded and interfingered with hemipelagic siltstone of the distal offshore (Lithofacies 8). The turbidity currents that developed at this time were of a markedly different character to the Montney Turbidite Zone deposits.

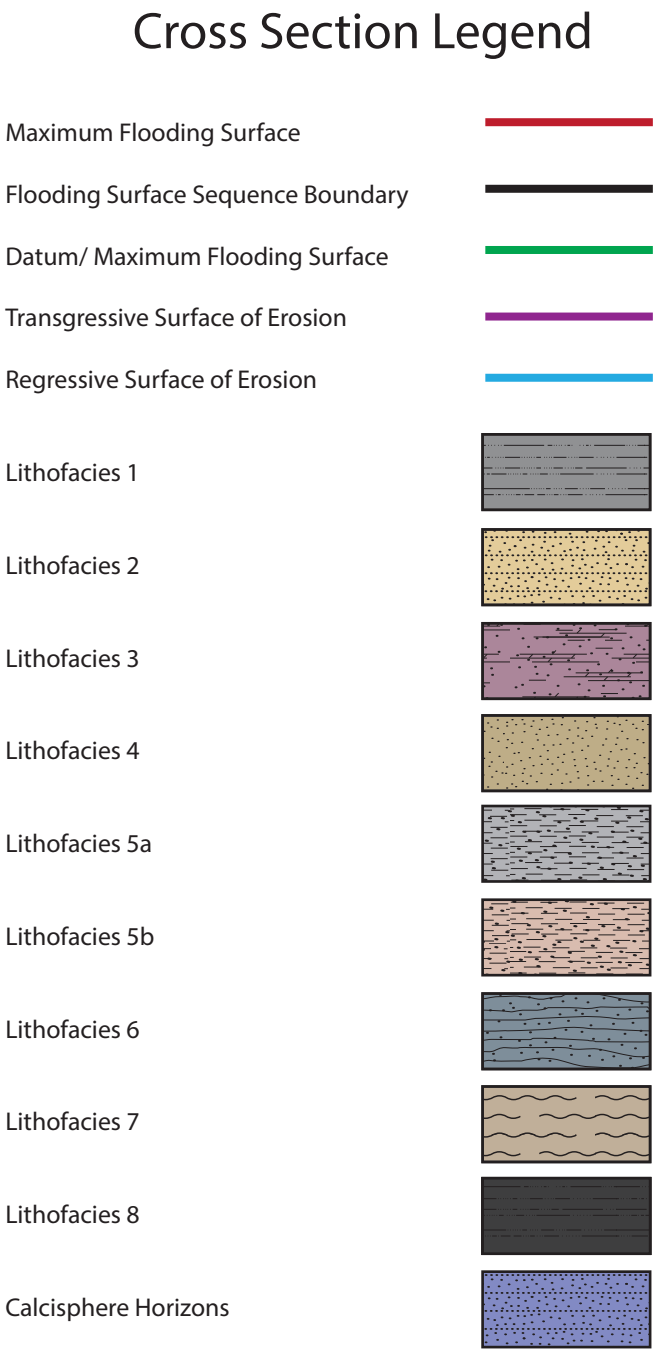

Figure 2.10 - Cross-Section A-A' oriented parallel to depositional dip. Datum is Maximum Flooding Surface that is represented by the occurrence of Lithofacies 4. The D1 horizon thins dramatically to the southwest. Lithofacies 5 gradually grades into the distal offshore deposits of Lithofacies 8 (5-9-76-13w6 is comprised primarily of Lithofacies 8). The D1-D2 Transition and the D2 Horizon thin to the southwest but much more gradually. The D2 horizon is characterized by multiple shoaling upwards sequences, resulting in multiple successions of Lithofacies 7 overlying Lithofacies 5. Cross section location shown in Fig. 2.2.

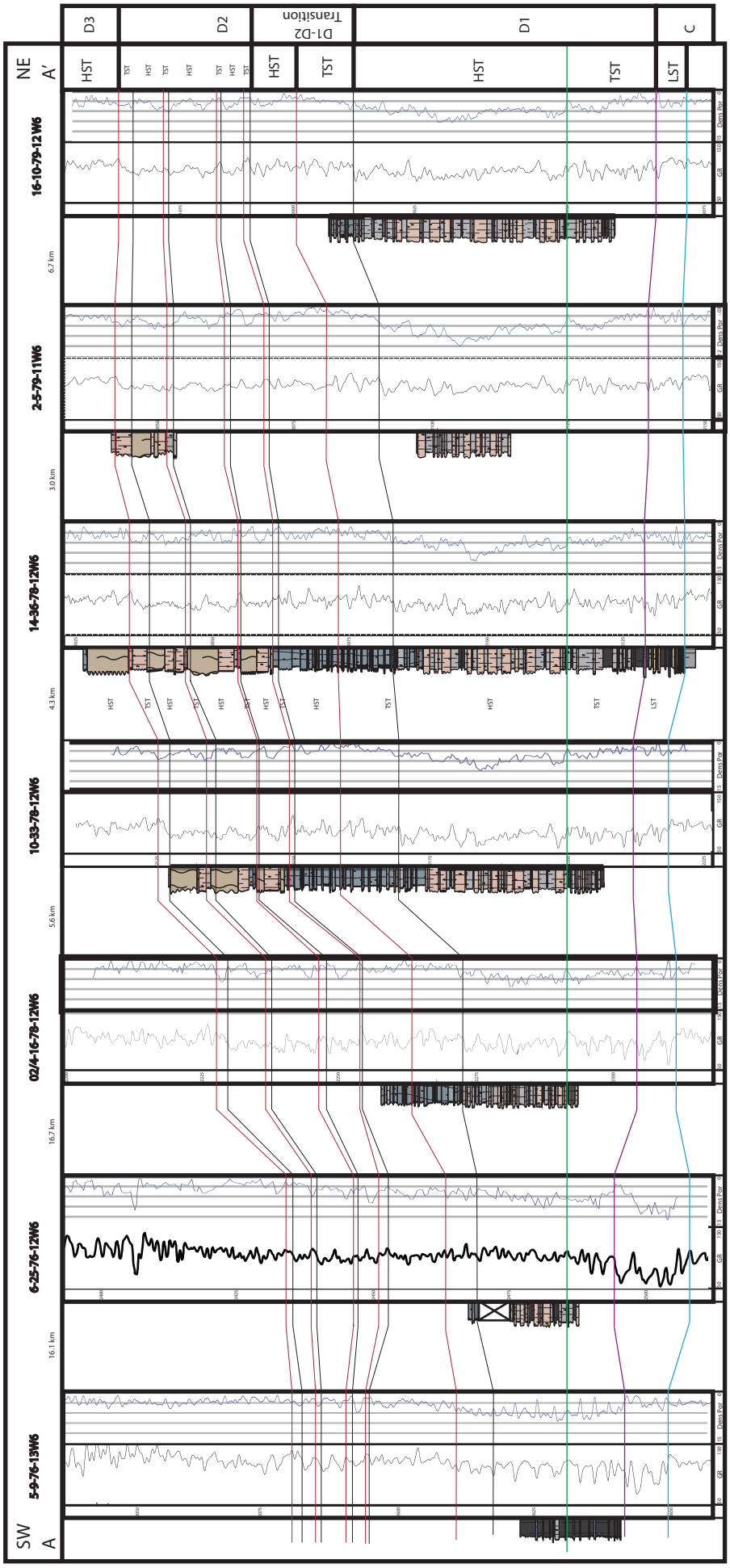

Figure 2.10 (Continued)- Cross Section A-A'

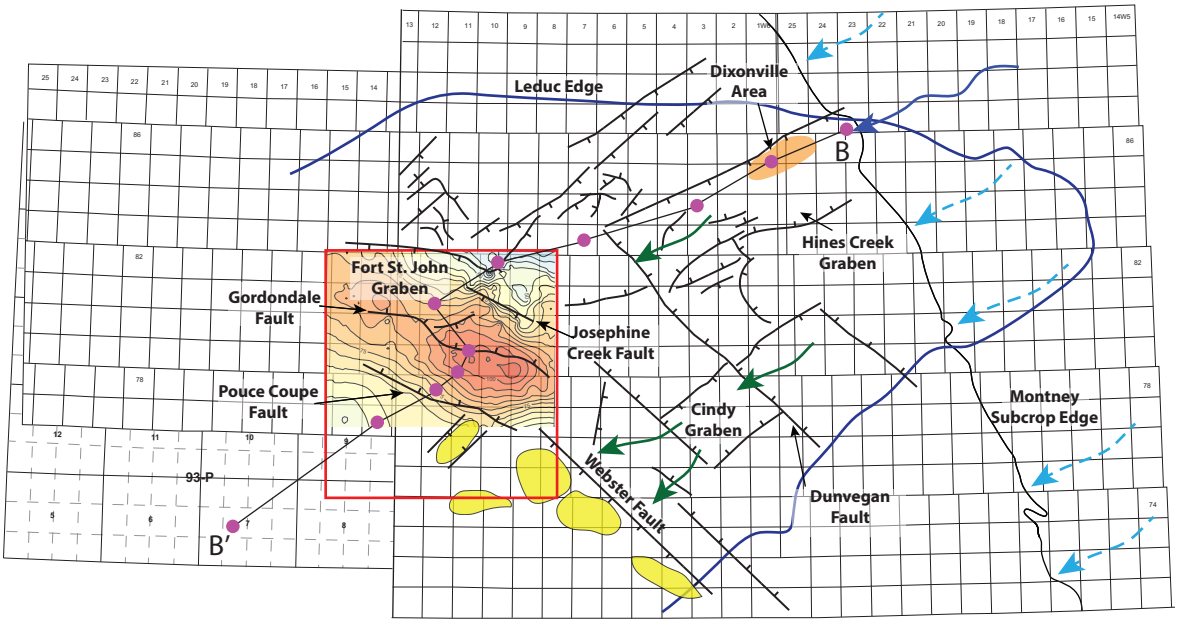

Figure 2.11- Regional map showing the position of the study area (outlined in red) in relation to the relative position of the major structural lineaments in the area and the Upper Devonian Leduc Reef trend. Dark blue arrow represents relative position of perennial deltaic system, dashed light blue lines represent inferred position of ephemeral river systems and green arrows show major sediment conduits in the area throughout the Dienerian-Smithian time. The Dixonville area is outlined in orange and has been interpreted to be deposited by a perennial deltaic system. The yellow outlines the relative position of the major Montney Turbidite Zone deposits. The contour map shows the distribution of the total D1 and D2 thickness; contour interval=5m; zoomed in view of contour map in Fig. 13D. Position of regional cross section A-A' shown on map. Map compiled and modified from Barclay et al, 1990; Mei, 2009; Panek, 2000; Richards et al., 1994; Zonneveld et al, 2010a; Zonneveld et al, 2010b; Zonneveld and Moslow, 2014; and Zonneveld, pers. comm.

Figure 2.12 (Next page)- Regional cross section running from the Montney subcrop edge to west of the study area. Montney is subdivided into three members, in addition the Montney Turbidite Zone, D1 horizon, D1-D2 transition, D2 horizon, and Dixonville Delta are highlighted.

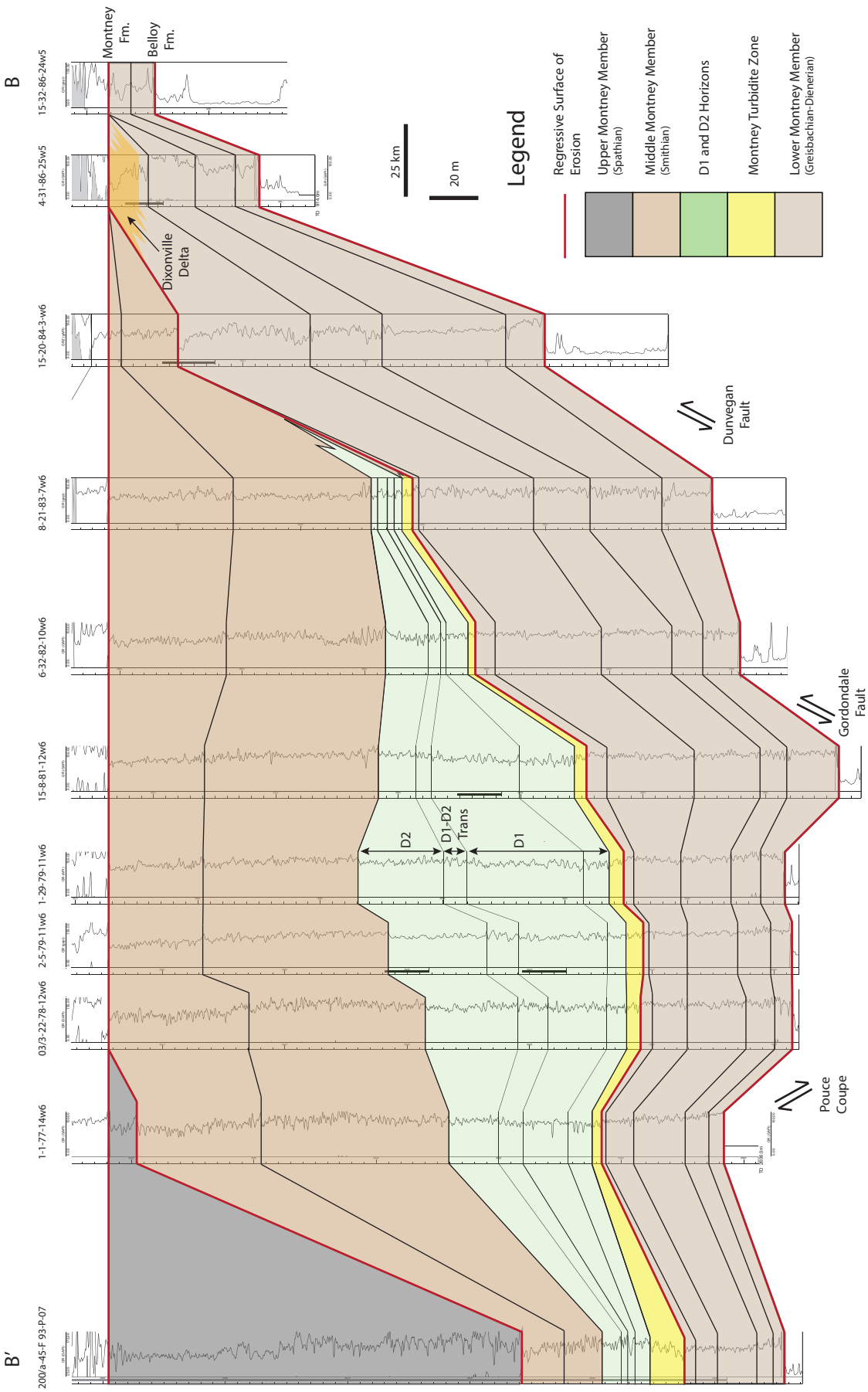
B
B′
15-32-86-24w5
4-31-86-25w5
15-20-84-3-w6
8-21-83-7w6
6-32-82-10w6
15-8-81-12w6
1-29-79-11w6
2-5-79-11w6
03/3-22-78-12w6
1-1-77-14w6
200/a-45-F 93-P-07
Montney Fm.
Belloy Fm.
Dixonville Delta
Dunvegan Fault
Gordondale Fault
Pouce Coupe
D2
D1-D2 Trans
D1
25 km
20 m
Legend
Regressive Surface of Erosion
Upper Montney Member (Spathian)
Middle Montney Member (Smithian)
D1 and D2 Horizons
Montney Turbidite Zone
Lower Montney Member (Griesbachian-Dienerian)

Increased accommodation trapped sand sized grains near the coastline and only silt-sized grains were available for deposition. The turbidity currents were no longer fed by a single point source, and as such main turbidite channels and lobes did not develop. Linear sourced turbidity currents resulted in laterally continuous sheet flow deposits.

A net thickness map of the D1 horizon shows thicknesses were distributed in a roughly linear fashion and thin towards the southwest, agreeing with the interpretation of linear turbidity currents sourced from the northeast (Fig. 2.13A). From the D1 isopach map the major roll that structural lineaments played on sedimentation throughout the deposition of the D1 becomes evident. During deposition of the D1, the Fort St John Graben (FSJG) was a tectonic low, its northern edge defined by the Bear Canyon fault. Directly south of the Josephine Creek Fault the D1 thickness increases markedly suggesting that there was a structural high north of the Josephine Creek Fault that was a major sediment source for linear sourced turbidity currents. Or alternatively, the Josephine Creek Fault was a down-drop block that acted as a major sediment trap. The thickest accumulations of the D1 occur north of the Gordondale Fault, and thicknesses remain fairly large until they markedly thin south of the Pouce Coupe Fault, showing that these two faults defined the southern edge of the FSJG. This relationship is also apparent in the regional cross section B-B' (Fig. 2.12), where the D1 thins significantly on the south side of the Pouce Coupe Fault.

The D1-D2 transition is characterized by the appearance of silty shale beds (Fig. 2.8). Appreciable clay is conspicuously absent from most Montney successions and has only been found in a few locales. These locations (Pedigree-Ring-Border and Dixonville) are interpreted to have been affected by deltas (Zonneveld and Moslow, 2014). The occurrence of clay in the D1-D2 transition suggests there is an active deltaic system proximal to the study area. The Hines

Creek satellite graben is situated approximately 75 km northeast of the study area (Fig. 2.11). Syndepositional movement of high-angle normal faults bounding the Hines Creek Graben provided a topographic low that a perennial river system flowed through and deposited the Dixonville Delta (Fig 2.12; Zonneveld and Moslow, 2014). The Dixonville area is situated near the Montney subcrop edge. As a result, strata coeval to the D1-D2 transition has been eroded away resulting in the erosion of any corresponding deltaic deposits linked to the hyperpycnal flows. It is likely though, that major river systems would have been prone to running through the Hines Creek Graben at times of tectonic reactivation (Davies, 1997; Kendall, 1999).

During deposition of the D1-D2 transition, renewed subsidence in the Hines Creek Graben may have caused a delta lobe to switch back into the area. Hyperpycnal flows were periodically generated, resulting in the transportation and deposition of beds with high amounts of clay. The interbedding of clay-rich beds and siltstone beds demonstrate fluctuations between linear sourced turbidity currents and hyperpycnal flows. A net thickness map of the D1-D2 transition shows that this unit was deposited in a lobate geometry, supporting the interpretation that there is a deltaic influence in the area (Fig. 2.13B). During this period, the main area of sedimentation shifted from north of the Gordondale fault and the thickest accumulations were found in between the Pouce Coupe and Gordondale faults, suggesting that this area was a topographic low during the deposition of the D1-D2 transition.

The Montney D2 horizon is characterized by repeated small-scale fluctuations in base level that cause interbedding of Lithofacies 5 and 7. The resulting deposits are much more lithologically variable than the underlying D1 horizon. The facies associations in the D2 horizon reflect multiple shallowing upwards packages from proximal offshore to the offshore transition zone. Lithofacies 7 is the most proximal of the facies, as shown by the increase in coarse

siltstone and the occurrence of combined flow ripples that mark deposition above storm wave base. The occurrence of interbedded clay rich beds suggests that there was still an active deltaic system in the region, generating periodic hyperpycnal flows. The resulting deposits are once again distributed in a lobate geometry insinuating continued deltaic influence (Fig. 2.13C). The thickest accumulations of the D2 are located between the Pouce Coupe and Gordondale faults, indicating that this area was still a topographic low during D2 deposition. Northeast of the Josephine Creek Fault the D2 thins significantly, suggesting this area was a topographic high that potentially acted as a sediment source for linear sourced turbidity currents.

Reservoir Lithologies

The D1 horizon is currently the main exploration target in the study area. It has high porosities (up to 9%) and produces liquids rich natural gas and oil in some parts of the study area and dry gas towards the southwest part of the study area. Lithofacies 5 is the main reservoir facies in the D1 and D2 horizons based on industry drilling activity. In the present study Lithofacies 5 has been broken into L5a and L5b based on the proportion of coarse-grained siltstone. Although the distinction is subtle in core (Figs. 2.5A,B and 2.8B-D) in thin section it is apparent that L5b (Fig. 2.6C,D) has a higher proportion of coarse-grained siltstone and higher porosity than L5a (Fig. 2.6E,F). Lithofacies 5 rarely contains calcite cement but is partially cemented by dolomite, which allows the rock to retain much of its primary porosity (Fig. 2.6C-F). The lack of cement has also resulted in limited contrast between the coarse-grained and fine- to medium-grained siltstone laminae, resulting in the lithofacie's distinctive dull and homogenous look. The relative homogeneity throughout the facies makes it suitable for completions, as there are few hydraulic fracture barriers throughout this facies.

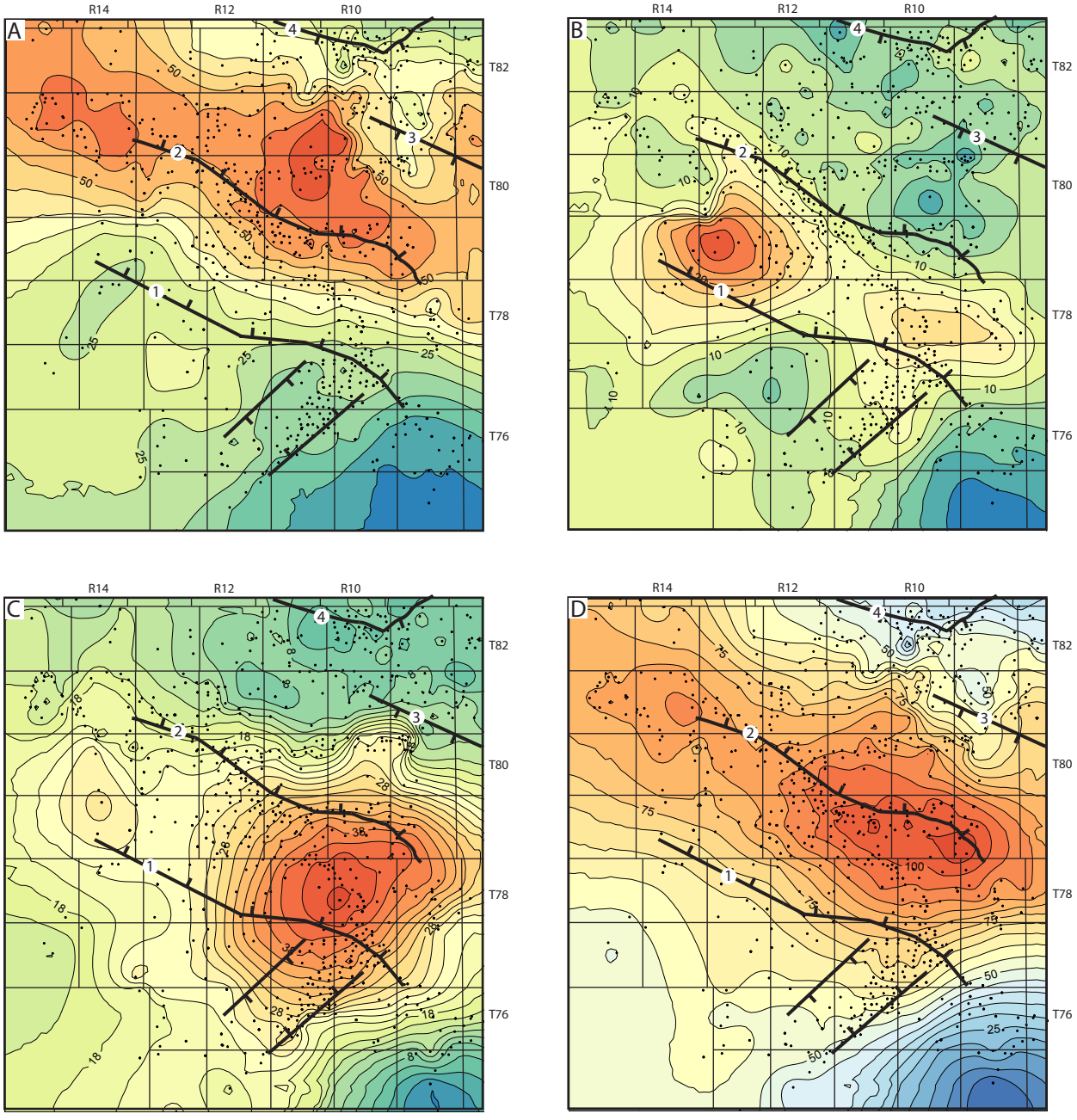

Figure 13- Net thickness distribution for the D1, D1-D2 transition and D2 horizons. Major faults in the study area outlined:1-Pouce Coupe Fault; 2- Gordondale Fault; 3- Josephine Creek Fault; 4- Bear Canyon Fault. **A.** Isopach of D1 horizon, note linear distribution of thickest interval; contour interval= 5m. **B.** Net thickness horizon of D1-D2 transition, deposits are in a lobate geometry; contour interval=2m. **C.** Net thickness isopach of D2 horizon; contour interval 2m. **D.** Total thickness of D1 horizon, D1-D2 transition and D2 horizon combined; contour interval=5m.

Fine to medium bituminous siltstone beds of Lithofacies 8 found in the southwest part of the study area, in both the D1 and D2 horizons, are important drilling targets. Wells producing from these beds are characterized by dry gas, but are often prolific. Thin section analysis shows quartz and feldspar are the dominant grain types, but there are significantly larger amounts of pyrobitumen in this unit compared to the other lithofacies studied. Porosity values in these beds range from 3-5%. Very little intergranular porosity was observed in thin section (Fig.2.6 K,L), suggesting the porosity in this unit comprises mainly micro and nano-porosity, possibly within pyrobitumen as Wood et al. (2013) and Wood (2015) observed in studies of reservoir quality through the Montney tight gas fairway.

The D2 horizon is highly heterogeneous and lithologically complex, with interbedded Lithofacies 5 and 7. Lithofacies 7 is highly cemented by calcite (Fig. 2.6H,I) and has interbedded silty shale. This results in lower reservoir and completions quality. It is thought that Lithofacies 7 had the highest paleo porosity and permeability, which encouraged diagenetic fluid flow through this unit and, as a result, Lithofacies 7 is now highly cemented and a poor reservoir candidate. The D2 horizon comprises multiple shallowing upwards sequences, which occur in a predictable gradually coarsening upwards succession of Lithofacies 5 being overlain by Lithofacies 7 (Fig. 2.10). Four of these cycles were observed, with the occurrence of Lithofacies 5 correlating to abrupt increases in the density porosity log values (Fig. 2.10). The occurrences of Lithofacies 5 in the D2 horizon are thinner (up to 5m) than in the D1 horizon (up to 20m). But multiple occurrences of Lithofacies 5 result in stacked thinner (3-5 m) pay zones. Multiple stacked pay zones make the D2 horizon a viable prospect as exploration continues.

Lithofacies 7 is interpreted to grade laterally into Lithofacies 5 as the distance from the source of the mass wasting event increases. And Lithofacies 5 is interpreted to laterally grade

into Lithofacies 8 as the turbidity current loses energy and sedimentation from suspension is the dominant process. Based on this interpretation it is suggested that the best reservoir quality in the D2 horizon will be located further southwest in the study area. In these more distal locations, instead of Lithofacies 5 being interbedded with Lithofacies 7, Lithofacies 5 will occur interbedded with Lithofacies 8. As a result, the two lithofacies with the highest reservoir quality are interbedded in these locations. As there were no cores in the distal part of the D2 horizon, this hypothesis could not be confirmed but warrants further investigation as development continues.

Conclusions

In the Greater Pouce Coupe Area, the Smithian-aged Middle Montney Member consists of a multicyclic, overall coarsening upwards succession of silty shale, siltstone and very fine-grained sandstone. Eight lithofacies were identified in the study area, representing deposition in the offshore transition to distal offshore areas. Sedimentation in the study area was dominated by turbidity currents, with cyclic fluctuations in sea level and varying deltaic influence causing changes in the coarse siltstone fraction as well as clay content. In contrast to deposits in the Montney Turbidite Zone, these gravity flows did not have a single point source. Instead they were linearly sourced creating sheet flows.

Linear sourced turbidity currents in the proximal offshore area deposited the units with the highest porosity and corresponding best reservoir quality (Lithofacies 5). In the offshore transition area close to the source of the mass wasting events, a higher proportion of coarse-grained siltstone was deposited by linear sourced turbidity currents (Lithofacies 7). These units would have had higher paleo-porosity/permeability, and as a result, diagenetic fluids

preferentially moved through these units leaving them highly cemented and with low preserved porosity. During times when there was an active delta in the area, silty shale beds deposited by hyperpycnal flows were interbedded with siltstone beds (Lithofacies 6). In the distal offshore area, suspension settling was the primary mode of deposition (Lithofacies 8). These deposits were found to have the second best reservoir quality based on porosity, and many prolific dry gas wells have produced from these beds.

The Montney coastline was characterized by rare perennial rivers with common ephemeral / seasonal river systems that only delivered sand and silt to the coast during major storms (Zonneveld and Moslow, 2014). These sudden, often catastrophic, ephemeral fluvial depositional episodes resulted in rapid, albeit short-lived sediment input and, concomitantly, produced over-steepened shoreface profiles (unusual in fine-grained coastal successions). This, coupled with syn-sedimentary tectonics, created an unstable ramp setting prone to mass wasting events. The occurrence of sharp-based, silty shale beds within the D1-D2 transition suggest that there may have been a perennial delta present in the area. The silty shale beds may be relict of hyperpycnal flows from such deltas.

References

Arnott, R.W.C. 2010. Deep-marine sediments and sedimentary systems, in James, N.P., and Dalrymple, R.W., eds., Facies Models 4: St. John's, Newfoundland, Geological Association of Canada, p. 295–322.

Barclay, J.E., Krause, F.F., Campbell, R.I. and Utting, J. 1990. Dynamic casting and growth faulting: Dawson Creek Graben Complex, Carboniferous-Permian Peace River Embayment, western Canada. *In:* Geology of the Peace River Arch. S.C. O' Connell and J.S. Bell (eds.). Bulletin of Canadian Petroleum Geology, v. 38, p. 115-145.

Beranek, L.P. and Mortensen, J.K. 2006. A Triassic link between Yukon-Tanana and North America; new detrital zircon age, geochemical, and biostrati- graphic data. Geological Society of America, Cordilleran Section, Abstracts with Program, v. 38, p. 5–6.

Beranek, L.P. and Mortensen, J.K. 2007. Latest Permian to Middle Triassic accretions of the Yukon-Tanana, Stikine and Quesnel terranes to North America; new detrital zircon age data from Triassic rocks in Yukon. Geological Society of America, Cordilleran Section, Abstracts with Program, v. 39, p. 69.

Bond, D.P.G., Wignall, P.B. 2010. Pyrite framboid study of marine Permian–Triassic boundary sections: a complex anoxic event and its relationship to contemporaneous mass extinction. Geolical Society of America Bulletin, v. 122, p. 1265–1279.

Botes, A., Henderson, J., Nakale, T., Nantanga, K., Schachtschneider, K., & Seely, M. 2003. Ephemeral rivers and their development: testing an approach to basin management committees on the Kuiseb River, Namibia. Physics and Chemistry of the Earth, v. 28, p. 853-858.

Bottjer, D.J. and Droser, M.L. 1991. Ichnofabric and siliciclastic depositional systems: integration for sequence stratigraphic analysis. American Association of Petroleum Geology Bulletin v. 75, p. 545.

Davies, G.R. 1997. The Triassic of the Western Canada Sedimentary Basin: tectonic and stratigraphic framework, Palaeogeography, Paleoclimate and biota. In: Triassic of the Western Canada Sedimentary

Basin. T.F. Moslow and J. Wittenberg (eds.). Bulletin of Canadian Petroleum Geology, v. 45, p. 434–460.

Davies, G.R., Hume, D. 2016. Lowstand / Slope-Onlap Wedges In The Montney: Stratigraphic And Sequence Framework, Reservoir Significance (Oral Presentation). GeoConvention 2016: May 7 – 11 2016, Calgary, AB. Available from http://www.geoconvention.com/uploads/2016abstracts/224_GC2016_Lowstand_Slope_Onlap_Wedges_in_the_Montney.pdf

Davies, G.R., Moslow, T.F. and Sherwin, M.D. 1997. The lower Triassic Montney Formation, west-central Alberta. In: Triassic of the Western Canada Sedimentary Basin. T.F. Moslow and J. Wittenberg (eds.). Bulletin of Canadian Petroleum Geology, v. 45, p. 474–505.

Dixon, J. 2000. Regional lithostratigraphic units in the Triassic Montney Formation of Western Canada. Bulletin of Canadian Petroleum Geology, v. 48, p. 80–83.

Drzewiecki, P.A. and Simo, J.A.T. 1997. Carbonate platform drowning and oceanic anoxic events on a mid-Cretaceous carbonate platform, south-central Pyrenees, Spain. Journal of Sedimentary Research, v. 67, p. 698-714.

Dzulynski, S. and Kotlarczyk, J. 1962. On load-casted ripples. Ann. Soc. Géol. Pologne v. 32, p. 148–159.

Ekdale, A. A. 1985. Paleoecology of the marine endobenthos. Palaeogeography, Palaeoclimatology, Palaeoecology, v. 50, p. 63-81.

Ekdale, A. A., & Mason, T. R. 1988. Characteristic trace-fossil associations in oxygen-poor sedimentary environments. Geology, v. 16, p. 720-723.

Erwin, D.H. 2006. Extinction: How life on earth nearly ended 250 million years ago. Princeton University Press, Princeton, New Jersey, 296 p.

Ferri, F. and Zonneveld, J-P. 2008. Were Triassic rocks of the Western Canada Sedimentary Basin deposited in a foreland? Canadian Society of Petroleum Geologists Reservoir, v. 35, p. 12–14.

Föllmi, K. B., & Grimm, K. A. 1990. Doomed pioneers: Gravity-flow deposition and bioturbation in marine oxygen-deficient environments. Geology, v. 18, p. 1069-1072.

Hayes, L.E., Beatty, T.W., Henderson, C.M., Love, G.D., and Summons, R.E. 2007. Evidence For Photic Zone Euxinia Through The End-Permian Mass Extinction In The Panthalassic Ocean (Peace River Basin, Western Canada). Palaeoworld, v. 16, p. 39-50. Jahnert, R., De Paula, O., Collins, L., Strobach, E., & Pevzner, R. 2012. Evolution of a coquina barrier in Shark Bay, Australia by GPR imaging: Architecture of a Holocene reservoir analog. Sedimentary Geology, v.281, p. 59-74.

Kelts, K., and Mckenzie, J.A., 1984, A Comparison Of Anoxic Dolomite From Deep-Sea Sediments: Quaternary Gulf Of California And Messinian Tripoli Formation Of Sicily, in Garrison, R.E., Kastner, M., and Zenger, D.H., eds., Dolomites of the Monterey Formation and Other OrganicRich Units: SEPM, Pacific Section, p. 19–28

Kendall, D.R. 1999. Sedimentology and stratigraphy of the Lower Triassic Montney Formation, Peace River Basin, subsurface of northwestern Alberta. . Unpublished M.Sc. Thesis, University of Calgary, Calgary, Alberta, 394 p.

Krapf, C. B., Stollhofen, H., & Stanistreet, I. G. 2003. Contrasting Styles Of Ephemeral River Systems And Their Interaction With Dunes Of The Skeleton Coast Erg (Namibia). Quaternary International, v. 104, p. 41-52.

Lumsden, D. N. 2003. Organodiagenetic Dolomite On A Deep Subtidal Shelf, Fort Payne Formation (Mississippian), Tennessee, U.S.A. In Ahr, W. M.; Harris, P. M.; Morgan, W. A.; and Somerville, I. D., eds. SEPM Special Publication 78: Permo-Carboniferous Carbonate Platforms and Reefs, p. 323–332.

MacEachern, J.A., Bann, K.L., Pemberton, S.G., And Gingras, M.K. 2007. The Ichnofacies Paradigm: High-Resolution Paleoenvironmental Interpretation Of The Rock Record, In MacEachern, J.A., Bann, K.L., Gingras, M.K., and Pemberton, S.G., eds., Applied Ichnology: SEPM, Short Course Notes 52, p. 27–64.

Martinsen, O. J., Lien, T. & Jackson, C. 2005. Turbidite systems offshore Norway. In: Dore, A. G. & Vining, B. A. (eds) Petroleum Geology: North-West Europe and Global Perspectives—Proceedings of the 6th

Petroleum Geology Conference, 1147–1164. q Petroleum Geology Conferences Ltd. Published by the Geological Society, London.

Mazzullo, S.J., 2000, Organogenic Dolomitization In Peritidal To Deep-Sea Sediments: Journal of Sedimentary Research, v. 70, p. 10–23.

Mei, S. 2009. New insights on faults in the Peace River arch region, northwest Alberta, based on existing well-log data and refined trend surface analysis, Can. J. Earth Sci. 46, no. 1, 41–65, doi: 10.1139/ E09-006

Moslow, T.F. 2000. Reservoir architecture of a fine-grained turbidite system: Lower Triassic Montney Formation, Western Canada Sedimentary Basin. In: Deep-water Reservoirs of the World, Conference Proceedings, Gulf Coast SEPM. P. Weimer, R.M. Slatt, J. Coleman, N.C. Rosen, H. Nelson, A.H. Bouma, M.J. Styzen, and D.T. Lawrence (eds.). p. 686–713.

Moslow, T.F. and Davies, G.R. 1997. Turbidite reservoir facies in the Lower Montney Formation, west-central Alberta. *In:* Triassic of the Western Canada Sedimentary Basin. T.F. Moslow and J. Wittenberg (eds.), Bulletin of Canadian Petroleum Geology v. 45, p. 507-536.

Myrow, P. M., Fischer, W., & Goodge, J. W. (2002). Wave-modified turbidites: combined-flow shoreline and shelf deposits, Cambrian, Antarctica. Journal of Sedimentary research, v. *72*, p. 641-656.

Mulder, T., and Alexander, J. 2001. The physical character of subaqueous sedimentary density currents and their deposits. Sedimentology, v. 48, p. 269–299.

Mutter, R.J. and Neuman, A.G. 2006. An enigmatic chondrichthyan with Paleozoic affinities from the Lower Triassic of Western Canada. Acta Palaeontologica Polonica, v. 51, p. 271–282.

Mutti, E. 1977. Distinctive thin-bedded turbidite facies and related depositional environments in the Eocene Hecho Group (South central Pyrenees, Spain). Sedimentology, v. 24, p. 107-131.

Nakajima, T. 2006. Hyperpycnites deposited 700 km away from river mouths in the Central Japan Sea. Journal of Sedimentary Research, v. 76, p. 60–73.

NASA. 2008. Phytoplankton Bloom off Namibia. Retrieved from: https://www.nasa.gov/multimedia/imagegallery/image_feature_975.html

Nickling, W. G., & Neuman, C. M. 2009. Aeolian sediment transport. In Geomorphology of desert environments. p. 517-555. Springer Netherlands.

Pemberton, S. G., and MacEachern, J. A. 1997. The ichnological signature of storm deposits: the use of trace fossils in event stratigraphy. Paleontological Events: Columbia University Press, New York, 73-109.

Pemberton, S.G., Mac Eachern, J.A., Ranger, M.J., 1992. Ichnology and event stratigraphy: the use of trace fossils in recognizing tempestites. In: Pemberton, S.G. (Ed.), Applications of Ichnology to Petroleum Exploration, a Core Workshop. Soc. Econ. Paleontol. Mineral., Core Workshop 17, p. 85–117.

Pisciotto, K.A., 1981, Review of secondary carbonates in the Monterey Formation, California, in Garrison, R.E., Kastner, M., and Zenger, D.H., eds., Dolomites of the Monterey Formation and Other OrganicRich Units: SEPM, Pacific Section, p. 119–140.

Playter, T. L. 2013. Petrographic and X-ray Microtomographic Analysis of the Upper Montney Formation, Northeastern British Columbia, Canada. Unpublished M.Sc. Thesis, University of Alberta, Canada. 113 p.

Posamentier, H. W., & Allen, G. P. 1993. Variability of the sequence stratigraphic model: effects of local basin factors. Sedimentary geology, v. 86, p. 91-109.

Raup, D.M. 1979. Size of the Permo-Triassic bottleneck and its evolutionary implications. Science, v. 206, p. 217-218.

Reading, H.G., and Richards, M. 1994. Turbidite systems in deep-water basin margins classified by grain size and feeder system. American Association of Petroleum Geologists Bulletin, v. 78, p. 792–822.

Seilacher, A. 1969. Fault-graded beds interpreted as seismites. Sedimentology, v. 13, p.155-159.

Reineck, H. E. and Singh, I. B. 1972. Genesis Of Laminated Sand And Graded Rhythmites In Storm-Sand Layers Of Shelf Mud. Sedimentology, v. 18, p.123-128.

Richards, B.C., Barclay, J.E., Bryan, D., Hartling, A., Henderson, C.M. and Hinds, R.C.,1994, Carboniferous strata of the Western Canada Sedimentary Basin; in Geological Atlas of the Western Canada Sedimentary Basin, G.D. Mossop and I. Shetsen (comp.), Canadian Society of Petroleum Geologists and Alberta Research Council, Special Report 4, 221–250

Seilacher, A. and Hemleben, C. 1966. Beiträge zur sedimentation und fossil-fürung des Hunsrückschiefers 14. Spurenfauna und Bildungstiefe der Hunsrückschiefer (Unterdevon). Notizblatt des Hessichen Landesamtes fur Bodenforschung zür Wiesbaden, v. 94, p. 40–53.

Sellwood, B. W. and Valdes, P.J. 2006. Mesozoic climates: General circulation models and the rock record. Sedimentary Geology, v. 190, p. 269-287.

Sholkovitz, E.R. and Soutar, A., 1975. Changes in the composition of the bottom water of Santa Barbara basin: effect of turbidity currents. Deep-Sea Research, v. 22, p. 13-22.

Smith, R.M,H., Mason, T.R. and Ward, J.D., 1993. Flash-flood sediments and ichnofacies of the Late Pleistocene Homeb Silts, Kuiseb River, Namibia. In: C.R. Fielding (Editor), Current Research in Fluvial Sedimentology. Sedimentary Geology, v. 85, p. 579-599.

Stollhofen, H., Stanistreet, I. G., von Hagke, C. and Nguno, A. 2014. Pliocene–Pleistocene climate change, sea level and uplift history recorded by the Horingbaai fan-delta, NW Namibia. Sedimentary Geology, v. 309, p. 15-32.

Svendsen, J., Stollhofen, H., Krapf, C. B., & Stanistreet, I. G. 2003. Mass and hyperconcentrated flow deposits record dune damming and catastrophic breakthrough of ephemeral rivers, Skeleton Coast Erg, Namibia. Sedimentary Geology, v. 160, p. 7-31.

Van Loon, A.J. and Wiggers, A.J. 1976. Primary and secondary synsedimentary structures in the lagoonal Almere Member (Groningen Formation, the Netherlands). Sedimentary Geology, v. 16, p. 89–97.

Velbel, M.A. 1990. Influence of temperature and mineral surface characteristics on feldspar weathering rates in natural and artificial systems: a first approximation. Water resources research 26: 3049-3053

Walker, R.G. 1967. Turbidite sedimentary structures and their relationship to proximal and distal depositional environments. Journal of Sedimentary Research, v. 37, p. 25-43.

Walker, R.G. 1985. Mudstones and thin-bedded turbidites associated with the Upper Cretaceous Wheeler Gorge conglomerates, California: a possible channel–levee complex. Journal of Sedimentary Research, v. 55, p. 279–290.

Wentworth, C.K. 1922. A scale of grade and class terms for clastic sediments: Journal of Geology, v. 30, p. 377–392.

Wetzel A. 2002. Modern Nereites in the South China Sea – Ecological association with redox conditions in the sediment. Palaios v. 17, p.507–515.

Wetzel, A., and Uchman, A. 1998. Deep-sea benthic food content recorded by ichnofabrics: A conceptual model based on observations from Paleogene flysch, Carpathians, Poland. Palaios, v. 13, p. 533–546.

Wilkin, R.T., Barnes, H.L., and Brantley, S.L. 1996. The size distribution of framboidal pyrite in modern sediments: An indicator of redox conditions: Geochimica et Cosmochimica Acta, v. 60, p. 3897–3912.

Windom, H.L. and Chamberlain, C.F. 1978. Dust-storm transport of sediments to the north Atlantic Ocean. Journal of Sedimentary Petrology, v. 48, p. 385–388.

Wood, J. M., Sanei, H., Curtis, M. E., & Clarkson, C. R. 2015. Solid bitumen as a determinant of reservoir quality in an unconventional tight gas siltstone play. International Journal of Coal Geology, v. 150, p. 287-295.

Woods, A.D., Bottjer, D.J. and Corsetti, F.A. 2007. Calcium carbonate seafloor precipitates from the outer shelf to slope facies of the Lower Triassic (Smithian-Spathian) Union Wash Formation, California, USA; sedimentology and palaeobiological significance. Palaeogeography, Palaeoclimatology, Palaeoecology, v. 252, p. 281-290.

Udden, J.A., 1914, Mechanical composition of clastic sediments: Geological Society of America, Bulletin, v. 25, p. 655–744.

Zaragosi, S., Le Suave, R., Bourillet, J. F., Auffret, G., Faugeres, J. C., Pujol, C., & Garlan, T. 2001. The deep-sea Armorican depositional system (Bay of Biscay), a multiple source, ramp model. Geo-Marine Letters, v. 20, p. 219-232.

Zonneveld, J. P., Gingras, M. K., & Beatty, T. W. 2010a. Diverse ichnofossil assemblages following the PT mass extinction, Lower Triassic, Alberta and British Columbia, Canada: evidence for shallow marine refugia on the northwestern coast of Pangaea. Palaios, v. 25, p. 368-392.

Zonneveld, J. P., MacNaughton, R. B., Utting, J., Beatty, T. W., Pemberton, S. G., & Henderson, C. M. 2010b. Sedimentology and ichnology of the Lower Triassic Montney Formation in the Pedigree-Ring/Border-Kahntah River area, northwestern Alberta and northeastern British Columbia. Bulletin of Canadian Petroleum Geology, v. 58, p. 115-140.

Zonneveld, J. P., Moslow, T.F. 2014. Perennial River Deltas of the Montney Formation: Alberta and British Columbia Subcrop Edge (Oral Presentation). GeoConvention 2014: May 12 – 16 2014, Calgary, AB. Available from http://cseg.ca/assets/files/resources/abstracts/2014/core/490_GC2014_Perennial_River_Deltas_of_the_Montney_Fm.pdf

Zonneveld, J. P., Moslow, T.F. 2017. Depositional history and Palaeogeographic evolution of the Montney in the Western Canada Sedimentary Basin (Oral Presentation). GeoConvention 2017: May 15 – 19, 2017, Calgary, AB. Available from http://www.geoconvention.com/uploads/2017abstracts/312_GC2017_Depositional_history_and_Palaeogeographic_evolution_Montney_WCSB.pdf

CHAPTER 3: CHEMOSTRATIGRAPHY OF THE MIDDLE MONTNEY D1 AND D2 HORIZONS IN THE GREATER POUCE-COUPE AREA, ALBERTA-BRITISH COLUMBIA

Introduction

Over the past decade the Montney Formation has evolved into western Canada's premier unconventional exploration play, containing an estimated 447 trillion cubic feet of natural gas in addition to natural gas liquids and condensate (Faraj et al., 2002; NEB Report, 2013). Historically, Montney exploration was focused on conventional reservoir intervals such as the turbidite interval and clastic and bioclastic shoreface intervals (Davies et al., 1997; Zonneveld et al., 2010). Although low porosity and low permeability siltstone intervals make up the largest portion of the Montney, until recently they were overlooked due to an inability to economically access the resource. With the advent of horizontal drilling and multistage hydraulic fracturing these intervals have become highly prospective (NEB Report, 2013). Restricted grain size and perceived macro-scale homogeneity have rendered traditional methods of reservoir characterization and stratigraphic correlation ineffective. In order for a mudrock play to be successful it is necessary to have a robust understanding of the stratigraphy to delineate areas with superior reservoir and completions quality. In the last decade inorganic whole-rock geochemistry has become a valuable tool, enabling stratigraphic correlations in fine-grained successions.

Chemostratigraphy relies upon recognizing changes in elemental concentrations through time and using those changes to model fluctuations in geological events such as paleoclimate and provenence (Ratcliffe et al., 2012). In the past geochemical datasets were used in fluvial successions where the lack of fossils precludes the use of more traditional stratigraphic correlation techniques such as biostratigraphy (Pearce et al., 2005; Ratcliffe, et al., 2010; Wright et al., 2010). Whole rock-geochemical datasets were also used to elucidate paleoredox conditions during oceanic anoxic events in organic rich mudstones (Jenkyns, 2010; Tribovillard et al., 2006). More recently there have been many studies applying these techniques to shale gas plays (Wright et al., 2010; Sano et al., 2013; Nance and Rowe, 2015). In most studies geochemical data is obtained from X-Ray Diffraction (XRD) and inductively coupled plasma mass spectrometry (ICP-MS), these destructive techniques require numerous closely spaced samples which becomes very expensive. Portable energy-dispersive X-ray fluorescence (ED-XRF) spectroscopy is a non-destructive method that has made it practical to acquire elemental measurements at desired scales, down to the sub centimeter scale (Nance and Rowe, 2015; Rowe et al. 2012).

This study uses ED-XRF measurements of three core to compliment detailed core descriptions. 18 samples were analyzed by ICP-MS to allow for the quantification of the qualitative XRF data. 6 samples were analyzed with XRD to allow for elemental concentrations to be related to mineral abundances. In the previous chapter detailed sedimentary lithofacies were identified and were interpreted to represent deposition in the proximal offshore to offshore transition area. The D1-D2 transition is marked by the conspicuous occurrence of silty shale beds, which were interpreted to mark the influence of a major deltaic system in the area. The clays could have also been sourced from an approaching volcanic island arc complex to the west,

at the onset of terrane accretion in the Early Triassic although this seems less likely. Elemental geochemistry can help refine the interpretation by showing the presence or absence of an igneous signature and changes in sediment source areas (Plank and Langmuir, 1998; Bracciali et al., 2007; Playter et al. 2017). The purpose of this study is threefold: firstly to use geochemical measurements as proxies for environmental conditions to compliment core based observations; secondly to determine the source of the clay in the D1-D2 transition; and thirdly to use as an aid in regional stratigraphic correlations and confirm sequence stratigraphic interpretations proposed in the first chapter of this thesis.

Geologic Setting

The Montney Formation is a complex accumulation of shale, siltstone and sandstone with bioclastic packstone and grainstone occurring in some areas (Zonneveld et al., 2011). Deposition took place in an arcuate shaped extensional basin along the northwestern margin of Pangaea (Davies, 1997). The thickest accumulations occur in the area of the collapsed Peace River Arch (Davies, 1997). Tectonic subsidence resulted in the formation of a system of grabens referred to as the Dawson Creek Graben Complex, which consisted of the primary Fort St John Graben and the satellite Hines Creek and Cindy grabens (Mei, 2009; Barclay, 1990). It was originally thought that the northwestern margin of Pangea was tectonically stable and inactive during this time (Davies, 1997; Moslow, 2000). However, recent work has suggested that terrane collisions on the western margin of North America may have occurred as early as the Early to Middle Triassic (Beranek and Mortensen, 2006; 2007; Ferri and Zonneveld, 2008).

During the Early Triassic western Canada was situated in a mid-latitudinal setting and was characterized by arid conditions with dominant northeast trade winds (Davies, 1997). The aridity of the region ,combined with exceptionally long sediment transport distances, resulted in dominantly fine-grained clastic deposition throughout all environments. Consequently, Montney depositional environments are not easily segregated on the basis of grain size alone (Zonneveld et al., 2011). Ephemeral fluvial transport is likely to be the dominant method of silt and sand delivery to the coast (Zonneveld et al., 2010), although aeolian input contributed a portion of the finer grained component. With the Montney coastline likely being characterized by few perennial rivers with abundant seasonal river systems that would only deliver sand and silt to the coast during major storms (Zonneveld et al., 2010). The lack of time sediments spent in subaqueous submersion in fluvial feeder channels prevented significant feldspar hydrolysis and is reflected by the lack of clay minerals observed in the Montney Formation. In two areas, the Pedigree-Ring-Border and the Dixonville Area, significant amounts of clay have been reported (Zonneveld and Moslow, 2014). These areas were interpreted to have accumulated under the influence of rare perennial deltas (Zonneveld and Moslow, 2014).

Study Area and Methods

This investigation focuses on the Middle Montney D1 and D2 horizons in the subsurface between Townships 75 to 82 and Ranges 10W6 to 15W6 (Fig. 1). The Montney D1 and D2 horizons directly overlie the Montney Turbidite interval and although stratigraphically equivalent successions are dry in surrounding areas, this area is characterized by liquids rich natural gas. There are 491 wells that have produced from the D1 horizon, whereas only 4 wells have produced from the D2 horizon. Thirty-one wells have been cored in the D1 and D2 horizons,

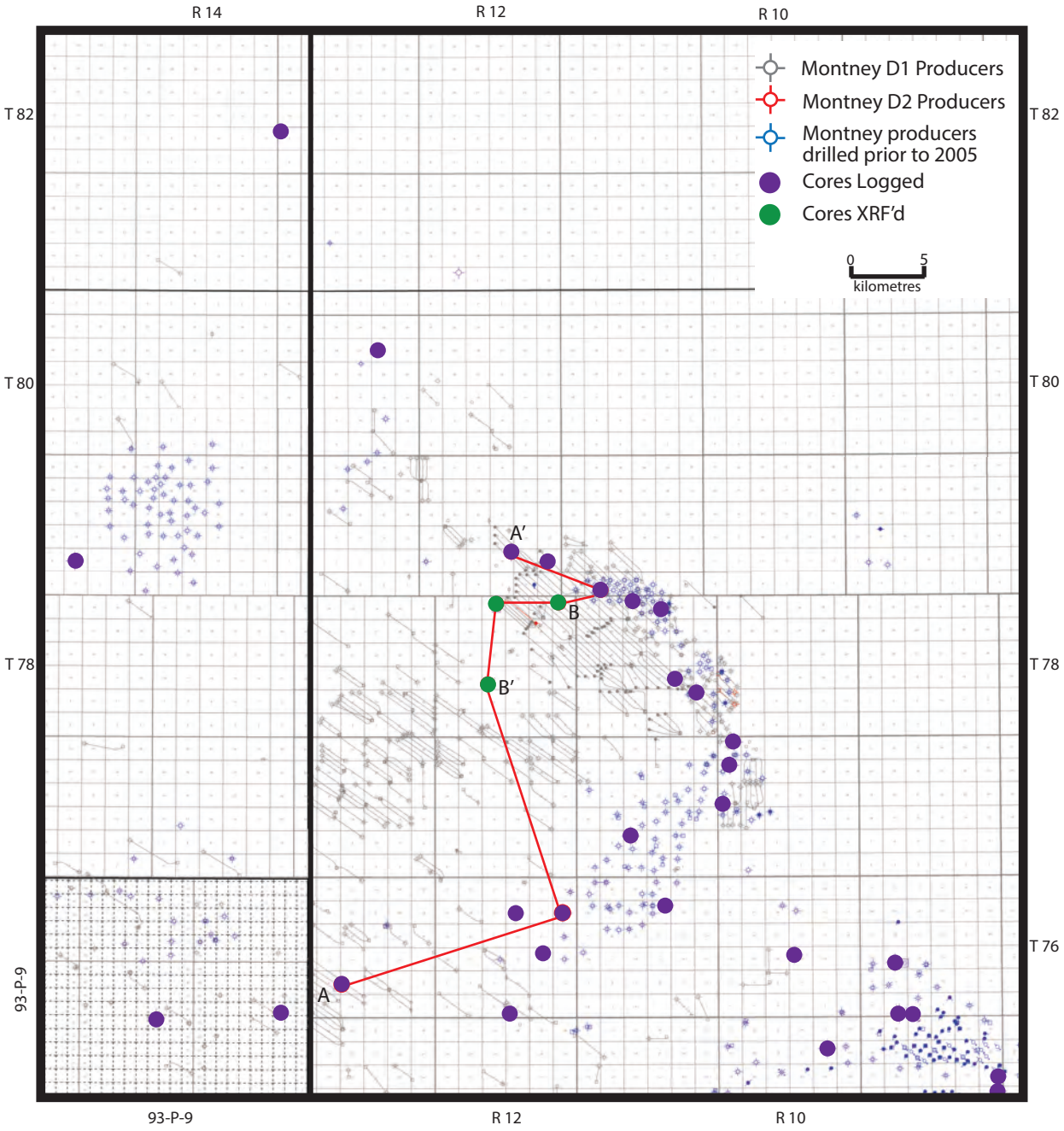

Figure 3.1- Location of wells in the study area. The three cores that were XRF'd for this study are marked in green. Location of cross sections A-A' and B-B' shown.

based on core length and availability three cores were selected for XRF measurements to acquire elemental data.

Sample spacing varied between approximately 1 m for 4-16-78-12w6 and approximately 0.5 m for 14-36-78-12w6 and 10-33-78-12w6. XRF analysis was done on 402 samples using a Thermo Scientific NITON XL3t 900 ED-XRF analyzer at the Alberta Geological Survey. A pressurized Helium canister was connected to the XRF machine to create an environment where lighter elements can be detected. Each sample was scanned for 180 seconds, to obtain readings for 40 elements (Ce, Ba, Te, Sb, Sn, Cd, Pd, Ag, Mo, Nb, Th, Zr, Y, Sr, U, Rb, Bi, As, Se, Au, Pb, Ge, W, Zn, Cu, Ni, Co, Fe, Mn, Cr, V, Ti, Ca, K, Al, P, Si, Cl, S, Mg). Accuracy and precision errors are element dependent. The following standards were each measured multiple times SiO2, SDO1, SGR1 to determine precision errors. The accuracy error was 19.7% and the precision error was 21.0%.

ICP methods

XRF methods require calibration of the XRF data with standards of known concentration, for this reason 10 samples from 14-36-78-12w6 and 6 samples from 10-33-78-12w6 were analyzed by inductively coupled plasma mass spectrometry (ICP-MS) and inductively coupled plasma optical emission spectrometry (ICP-OES). ICP-MS and ICP-OES analyses for the 14-36-78-12w6 core were done at Chemostrat laboratories in Houston, Tx and for the 10-33-78-12w6 core at Bureau Veritas Mineral Lab in Vancouver, BC. Both labs are accredited to ISO 17025:2005 (equivalent to ISO 9000). Following procedures outlined in Hildred *et al.* (2010), samples were cleaned using water and solvent to remove surface contamination. Subsequently, samples were pulverized using an Agate mortar and subjected to a Li-metaborate fusion procedure (Jarvis and Jarvis, 1992). Major elements analyzed for include: SiO_2, TiO_2, Al_2O_3,

Fe_2O_3, MgO, MnO, CaO, Na_2O, K_2O, and P_2O_5. Data was also collected for 25 trace elements (Ba, Be, Co, Cr, Cs, Cu, Ga, Hf, Mo, Nb, Ni, Pb, Rb, Sc, Sn, Sr, Ta, Tl, Th, U, V, W, Y, Zn, and Zr) and 14 rare earth elements (REE: La, Ce, Pr, Nd, Sm, Eu, Gd, Tb, Ho, Dy, Er, Tm, Yb, and Lu). Major-element data and high-abundance trace elements (such as Cr, Sc, Sr, Zn, and Zr) were determined using ICP-OES. Precision error, measured by running select samples in triplicate, associated with ICP-OES for the major-element data is 2%; error associated with high abundance trace elements is approximately 3%. Low-abundance trace element data was collected using an ICP-MS, with a precision error of 5%. The accuracy, measured by use of an internal standard, of major element analysis is ±1%. Additionally, in order to assess uncertainty values, 11 batches of five certified reference materials were analyzed in duplicate. The associated two-sigma uncertainty is 5-7% for major elements and 7-12% for trace elements. Trace element accuracy ranges from ± 3 to 7ppm, decreasing with higher abundance.

XRD methods

Six samples from 14-36-78-12w6 were analyzed by XRD to ascertain mineralogical controls on elemental compositions. XRD analysis was performed at the University of Greenwich, UK, using a Bruker AXS D8 Advance Diffractometer, and Co radiation at 30 kV and 30 mA to ascertain mineralogical controls on elemental composition. Scans were taken stepwise at 0.02° intervals, with a step time of 0.2s, and a 2Θ range from 3-70°. Spectral interpretations were made using PDF2/PDF4 powder diffraction databases issued by the International Center for Diffraction Data (ICDD), and DiffracPlus Eva software, quantification of mineral phases was via peak fitting using the RockJock software package. The detection limit is 0.5-2% (dependent on crystallinity).

XRF-ICP calibration

XRF and ICP data from the same depths were plotted against each other for each element (Figure 2). Correlation coefficients(R-squared values) were obtained, values above 0.7 showed high positive correlations and were sufficient to be used. The equation of the line in the scatterplots is the calibration factor, and that equation is used for each XRF measurement to calibrate the data. If R-squared values were <0.7 for an element in one well but >0.7 for that element in the other well the calibration factor from the well with a higher R-squared value was used. As no ICP data was obtained for 4-16-78-12w6 core (could not destroy any of the core) calibration factors from 10-33-78-12w6 were used. After calibrating the data only elements with high correlation coefficients were used in the rest of the study. The remaining elements that are used for the study are: SiO_2, TiO_2, Al_2O_3, Fe_2O_3, MgO, MnO, CaO, K_2O, Ba, Cr, Sr, Zn, Zr, V, S, Nb, Y, Rb, Mo.

Sedimentology/Stratigraphy

Detailed core analysis of thirty-one core within the D1 and D2 horizons resulted in the identification of eight lithofacies. These lithofacies are summarized in table 1, and are explained in great detail in chapter 1 of this thesis, as a result they will not be discussed in much detail. During deposition of the Montney D1 and D2 horizons the Pouce Coupe area was situated in a distal offshore to offshore transition zone. Throughout this period the dominant mechanism for sedimentation was subaqueous density flows. The Montney coast is interpreted to have been extremely arid, composed of numerous ephemeral rivers that only delivered sediment to the

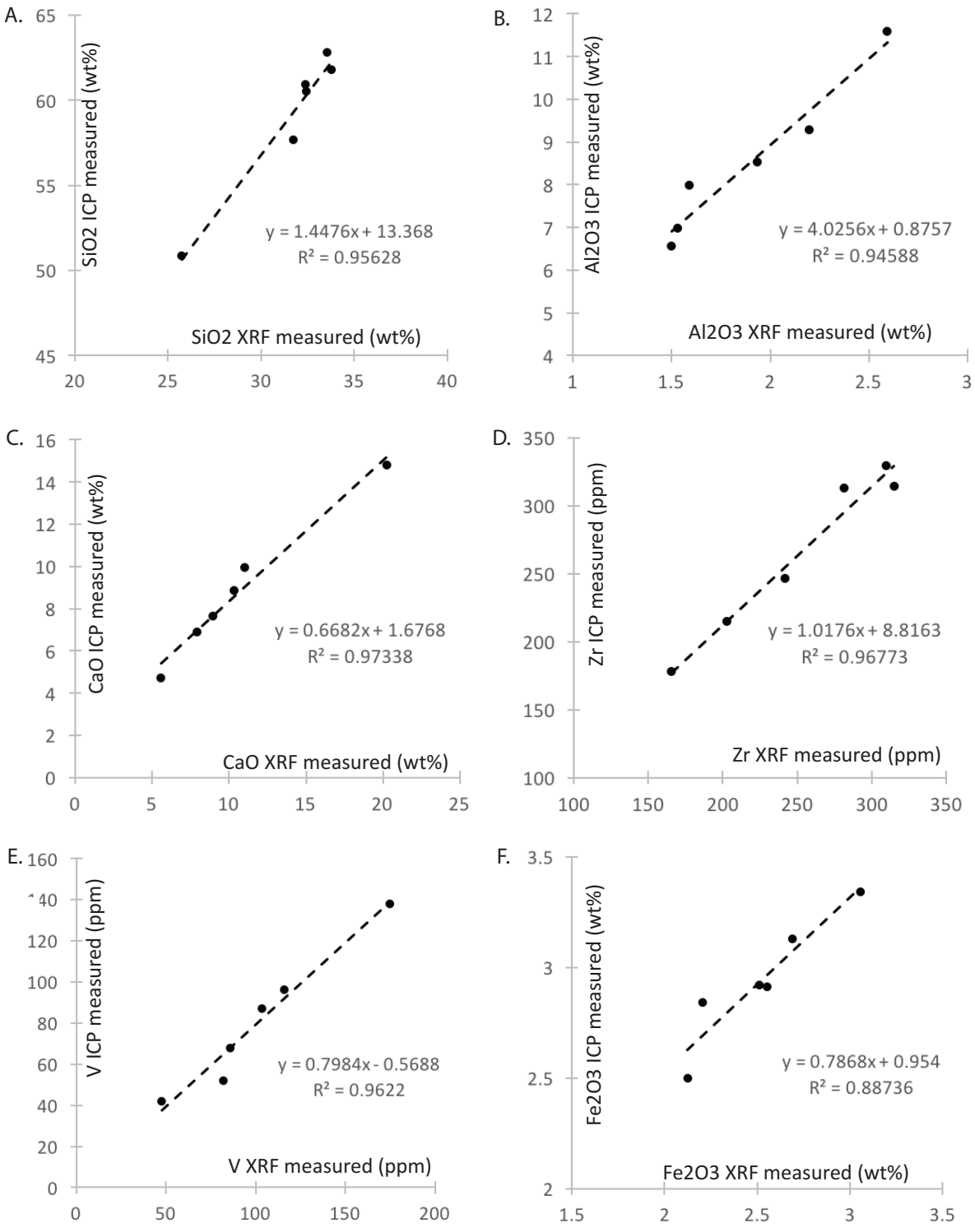

Figure 3.2- Comparison of ED-XRF measurements and ICP-MS or ICP-OES measurements for selected elements. The correlation coefficient and the equation of the line which was used as the correlation factor are listed.

Lithofacies	Descriptions	Interpretations
1 Interbedded parallel laminated and burrowed siltstones	•Planar laminated fine siltstone interbedded with highly bioturbated coarse siltstone beds •Carbonaceous debris found throughout •Ammonoid impressions and Ganoid fish scales found on bedding planes •Thin (<5cm) coarse siltstone interbeds have been highly bioturbated (BI-6) traces include *phycosiphon, skolithos and teichichnus*.	•Deposited in a distal ramp/ offshore position •Coarser beds are deposited by turbidity flows •Burrowed beds represent doomed pioneer assembledge
2 Interbedded sandstone and siltstone with abundant soft sediment deformation	•Interbedded very-fine sandstone, siltstone and shale. •Beds commonly erosively based with phosphatic grains and rip up clasts at base •Abundant soft sediment deformation, dewatering structures, climbing ripples, and planar laminations •Well developed Bouma Sequences in some cores. •No bioturbation observed	•Deposited by point-sourced turbidity flows •Major accumulations controlled by syn-sedimentary tectonism •Thick accumulations are not found throughout study area indicating inter channel or channel levee deposition
3 *Claria* Shell Beds	•Finely laminated fine-coarse siltstone with low relief planar wavy bedding •Abundant disarticulated and fragmented small (<3mm long) dolomitized Claraia shells oriented roughly parallel to bedding	•Following turbidite deposition the ensuing transgression caused erosion and redeposition of fragmented Claraia shells from the further up-dip Coquinal Dolomite Member •Deposited as transgressive lag
4 Massive Brown Dolostone	•Massive brown finely crystaline dolostone •Abundant small (<5 micron) pyrite framboids •Often has sub-vertical calcite filled fractures cutting through the beds.	•Deposited in distal ramp/offshore position •Deposited when sea level was at its highest, there was no sediment input into this part of the basin and anoxic conditions developed
5 WavyPlanar Laminated Siltstone	•Planar to wavy parallel laminated fine-coarse siltstone •Starved ripples, erosionally scoured beds, minor soft sediment deformation . •Low contrast between fine and coarse siltstone laminae •Low calcite cementation. •Low bioturbation (BI-1) consisting of isolated *nereites, planolites*.	•Deposited in proximal offshore position •Deposited by linear sourced turbidity currents
6 Pinstripe Laminated Siltstone	•Thin (<5cm) dark black beds of silty shale interbedded with fine to coarse siltstone. •Wavy parallel bedding is common, starved ripples and soft sediment deformation occur. • The coarser siltstone laminae are often highly cemented by both calcite and dolomite	•deposited in proximal offfshore position •Dark black silty shale beds are deposited by hyperpycnal flows •Interbedded siltstone beds are deposited by linear sourced turbidity currents
7 Lenticular Bedded Siltstones	•Lenticular bedded coarse to fine siltstone interbedded with silty shale beds •Abundant asymmetric and climbing ripples •Sediment loading and flame structures are common. •Coarser siltstone beds are cemented by calcite and dolomite.	•Deposited in the distal offshore transition to proximal offshore position •Interbedded hyperpycnal flows and linear sourced turbidity currents
8 Planar Laminated Bituminous Siltstone	•Planar laminated fine-medium siltstone •Rare pyritized starved ripples •Calcisphere beds are common	•Deposited in the distal offshore setting •Calcisphere beds associated with organisms that inhabited an unstable eutrophic environment

Table 3.1 - Summary of sedimentary lithofacies characteristics in the D1 and D2 Horizons in the Greater Pouce Coupe Area, Alberta and British Columbia

ocean during major storms (Davies, 1997; Zonneveld et al., 2010; Zonneveld and Moslow, 2014). During major storms runoff is intense and carries large sediment loads, due in part to lack of vegetation in sediment source areas (Krapf et al., 2003; Stollhoven et al., 2014; Zonneveld at al., 2010). These ephemeral river deposits all along the coastline are prone to over-steepening and susceptible to mass wasting events, producing linear sourced turbidity currents.

Based on core observation and geophysical log correlations the Middle Montney in the study area has been broken down into 4 units. The Montney Turbidite Zone, the D1 horizon, the D1-D2 transition and the D2 horizon (Fig. 3.3). The Montney Turbidite Zone was deposited during a lowstand systems tract. During this time coarser sediment (fine-grained sand) bypassed the shoreface and was brought out to the outer ramp, the Cindy Graben acted as a conduit (Moslow, 2000). Sub-aqueous density flows with a single point source developed; major accumulations were controlled by localized syn-sedimentary tectonism (Moslow, 2000).

The D1 horizon was deposited during the ensuing transgressive and highstand systems tract. At this time the study area was situated in the proximal- distal offshore area and deposition was dominated by point sourced turbidity currents in the proximal offshore and settling out of suspension in the distal offshore area. The Gordondale, Pouce Coupe and Josephine Creek faults were active at this time and controlled where the thickest accumulations of sediment occurred.

The D1-D2 transition is characterized by the appearance of silty-shale beds. Appreciable clay is conspicuously absent from most Montney successions and has only been found in a few locales. These locations (Pedigree-Ring-Border and Dixonville) are interpreted to have been affected by perennial deltas (Zonneveld and Moslow, 2014). The occurrence of clay in the D1-D2 transition suggests there is an active deltaic system proximal to the study area. Clay can

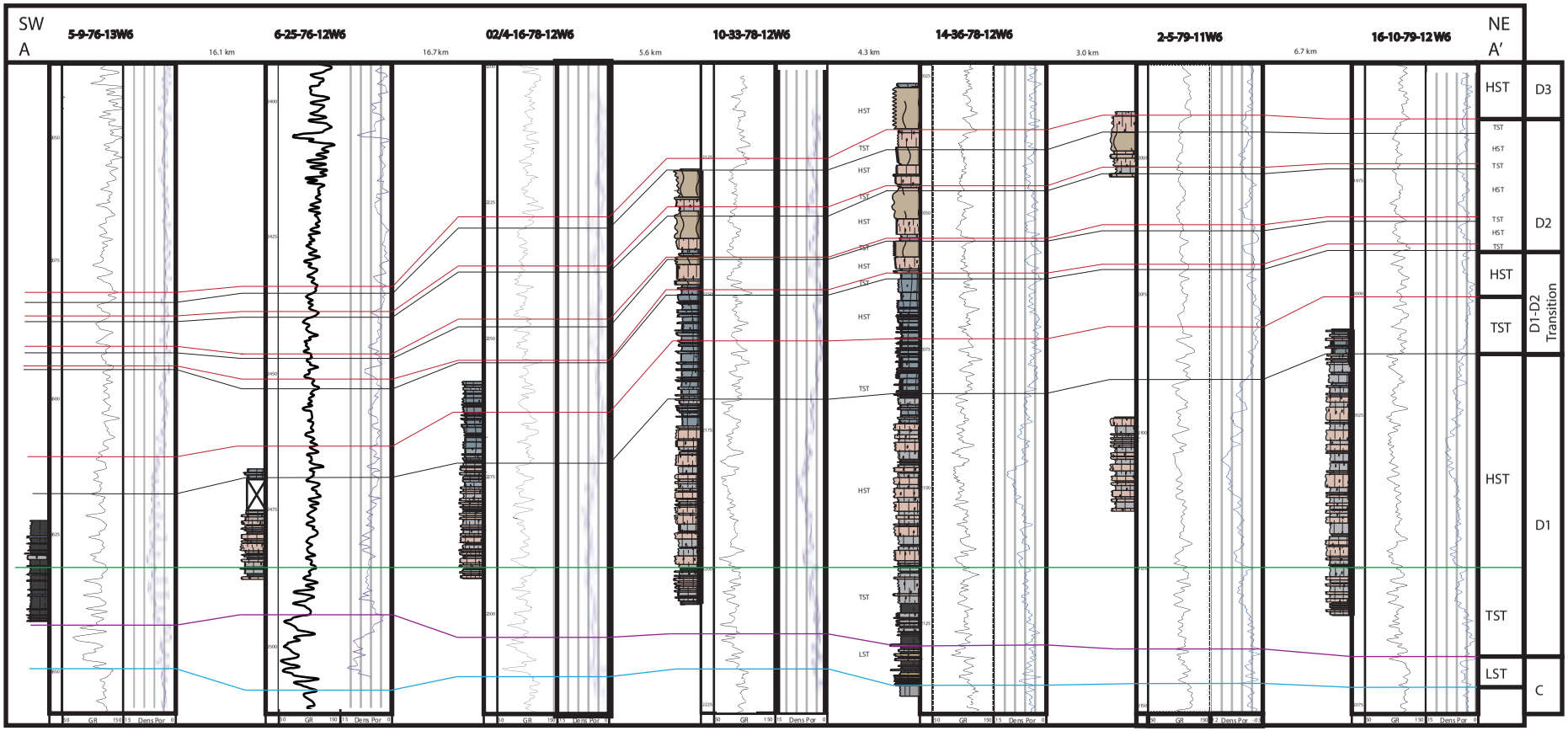

Figure 3.3 - Cross-Section A-A' oriented parallel to depositional dip. Datum is Maximum Flooding Surface that is represented by the occurrence of Lithofacies 4. Shows the major stratigraphic surfaces as well as the distribution of the D1 horizon, D1-D2 transition and D2 horizon. For larger view and legend see Figure 2.10.

occur in a variety of depositional settings but it most commonly occurs in areas where fresh water, rich in dissolved load, enters a body of salt water (REF).

The Hines-Creek satellite graben is situated approximately 75 km northeast of the study area and is known to have provided a topographic low that a perennial river flowed through at other times during deposition of the Montney. It is likely that during the D1-D2 transition a major fluvial system once again flowed through the Hines-Creek Graben, seasonally generating hyperpycnal flows.

The D2 horizon reflects deposition in the offshore transition to proximal offshore zone by linear sourced turbidity currents. Repeated small-scale fluctuations in base level cause the resulting deposits to be much more lithologically variable than the D1 horizon. Multiple shallowing upwards packages of Lithofacies 7 overlying Lithofacies 5 are present. Lithofacies 7 is the most proximal of the facies as shown by the increased coarse siltstone fraction and presence of combined flow ripples insinuating deposition above storm wave base.

Results

Principal Component Analysis

All XRF data was analyzed by Principal Component Analysis (PCA). PCA is an advanced statistical method used to reduce the dimensionality of large, complex datasets, in this case elemental concentrations (Shaw, 2003). A principal component score is assigned to each sample as determined by the eigenvectors, the eigenvectors are then plotted against each other (Sano et al., 2013). The closer the elements plot to one another on the eigenvector plots, the more closely associated they are to one another in the sediment (Ratcliffe and Wright, 2012).

Figure 3.4 summarizes the results of the PCA carried out on data acquired from three wells in the Middle Montney D1 and D2 horizons. 55 percent of the variation in the dataset is accounted for by principal components 1 and 2. Four broad grouping have been recognized as follows:

Group 1: includes SiO_2 and Zr. SiO_2 is typically associated with the amount of silt-size quartz grains in mudstones (Pearce et al., 2005; Ratcliffe et al., 2010; Sano et al., 2013). Zr is commonly associated with detrital zircon, which is typically found in the fine-sand or silt-sized particles (Sano et al., 2013). This group of elements is associated with the coarser fraction of terrigenous derived sediment.

Group 2: includes CaO, MnO, MgO, Sr and Ba. CaO is strongly associated with calcite, so it is likely the other elements in the group are also associated with carbonates.

Group 3: includes Mo, S and Zn. Mo is a redox sensitive element that tends to be less soluble under reducing conditions which results in authigenic enrichments in oxygen depleted environments (Tribovillard et al., 2006). The presence of S and Zn in this group likely reflects the presence of pyrite, an authigenic mineral often associated with reducing conditions/anoxia (Sano et al.,2013). Group 3 elements are associated with oxygen-depleted environments and are likely to be found in relatively high concentrations in facies that have high total organic carbon (TOC) content.

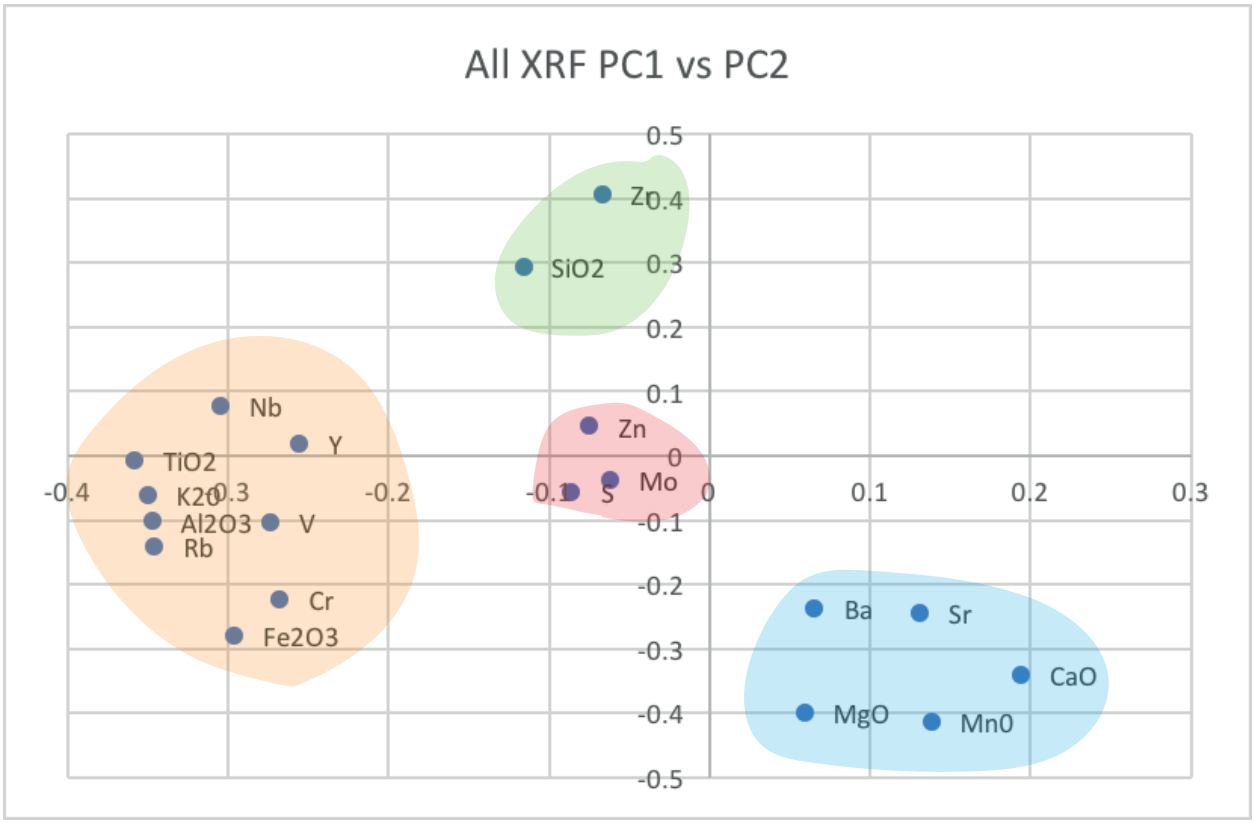

Figure 3.4 - Eigenvector cross plots for data derived by principal component analysis for samples in all the wells described in the study. Four broad groupings were recognized: Group 1 outlined in green; Group 2 outlined in blue; Group 3 outlined in red; Group 4 outlined in orange.

Group 4: includes Al_2O_3, K_2O, TiO_2, Rb, Fe_2O_3, Cr, Nb, Y and V. Al_2O_3 is related to clay mineral content, therefore the elements associated with Al_2O_3 are likely to be primarily controlled by clay mineral content as well (Sano et al., 2013; Ratcliffe et al., 2010). Rb and K_2O are commonly found in association with illite/smectite (Ratcliffe et al., 2010). Comparison with XRD data shows that these elements are closely associated with the presence of clay minerals (Table 2 [Pearson Product Correlations between XRD and ICP MS data])

Key Elements and Ratios- Mineralogical Interpretations

Comparison of elements and elemental ratios with mineralogical data obtained by XRD analysis (Table 2) allows for the determination of the basic mineralogical controls on element concentrations. The main elemental and elemental ratios used in this study for correlative purposes as well to ascertain controls on the depositional environment are:

SiO_2/Al_2O_3 –closely mimics the quartz content based on comparison of ICP-MS data and XRD data (Figure 5), and can be used as a grain size proxy.

Terrigenous Indicators ($Al_2O_3+K_2O+TiO_2+Fe_2O_3$)– closely associated with the amount of total clays in the sediment; high terrigenous indicator (TI) values define areas with high clay mineral abundance (Sano et al., 2013).

Fe_2O_3/MgO –as discussed in Sano et al. (2013) this ratio mimics pyrite abundance. Comparison with XRD and ICP data shows strong correlation, with a R^2 value of 0.95 (Figure 5).

Zr –is commonly associated with silt-grade detrital zircons and as such it can be used as a proxy for grain size (Sano et al., 2013). Zr has been shown to be a good indicator of siliciclastic detrital input in the Montney Formation as it is associated with the quartz-feldspar-mica detrital components rather than the clay mineral component (Chatellier et al., 2014)

Rb/K_2O –Both of these elements are present in clay minerals as well as Potassium Feldspar, however the Rb/K_2O ratio is typically higher in K-Feldspar than in clay minerals (Elwood et al., 2008; Sano et al., 2013). Based on the XRD data the amount of K Feldspar stays relatively constant in all samples therefore variations in this ratio are primarily controlled by changes in the clay mineral proportions.

V, Mo –are found to be relatively enriched in anoxic-euxinic settings and as such can be used as a proxy for periods of severe oxygen deficiencies, these settings are often characterized by high total organic content (Tribovillard et al., 2006; Sano et al., 2013). Source rock analysis was beyond the scope of the project so correlations between TOC and V and Mo concentrations were not established.

CaO – is directly proportionate to the amount of Calcite, with a correlation coefficient of 0.96.

Zr/Nb –As mentioned previously Zr is typically associated with the coarser-grained fraction of the sediment, Nb is commonly associated with clay minerals typically illite (Ratcliffe et al., 2012). The Zr/Nb is a good indicator of grain size.

	Al2O3 (wt %)	SiO2 (wt %)	TiO2 (wt %)	Fe2O3 (wt %)	MnO (wt %)	MgO (wt %)	CaO (wt %)	Na2O (wt %)	K2O (wt %)	P2O5 (wt %)	Ba (ppm)	Cr (ppm)
Quartz	-0.938	0.648	-0.931	-0.878	0.01	-0.471	0.514	0.597	-0.864	-0.66	-0.024	-0.901
K feldspar	0.57	0.015	0.651	0.34	-0.479	-0.259	-0.786	-0.033	0.707	0.013	0.386	0.469
Plagioclase	-0.565	0.539	-0.455	-0.534	-0.33	-0.672	-0.093	0.536	-0.516	-0.501	-0.047	-0.57
Calcite	-0.389	-0.381	-0.481	0.021	0.95	0.483	0.962	-0.329	-0.655	0.316	-0.202	-0.297
Dolomite	-0.588	0.186	-0.556	-0.367	0.532	-0.19	0.617	0.292	-0.676	-0.219	0.388	-0.551
Ankerite	-0.779	0.25	-0.784	-0.581	0.401	-0.037	0.772	0.438	-0.888	-0.254	-0.08	-0.67
Siderite	-0.638	0.057	-0.637	-0.387	0.55	0.122	0.802	0.332	-0.82	-0.058	-0.047	-0.513
Chlorite	0.841	-0.423	0.82	0.623	-0.394	0.433	-0.624	-0.346	0.854	0.471	-0.26	0.832
Barite	-0.241	0.457	-0.171	-0.296	-0.151	-0.667	-0.193	0.236	-0.071	-0.487	0.574	-0.349
Fluorapatite	0.716	-0.894	0.68	0.925	0.454	0.719	-0.046	-0.783	0.451	0.888	-0.268	0.743
Total Non-Clays	-0.881	0.371	-0.86	-0.638	0.41	-0.313	0.71	0.411	-0.951	-0.398	0.089	-0.826
Pyrite	0.847	-0.717	0.833	0.899	-0.026	0.473	-0.5	-0.745	0.708	0.733	-0.381	0.82
Illite	0.862	-0.326	0.842	0.617	-0.4	0.234	-0.724	-0.428	0.96	0.34	0.007	0.785
Total Clays	0.881	-0.371	0.86	0.638	-0.41	0.313	-0.71	-0.411	0.951	0.398	-0.089	0.826

	Sr (ppm)	Zn (ppm)	Zr (ppm)	V (ppm)	Rb (ppm)	Y (ppm)	Nb (ppm)	Mo (ppm)	Pb (ppm)	Th (ppm)	U (ppm)
Quartz	-0.15	0.278	0.505	-0.506	-0.931	-0.784	-0.941	0.337	-0.976	-0.91	-0.844
K feldspar	-0.268	-0.034	0.116	0.186	0.468	0.361	0.643	-0.813	0.774	0.678	0.307
Plagioclase	-0.325	0.694	0.403	-0.719	-0.625	-0.452	-0.552	-0.607	-0.344	-0.44	-0.5
Calcite	0.791	-0.333	-0.534	-0.409	-0.234	-0.239	-0.467	0.54	-0.287	-0.55	0.163
Dolomite	0.601	-0.1	0.052	-0.652	-0.541	-0.44	-0.577	-0.107	-0.263	-0.575	-0.14
Ankerite	0.357	0.247	0.151	-0.402	-0.716	-0.462	-0.816	0.527	-0.864	-0.793	-0.439
Siderite	0.58	0.206	-0.023	-0.382	-0.559	-0.285	-0.681	0.463	-0.678	-0.66	-0.195
Chlorite	-0.301	0.038	-0.206	0.863	0.801	0.768	0.832	0.123	0.486	0.833	0.471
Barite	-0.117	-0.177	0.346	-0.546	-0.302	-0.447	-0.161	-0.772	0.236	-0.151	-0.243
Fluorapatite	0.522	-0.215	-0.859	0.157	0.791	0.694	0.659	-0.188	0.827	0.612	0.96
Total Non-Clays	0.335	0.161	0.178	-0.79	-0.83	-0.684	-0.895	0.068	-0.665	-0.875	-0.477
Pyrite	-0.007	-0.02	-0.662	0.252	0.86	0.704	0.807	-0.435	0.913	0.789	0.804
Illite	-0.339	-0.261	-0.154	0.715	0.808	0.607	0.889	-0.168	0.731	0.858	0.459
Total Clays	-0.335	-0.161	-0.178	0.79	0.83	0.684	0.895	-0.068	0.665	0.875	0.477

Table 3.2 - Pearson product moment correlation coefficients between mineralogical abundances (derived from XRD analysis) and elemental concentrations (derived from ICP-MS and ICP-OES analysis)

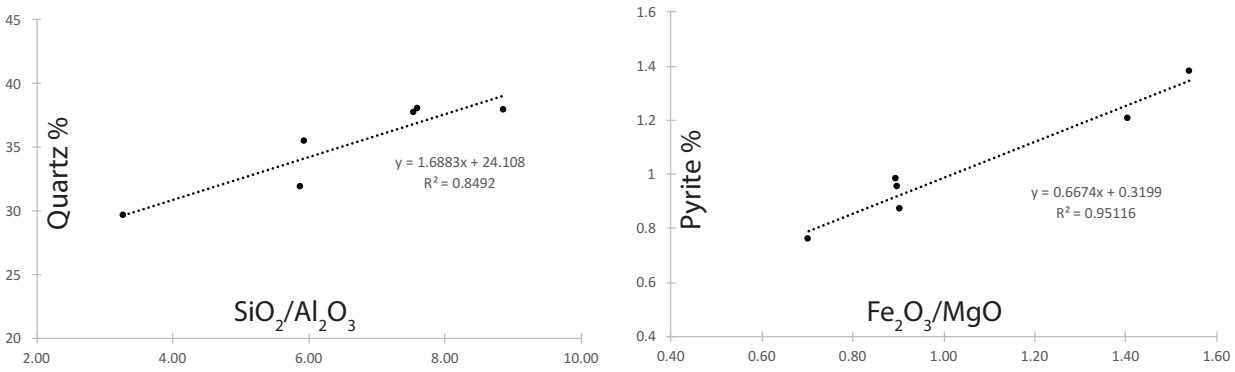

Figure 3.5 - ICP-MS and ICP-OES derived elemental compositions plotted against XRD derived mineralogical data for selected minerals and elemental ratios.

Chemostratigraphic Units

Chemostratigraphy in this study is used as a way to refine and confirm stratigraphic correlations that were initially based on core and well log data. Changes in elemental concentrations produce recognizable patterns and trends, which allows for the recognition of distinctive geochemical packages (Pearce et al., 2005; Playter et al., in review). These packages are termed chemofacies which Playter et al. (in review) define as "bodies of rock characterized by a particular combination of oxide elemental patterns, trace element signatures and element ratio values dependent on underlying mineralogical controls (including organic matter) that distinguish it from adjacent bodies of rock. Chemofacies inherently represent both provenance characteristics and paleoredox conditions."

As in the work of Pearce et al. (1999), Pearce et al. (2005), Ratcliffe et al. (2010) and Sano et al. (2013), chemofacies were defined based on changes in the geochemical profiles. In addition this data has been tied in with gamma ray logs, density porosity logs and detailed lithologs (Fig. 3.6). As geochemical data is rare in the area, tying in well log profiles with geochemical profiles allows for interpolation of important stratigraphic surfaces across the region. Trace elements with limited mobility, such as Zr, Al, Ti and Cr, were used for correlations, as their limited mobility makes them less susceptible to diagenetic alteration by clay and feldspar weathering than are some of the more mobile elements (Pearce et al., 1999; Playter et al., in review). Six chemofacies were recognized based on the geochemical profiles of major oxides, trace elements and elemental ratios.

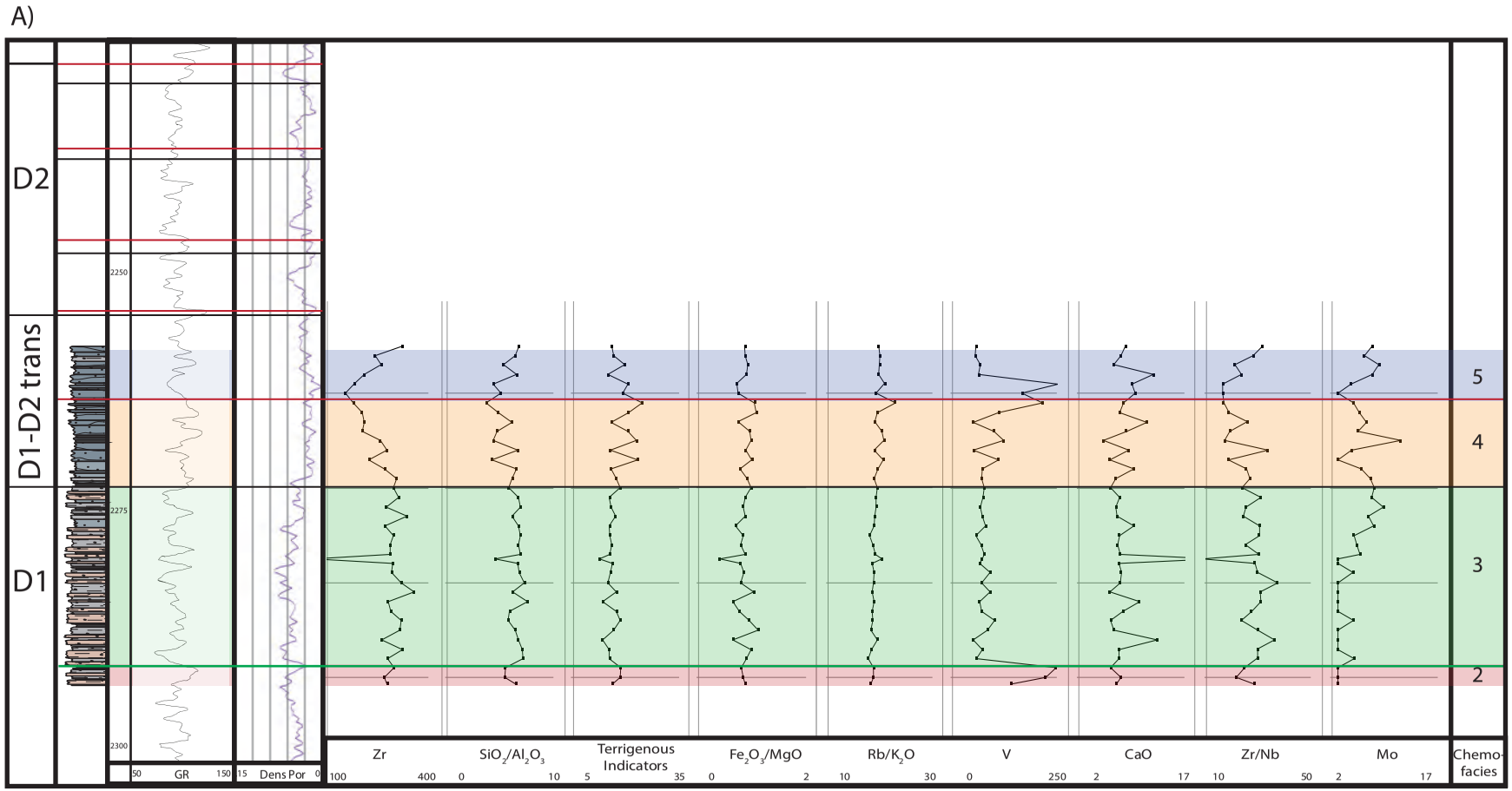

Figure 3.6 - Elemental profiles for the three wells that ED-XRF was acquired. Litholog, gamma ray and density porosity curves are included for comparison and correlation purposes. Three main lithostratigraphic packages are labeled and seven chemostratigraphic intervals are outlined and colored for visualization. Stratigraphic surfaces and lithology colors are the same as those used in Figure 3.3. Black squares indicate sample locations. **A)** Elemental profile for 4-16-78-12w6; **B)** Elemental profile for 10-33-78-12w6; **C)** Elemental profile for 14-36-78-12w6.

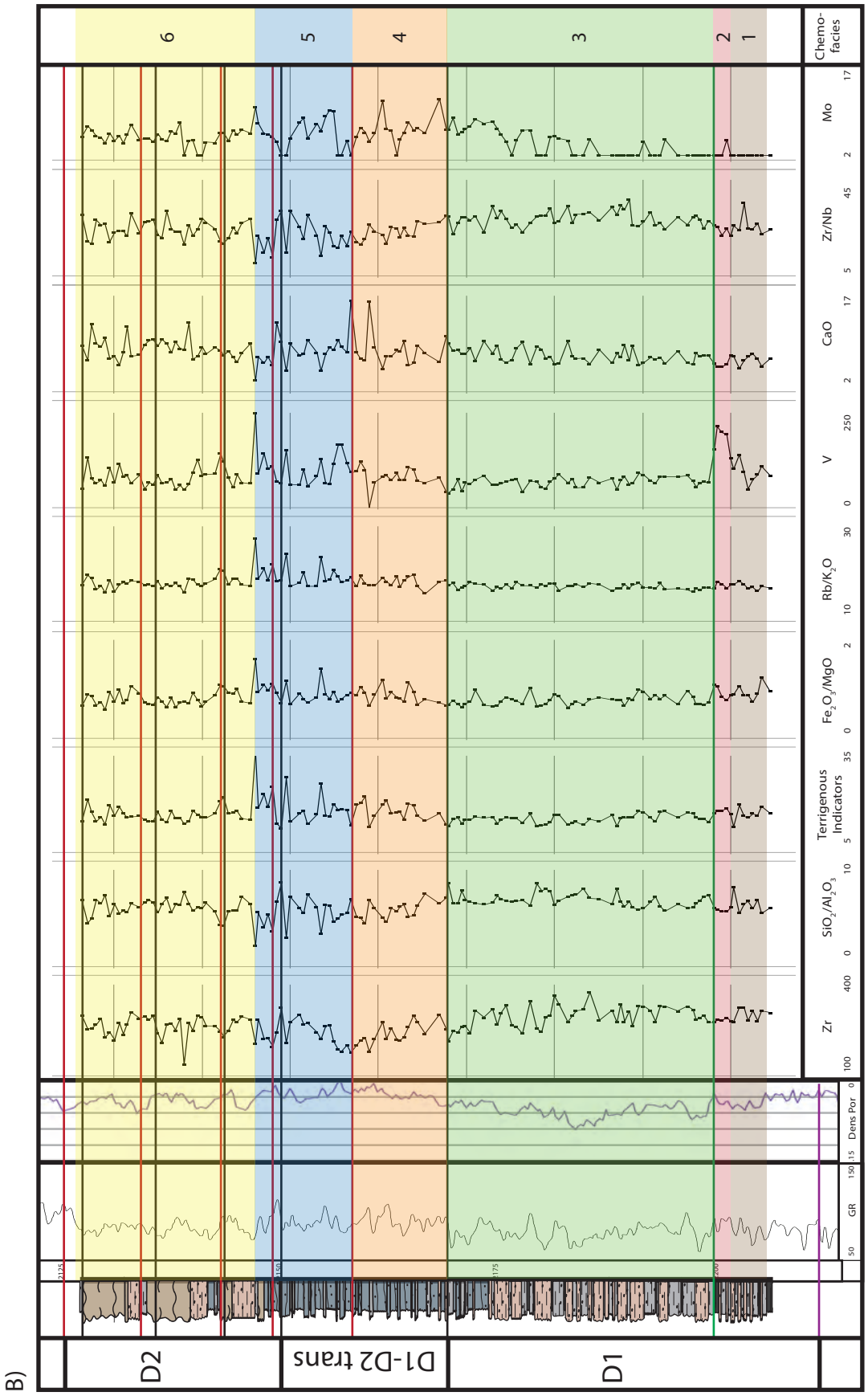
B)
D2
D1-D2 trans
D1
6
5
4
3
2
1
Chemo-facies
Mo
Zr/Nb
CaO
V
Rb/K2O
Fe2O3/MgO
Terrigenous Indicators
SiO2/Al2O3
Zr
Dens Por
GR


C)
D2
D1-D2 trans
D1
7
6
5
4
3
2
1
Chemo-facies
Mo
Zr/Nb
CaO
V
Rb/K2O
Fe2O3/MgO
Terrigenous Indicators
SiO2/Al2O3
Zr
Dens Por
GR
2025
2050
2075
2100
2125

Chemofacies 1

This chemofacies occurs in the Montney Turbidite Zone and the basal part of the overlying Middle Montney D1 member. When examining major oxides, this chemofacies is characterized by high CaO, MgO and MnO values. The Terrigenous Indicators, Ze, Fe_2O_3/MgO and Mo concentrations are all low throughout this chemofacies.

Chemofacies 2

The lower boundary of Chemofacies 2 is marked by an abrupt increase in V and Mo values. High values of V and Mo are characteristic of Chemofacies 2. Concentrations of Zr decrease upwards and values of SiO_2/Al_2O_3 are low throughout this chemofacies. In core, the top of Chemofacies 2 is marked by a thin layer (<30cm) of finely crystalline dolomite; this dolomite is interpreted to be formed by organogenesis in anoxic settings (Pisccioto, 1981; Lumsden, 2003). This dolostone was only sampled in the 14-36-78-12w6 well and is marked by a spike in CaO and MgO values and a drop in V and Mo values. Because it is such a thin unit and depending on the sampling resolution would not always be measured it was not made its own chemofacies.

Chemofacies 3

The transition to Chemofacies 3 is marked by abrupt increases in the Zr and SiO_2/Al_2O_3 values along with major decreases in the value of the Terrigenous Indicators, V, and Mo. The values of Zr and SiO_2/Al_2O_3 remain high throughout Chemofacies 3 but start to decrease near the top of the unit. Values of Terrigenous Indicators, Fe_2O_3/MgO, Rb/K_2O, V, Mo, and CaO are low throughout.

Chemofacies 4

The base of Chemofacies 4 is marked by abrupt increases in the Zr concentration and SiO_2/Al_2O_3 values which then decrease through this interval. Terrigenous Indicator values are generally higher than in the underlying facies and increase throughout the interval. After an initial sharp increase, Zr/Nb values decrease upwards throughout the unit and are the lowest values observed throughout any of the units

Chemofacies 5

The transition to Chemofacies 5 is marked by increases in Zr, SiO_2/Al_2O_3 and Zr/Nb values. Concentrations of V initially increase sharply before declining and remaining low throughout the rest of the unit. Values of CaO are irregular throughout the unit, but generally higher than in any of the other chemofacies. Terrigenous Indicator values are slightly lower than those observed in Chemofacies 4 but generally remain higher than the values observed in chemofacies 1, 2 and 3.

Chemofacies 6

The base of Chemofacies 6 is marked by a sharp increase in Zr and SiO_2/Al_2O_3 values, with a corresponding sharp drop in Terrigenous Indicator values. After the initial spike Zr and SiO_2/Al_2O_3 values quickly decrease to values similar to those observed in Chemofacies 4 before steadily increasing throughout the rest of the unit. The Terrigenous Indicator values remain low throughout the unit with a few positive excursions. Concentrations of CaO are generally lower than those observed in Chemofacies 5, but there are many major positive spikes; values of CaO are higher than those observed in Chemofacies 3.

Chemofacies 7

The transition to Chemofacies 7 is marked by steadily decreasing values of Zr and SiO_2/Al_2O_3 which continue to decrease until near the top of the unit when they start to gradually increase. Values of Fe_2O_3/MgO are constant throughout the unit and are slightly higher than in the underlying chemofacies. Concentrations of CaO are generally higher than those observed in the other chemofacies aside from Chemofacies 1.

Discussion

Depositional Trends

Variations in inorganic geochemistry during deposition of the Middle Montney D1 and D2 Members elegantly compliment lithologic descriptions of the core. Broadly speaking, the trends observed agree with interpretations of sedimentary environments proposed in Chapter 1. At the base of the succession, during deposition of the Montney Turbidite Zone, clay indicator values are low, supporting the interpretation that, at this time, a lowstand systems tract developed. As a result, coarser grained sediment bypassed the shoreface region and was brought out to the proximal offshore area. During this time very little clay-sized sediment was deposited. Values of CaO are consistently high throughout this unit, because the coarser sediment was preferentially cemented post-depositionally. The geochemical signature associated with the Montney Turbidite Zone extends further up the section than was observed in core analysis. This implies that the transgression following the lowstand systems tract was gradual, and coarser grained sediment continued to be deposited in this area.

The position of the maximum flooding surface (MFS) in the lithostratigraphic cross section was based on the occurrence of a finely crystalline dolostone with abundant small pyrite framboids distributed throughout the unit. As this finely crystalline dolostone was very thin (<30cm), it was only sampled by XRF in the 10-33-78-12w6 core, preventing it from being used as a marker across the entire area. Even withstanding the absence of that marker, the MFS can be readily observed in all three cores by high values in Mo and V. These elements are commonly found to be enriched in oxygen deficient settings (Tribovillard et al., 2006). Chemofacies 2 marks a time that the relative sea level was high, there was little sediment input into the basin, and anoxic-euxinic conditions developed.

Above the MFS the D1 HST develops. This unit comprises much of the D1 horizon and horizontal wells producing from the D1 generally land at the base of this unit. Based on detailed core analysis, this unit was interpreted to be deposited by linear sourced turbidity currents. In core and thins section analysis it was recognized that the unit's superior reservoir quality was due to low clay and calcite cement content. The inorganic geochemistry agrees with the interpretation as terrigenous indicators and CaO values are low throughout the unit. Values of Zr and SiO_2/Al_2O_3 increase from the base of the unit to approximately half way up the unit, which agrees with the interpretation that this is a shallowing upwards succession with the proportion of coarse siltstone increasing upwards. Towards the top of the unit the values of Zr and SiO_2/Al_2O_3 begin to decrease showing that there was a gradual increase in relative sea level, decreasing the coarse siltstone fraction near the top of this unit.

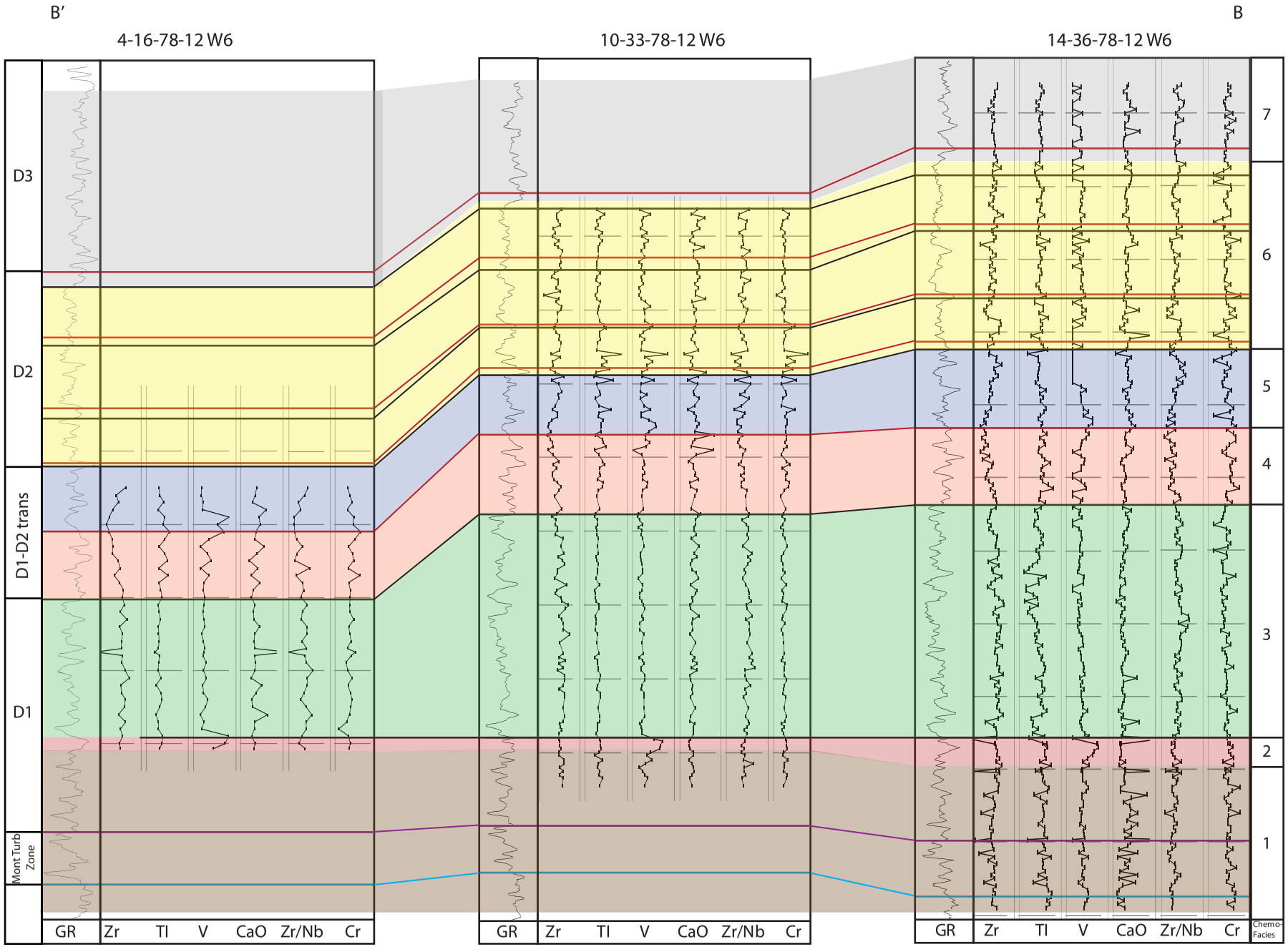
B'
4-16-78-12 W6
10-33-78-12 W6
B
14-36-78-12 W6
D3
D2
D1-D2 trans
D1
Mont Turb Zone
7
6
5
4
3
2
1
GR
Zr
Tl
V
CaO
Zr/Nb
Cr
Chemo-Facies

Figure 3.7 (Previous Page) - Cross Section of the three wells that ED-XRF was acquired correlating the chemofacies. Datum is Maximum Flooding Surface in D1 Horizon.

The D1-D2 transition is marked in core by the occurrence of silty shale beds. Appreciable amounts of clay minerals are rare in the Montney Formation and are only found in two areas: Pedigree-Ring-Border and Dixonville area. These areas are interpreted to have been deposited near perennial deltaic systems. The initial stages of the D1-D2 transition took place during a Transgressive System Tract. Values of Mo and V increase upwards, indicating increasing levels of anoxia. In contrast, values of Zr and SiO_2/Al_2O_3 decrease upwards, indicating a fining upwards grain size trend. Terrigenous Indicator values throughout Chemofacies 4 are higher than in the underlying D1 horizon and increase upwards showing increasing amounts of clay being deposited throughout the unit.

The D1-D2 transition highstand system tract continues to display high Terrigenous Indicator and Rb/K_2O values, indicating a high amount of clay through this interval. Zr and SiO_2/Al_2O_3 values increase upwards, indicating a shallowing upwards succession and support the interpretation that Chemofacies 5 was deposited during a HST. Values of CaO are inconsistent throughout the unit, with numerous positive excursions related to the observation that the coarse grained intervals within the D1-D2 transition were highly cemented with calcite. Vanadium and Mo values are erratic through the unit but are generally high relative to the D1 and D2 units. Values of Fe_2O_3/MgO are high in some intervals. These values suggest there was some degree of oxygen deficiency occurring during the deposition of Chemofacies 5.

In core the D2 horizon is characterized by interbedding of strata deposited by linear sourced turbidity currents in the proximal offshore (Lithofacies 5) and offshore transition (Lithofacies 7) areas. Values of Zr and SiO_2/Al_2O_3 increase upwards in the unit, reflecting an

overall progradation during the deposition of the D2 horizon. The terrigenous indicators and Rb/K_2O values are generally low, with a few positive excursions reflecting periodic influence of hyperpycnal flows during the deposition of the D2 Horizon. Lithofacies 7 was the coarsest of all the lithofacies observed and was highly cemented with calcite, this is reflected in the numerous positive excursions in the CaO values throughout this unit.

Above the D2 horizon in the 14-36-78-12w6 core the basal part of the D3 horizon was measured. This area is characterized by increasing Zr and SiO_2/Al_2O_3 values reflecting a coarsening upwards package. This is consistent with the sequence stratigraphic interpretations of Davies and Hume (2016) and Davies (1997) that the Middle Montney (Members D1-D4) were deposited during a third order HST after the TST that followed the deposition of the Montney Turbidite Zone.

Origin of Clays

Deposition of the Montney Formation was originally thought to have occurred along the tectonically stable and inactive northwestern margin of Pangea (Davies, 1997; Moslow, 2000). However recent work has suggested terrane accretions on the western margin may have occurred as early as the Early to Middle Triassic (Beranek and Mortensen, 2006; 2007; Ferri and Zonneveld, 2008). Obduction of ophiolites, volcanic arc complexes and the Yukon-Tanana Terrane, which resulted from the closing of a back-arc basin, would have depressed the crust and led to the development of a foreland basin (Ferrie and Zonneveld, 2008). The obduction created a topographic high that may have acted as a western sediment source; based on the metamorphic

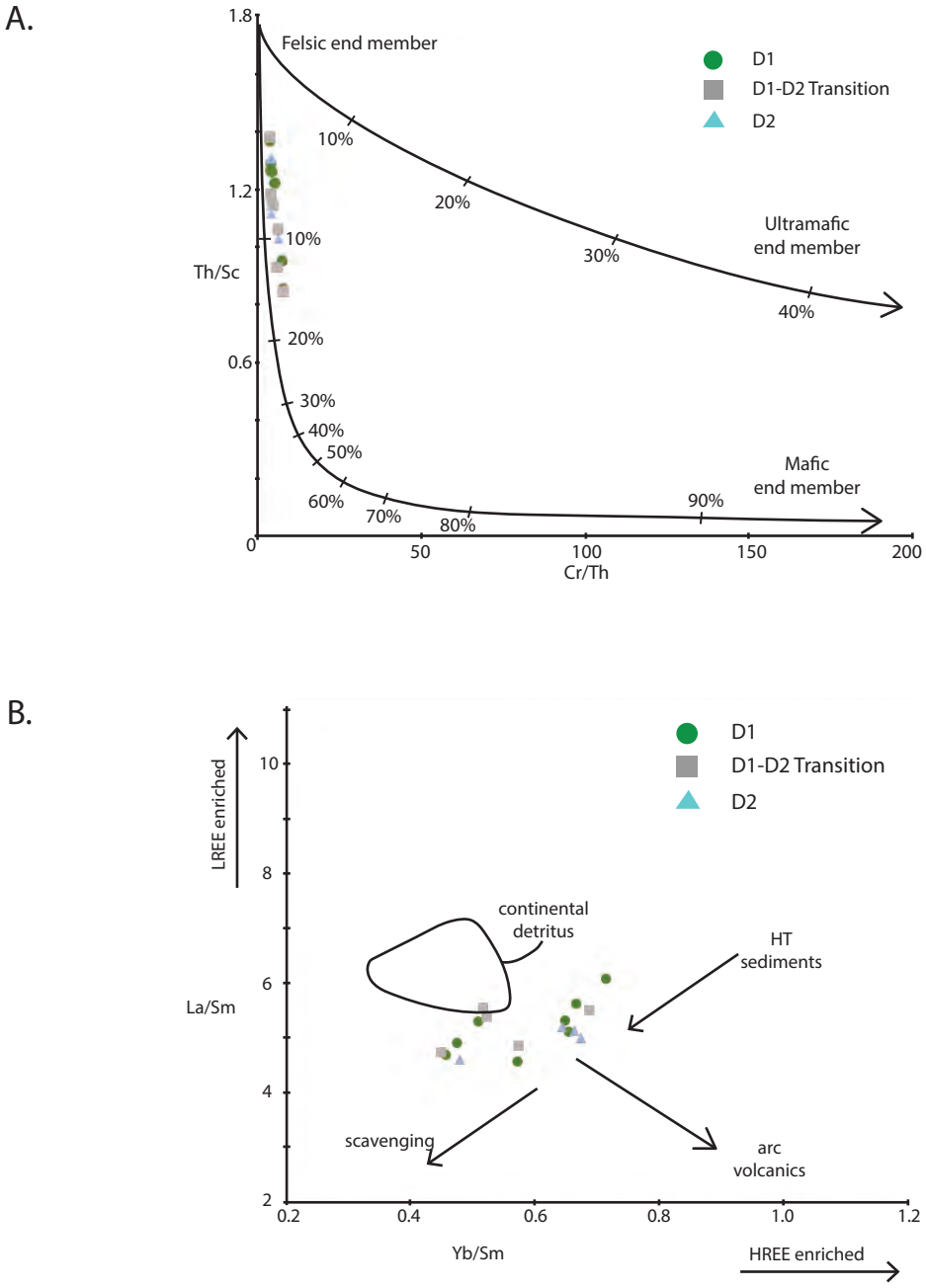

Figure 3.8 - A) Cr/Th versus Th/Sc cross plot from ICP-MS and ICP-OES samples. Two mixing curves have been calculated between a felsic and mafic endmember and between a felsic and ultramafic endmember after Bracciali et al. (2007) and Totten et al. (2000). Our samples plot close to the felsic endmember insinuating sediment source was upper crustal rocks from the east. **B)** Yb/Sm versus La/Sm cross plot from ICP-MS and ICP-OES samples. Yb/Sm reflects HREE enrichment while La/Sm reflects LREE enrichment after Plank and Langmuir (1998). Felsic rocks are enriched in LREE in contrast to mafic-ultramafic rocks which are enriched in HREE. Our samples plot closer to the continental detritus and are unlikely to be sourced from a mafic-ultramafic rocks.

and volcanic nature of the accreted terranes, they are likely to weather easily and produce clays. It is possible that clays in the D1-D2 transition could have been sourced from volcanic terrane to the west instead of being sourced from perennial river systems from the east.

Previous studies on the provenance of shales have used cross plots of Th/Sc versus Cr/Th and Yb/Sm versus La/Sm to distinguish felsic, mafic and ultramafic sediment sources (Plank and Langmuir, 1998; Bracciali et al., 2007; Totten et al., 2000; Playter et al. 2017). High values of Th/Sc reflect an enrichment in felsic components whereas high values of Cr/Th reflect an enrichment in the mafic-ultramafic components (Bracciali et al., 2007; Playter et al., 2017). Felsic rocks have also been shown to be enriched in LREE in contrast to mafic-ultramafic rocks, which are enriched in HREE, making the Yb/Sm versus La/Sm cross plot ideally suited to show the primary source of sediments (Bracciali et al., 2007; Plank and Langmuir, 1998). Analysis of these plots for samples from the D1 and D2 horizons show no major changes in sediment sources throughout the period (Fig. 3.7). This suggests that the clays deposited during the D1-D2 transition were sourced from upper crustal rocks from the eastern land mass and if terrane accretion had commenced the study area was not affected.

Conclusions

ED-XRF analysis was used to obtain geochemical profiles of three cores in the D1 and D2 horizons in the Pouce Coupe Area. Inorganic whole-rock geochemical data was used as a proxy for environmental conditions occurring at the time of deposition, to determine the source of the clays in the D1-D2 transition (by identifying the presence or absence of an igneous geochemical signature during the D1-D2 transition), to aid in stratigraphic correlations

throughout the area, and to confirm the sequence stratigraphic interpretation proposed in Chapter 2 of this thesis.

Elemental compositions were found to elegantly compliment sedimentologic core descriptions. With increases in the values of Zr and SiO_2/Al_2O_3 strongly correlating with increases in the coarser siltstone/v. fine sandstone fraction and increases in the Terrigenous Indicators ($Al_2O_3 + K_2O + Fe_2O_3 + TiO_2$) and Mo and V values being associated with increasing amounts of clay. Th/Sc versus Cr/Th and Yb/Sm versus La/Sm cross plots showed that clays deposited throughout the D1-D2 transition were sourced from easterly upper crustal rocks and terrane accretion on the western margin had yet to commence. Geochemical profiles enabled the recognition of 7 distinct chemofacies that are identifiable across the area. Chemostratigraphy was also found useful to compliment the sequence stratigraphic architecture erected in Chapter 2. The sampling resolution (~50cm) was found to be too large to resolve the parasequences within the D2 horizon and it is suggested that any future studies have a smaller sampling interval in the more lithologically complex zones throughout the Montney Formation.

References

Barclay, J.E., Krause, F.F., Campbell, R.I. and Utting, J. 1990. Dynamic casting and growth faulting: Dawson Creek Graben Complex, Carboniferous-Permian Peace River Embayment, western Canada. *In:* Geology of the Peace River Arch. S.C. O' Connell and J.S. Bell (eds.). Bulletin of Canadian Petroleum Geology, v. 38, p. 115-145.

Beranek, L.P. and Mortensen, J.K. 2006. A Triassic link between Yukon-Tanana and North America; new detrital zircon age, geochemical, and biostrati- graphic data. Geological Society of America, Cordilleran Section, Abstracts with Program, v. 38, p. 5–6.

Beranek, L.P. and Mortensen, J.K. 2007. Latest Permian to Middle Triassic accretions of the Yukon-Tanana, Stikine and Quesnel terranes to North America; new detrital zircon age data from Triassic rocks in Yukon. Geological Society of America, Cordilleran Section, Abstracts with Program, v. 39, p. 69.

Bracciali, L., Marroni, M., Luca, P.,Sergio, R. 2007. Geochemistry and petrography of Western Tethys Cretaceous sedimentary covers (Corsica and Northern Apennines): from source areas to configuration of margins. Geological Society of America Special Papers, v. 420, p.73-93.

Chatellier J.D., Moslow, T.F., Haverslew, B. 2014. The Use of X-Ray Fluorescence for Sequence Stratigraphy and Geomechanics of Shale. GeoConvention 2014: May 12 – 16 2014, Calgary, AB. Available from http://www.geoconvention.com/archives/2014/418_GC2014_The_use_of_X-Ray_Fluorescence.pdf

Davies, G.R., Moslow, T.F., Sherwin, M.D. 1997. The lower Triassic Montney Formation, west-central Alberta; *in* Triassic of the Western Canada Sedimentary Basin, T.F. Moslow and J. Wittenberg (ed.). Bulletin of Canadian Petroleum Geology, v. 45, p. 474–505.

Davies, G.R. and Hume, D. 2016. Lowstand / Slope-Onlap Wedges In The Montney: Stratigraphic And Sequence Framework, Reservoir Significance (Oral Presentation). GeoConvention 2016: May 7 – 11 2016, Calgary, AB. Available from http://www.geoconvention.com/uploads/2016abstracts/224_GC2016_Lowstand_Slope_Onlap_Wedges_in_the_Montney.pdf

Faraj, B., Harold, W., Addison, G., McKinstry, B., Donaleshen, R., Sloan, G., Lee, J., Anderson, T., Leal, R., Anderson, C., Lafleur, C., Ahlstrom, A. 2002. Shale gas potential of selected Upper Cretaceous, Jurassic, Triassic and Devonian shale formations in the WCSB of Western Canada: Implications for shale gas production. *Gas Technology Institute.* Des Plaines, Illinois. 103 pages

Ferri, F. and Zonneveld, J-P. 2008. Were Triassic rocks of the Western Canada Sedimentary Basin deposited in a foreland? Canadian Society of Petroleum Geologists Reservoir, v. 35, p. 12–14.

Hildred, G.V., Ratcliffe, K.T., Wright, A.M., Zaitlin, B.A., Wray, D.S. 2010. Chemostratigraphic applications to low-accomodation fluvial incised-valley settings: an example from the lower Mannville Formation of Alberta, Canada. Journal of Sedimentary Research, v. 80, p. 1032-1045.

Jarvis, I., and Jarvis, K. 1992. Plasma spectrometry in the earth sciences: techniques, applications and future trends. Chemical Geology, v. 95, p.1-33.

Jenkyns, H.C., 2010. Geochemistry of oceanic anoxic events. Geochemistry, Geophysics, Geosystems 11, Q03004. doi:10.1029/2009GC002788.

Krapf, C. B., Stollhofen, H., Stanistreet, I. G. 2003. Contrasting Styles Of Ephemeral River Systems And Their Interaction With Dunes Of The Skeleton Coast Erg (Namibia). Quaternary International, v. 104, p. 41-52.

Lumsden, D. N. 2003. Organodiagenetic Dolomite On A Deep Subtidal Shelf, Fort Payne Formation (Mississippian), Tennessee, U.S.A. In Ahr, W. M.; Harris, P. M.; Morgan, W. A.; and Somerville, I. D., eds. SEPM Special Publication 78: Permo-Carboniferous Carbonate Platforms and Reefs, p. 323–332.

Mei, S. 2009. New insights on faults in the Peace River arch region, northwest Alberta, based on existing well-log data and refined trend surface analysis, Can. J. Earth Sci. 46, no. 1, 41–65, doi: 10.1139/ E09-006

Moslow, T.F. 2000. Reservoir architecture of a fine-grained turbidite system: Lower Triassic Montney Formation, Western Canada Sedimentary Basin. In: Deep-water Reservoirs of the World, Conference Proceedings, Gulf Coast SEPM. P. Weimer, R.M. Slatt, J. Coleman, N.C. Rosen, H. Nelson, A.H. Bouma, M.J. Styzen, and D.T. Lawrence (eds.). p. 686–713.

Nance, H. S. and Rowe, H. 2015. Eustatic controls on stratigraphy, chemostratigraphy, and water mass evolution preserved in a Lower Permian mudrock succession, Delaware Basin, west Texas, USA. Interpretation, v. 3, p. SH11-SH25.

National Energy Board, BC Oil and Gas Commission, Alberta Energy Regulator and BC Ministry of Natural Gas Development. 2013. Energy briefing note: the ultimate potential for unconventional petroleum from the Montney Formation of British Columbia and Alberta; National Energy Board, BC Oil and Gas Commission, Alberta Energy Regulator and BC Ministry of Natural Gas Development, 17 p.

Pearce,T.J., Wray, D. S., Ratcliffe, K. T., Wright, D. K., Moscariello, A. 2005. Chemostratigraphy of the Upper Carboniferous Schooner Formation, southern North Sea. In: Carboniferous Hydrocarbon Geology: The Southern North Sea and Surrounding Onshore Areas. J.D. Collinson, D.J. Evans, D.W. Holliday and N.S. Jones (eds.). Yorkshire Geological Society, Occasional Publications series, v. 7, p. 147–164.

Pearce, T. J., Besly, B. M., Wray, D. S., Wright, D. K. 1999. Chemostratigraphy: a method to improve interwell correlation in barren sequences—a case study using onshore Duckmantian/Stephanian sequences (West Midlands, UK). Sedimentary Geology, v. 124, p.197-220.

Plank, T., & Langmuir, C. H. 1998. The chemical composition of subducting sediment and its consequences for the crust and mantle. Chemical geology, v. 145, p. 325-394.

Pisciotto, K.A., 1981, Review of secondary carbonates in the Monterey Formation, California, in Garrison, R.E., Kastner, M., and Zenger, D.H., eds., Dolomites of the Monterey Formation and Other OrganicRich Units: SEPM, Pacific Section, p. 119–140.

Playter T, Corlett H, Konhauser K, Robbins L, Zonneveld J.P. In Review. New Evidence for Global Volcanism Following the End-Permian Mass Extinction.

Playter T, Corlett H, Konhauser K, Robbins L., Rohais, S., Crombez, V., MacCormack, K., Rokosh, D., Prenoslo, D., Furlong, C.M., Pawlowicz, J., Gingras, M.K., Lalonde, S., Lyster, S., Zonneveld, J.P. In Review.Clinoform identification and correlation in fine-grained sediments: case study using the Triassic Montney Formation

Ratcliffe, K.T., Wright, A.M., Montgomery, P., Palfrey, A., Vonk, A., Vermeulen, J., Barrett, M., 2010. Application of chemostratigraphy to the Mungaroo Formation, the Gorgon field, offshore northwest Australia. APPEA Journal, 50th Anniversary Issue, p. 371–388.

Ratcliffe, K. T., Wright, A. M., Schmidt, K. 2012. Application of inorganic whole-rock geochemistry to shale resource plays: an example from the Eagle Ford Shale Formation, Texas. The Sedimentary Record, v. 10, p. 4-9.

Ratcliffe, K., Wright, M., 2012. Unconventional methods for unconventional plays: using elemental data to understand shale resource plays. PESA News Resour. 2012, p. 55-60.

Rowe, H., Hughes, N., Robinson, K. 2012. The quantification and application of handheld energy-dispersive x-ray fluorescence (ED-XRF) in mudrock chemostratigraphy and geochemistry. Chemical Geology, v. 324, p. 122-131.

Sano J.L., Ratcliffe K. T., D.R. Spain, 2013, Chemostratigraphy of the Haynesville Shale, *in* U. Hammes and J. Gale, eds., Geology of the Haynesville Gas Shale in East Texas and West Louisiana, U.S.A. AAPG Memoir 105, p. 137–154.

Shaw, P. J. (2003). Multivariate statistics for the environmental sciences. 1st ed. Hodder-Arnold. P. 233

Stollhofen, H., Stanistreet, I. G., von Hagke, C., Nguno, A. 2014. Pliocene–Pleistocene climate change, sea level and uplift history recorded by the Horingbaai fan-delta, NW Namibia. Sedimentary Geology, v. 309, p. 15-32.

Totten, M. W., Hanan, M. A., Weaver, B. L. 2000. Beyond whole-rock geochemistry of shales: The importance of assessing mineralogic controls for revealing tectonic discriminants of multiple sediment sources for the Ouachita Mountain flysch deposits. Geological Society of America Bulletin, v. 112, p. 1012-1022.

Tribovillard, N., Algeo, T., Lyons, T.W., Riboulleau, A., 2006. Trace metals as paleoredox and paleoproductivity proxies: an update. Chemical Geology, v. 232, p. 12–32

Wright, A.M., Ratcliffe, K.T., Zaitlin, B.A., Wray, D.S., 2010. The application of chemostratigraphic techniques to distinguish compound incised valleys in lowaccommodation incised-valley systems in a foreland-basin setting: an example from the Lower Cretaceous Mannville Group and Basal Colorado Sandstone (Colorado Group), Western Canadian Sedimentary Basin. In: Ratcliffe, K.T., Zaitlin, B.A. (Eds.), Application of Modern Stratigraphic Techniques: Theory and Case Histories: SEPM Special Publication, 94, p. 93–107.

Zonneveld, J-P., MacNaughton, R.B., Utting, J., Beatty, T.W., Pemberton, S.G. and Henderson, C.M. 2010. Ichnology and sedimentology of the Lower Montney Formation (Lower Triassic), Kahntah River and Ring Border gas fields, Alberta and British Columbia; *in* Applications of Ichnology to Petroleum Exploration, J-P. Zonneveld, M.K. Gingras and J.A. MacEachern (ed.), Bulletin of Canadian Petroleum Geology, v. 58, p. 115–140.

Zonneveld, J.P., Golding, M., Moslow, T.F., Orchard, M.J., Playter, T. and Wilson, N. 2011. Depositional framework of the Lower Triassic Montney Formation, west-central Alberta and northeastern British Columbia; *in* recovery – 2011 CSPG CSEG CWLS Convention, p. 1–4.

Zonneveld, J. P. and Moslow, T.F. 2014. Perennial River Deltas of the Montney Formation: Alberta and British Columbia Subcrop Edge (Oral Presentation). GeoConvention 2014: May 12 – 16 2014, Calgary, AB. Available from http://cseg.ca/assets/files/resources/abstracts/2014/core/490_GC2014_Perennial_River_Deltas_of_the_Montney_Fm.pdf

CHAPTER 4: SUMMARY AND CONCLUSION

Detailed sedimentological and ichnological analysis of 31 cores in the Middle Montney Member in the Pouce Coupe Area resulted in the identification of 8 distinct lithofacies. Microscopic properties and reservoir quality for each of the lithofacies were analyzed by thin section and Scanning Electron Microscope (SEM) imaging. Important surfaces recognized on the core were extrapolated, using geophysical logs, to 1000 vertical wells in the area, allowing for these surfaces to be correlated and for the distribution of the units to be mapped throughout the entire study area. Energy Dispersive X Ray Fluorescence (ED-XRF) was used to obtain geochemical profiles of 3 cores to compliment sedimentological descriptions.

The study area is situated along the southeastern extension of the Fort St. John Graben Complex (FSJG), where reactivation of structural lineaments are thought to have played a major role in sedimentation. Detailed mapping allowed for the identification of structural elements active during the deposition of the Montney D1 and D2 horizons. Net thickness maps of the D1 and D2 horizons show that the FSJG was a tectonic low at this time. The northern edge of the FSJG was defined by the Bear Canyon and Josephine Creek faults, and its southern most extent controlled by the Pouce Coupe and Gordondale faults. The thickness of the D1 horizon is distributed in a linear fashion and thins towards the southwest, supporting the interpretation of linear turbidity currents sourced from the northeast. The net thickness isopach of the D1-D2 transition is distributed in a more lobate fashion, suggesting a deltaic influence in the area.

In Chapter 2, lithofacies analysis determined that the study area was situated in the offshore transition to distal offshore area during deposition of the Middle Montney D1 and D2 horizons. Sedimentation in the study area was dominated by turbidity currents. Cyclic fluctuations in sea level and varying deltaic influence caused changes in the coarse siltstone

fraction as well as clay content. In contrast to deposits in the underlying Montney Turbidite Zone, these gravity flows do not have a single point source. Instead they were linearly sourced creating sheet flows.

Linear sourced turbidity currents in the proximal offshore area deposited the units with the highest porosity and correspondingly best reservoir quality (Lithofacies 5). In the offshore transition area, (close to the source of the mass wasting events), a higher proportion of coarse-grained siltstone was deposited (Lithofacies 7). These units likely had higher paleo-porosity/permeability, and thus diagenetic fluids preferentially moved through these units leaving them highly cemented and with low porosity. During times when there was an active delta in the area, silty shale beds deposited by hyperpycnal flows are interbedded with siltstone beds (Lithofacies 6). In the distal offshore area, suspension settling was the primary mode of deposition (Lithofacies 8).

The Montney coastline was characterized by rare perennial rivers with common ephemeral / seasonal river systems that only delivered sand and silt to the coast during major storms (Zonneveld and Moslow, 2014). These sudden, often catastrophic, ephemeral fluvial depositional episodes resulted in rapid, albeit short-lived, sediment input and, concomitantly, produced over-steepened shoreface profiles (unusual in fine-grained coastal successions). This, coupled with syn-sedimentary tectonics, created an unstable ramp setting prone to mass wasting events. The occurrence of sharp-based, silty shale beds within the D1-D2 transition suggest that there may have been a perennial delta present in the area. The silty shale beds may be relict of hyperpycnal flows from such deltas.

Inorganic whole-rock geochemical data has become a popular tool in unconventional mudstone plays in which the restricted grain size and perceived macro scale homogeneity

precludes the use of more traditional stratigraphic methods. In Chapter 3 of this thesis, ED-XRF analysis was used to obtain geochemical profiles of three cores in the D1 and D2 horizons. Elemental data was used as a proxy for environmental conditions occurring at the time of deposition, to determine the source of the clays in the D1-D2 transition (by identifying the presence or absence of an igneous geochemical signature), to aid in stratigraphic correlations throughout the area, and to confirm the sequence stratigraphic interpretation proposed in Chapter 2 of this thesis.

Elemental compositions were found to elegantly compliment sedimentologic core descriptions. Increases in the values of Zr and SiO_2/Al_2O_3 strongly correlated with increases in the coarser siltstone/v. fine sandstone fraction and increases in the Terrigenous Indicators (Al_2O_3 + K_2O+ Fe_2O_3 + TiO_2) and Mo and V values were associated with increasing amounts of clay. Th/Sc versus Cr/Th and Yb/Sm versus La/Sm cross plots showed that clay deposited throughout the D1-D2 transition was sourced from easterly upper crustal rocks and not accreted terranes to the west. Geochemical profiles enabled the recognition of 7 distinct chemofacies that are identifiable across the area. Chemostratigraphy was also found useful to compliment the sequence stratigraphic architecture erected in Chapter 2. The sampling resolution (~50cm) was found to be too large to resolve the high order parasequences within the D2 horizon. It is suggested that any future studies use smaller sampling intervals to appreciate the highly variable geochemistry throughout mudstones.

REFERENCES

Arnott, R.W.C. 2010. Deep-marine sediments and sedimentary systems, in James, N.P., and Dalrymple, R.W., eds., Facies Models 4: St. John's, Newfoundland, Geological Association of Canada, p. 295–322.

Barclay, J.E., Krause, F.F., Campbell, R.I. and Utting, J. 1990. Dynamic casting and growth faulting: Dawson Creek Graben Complex, Carboniferous-Permian Peace River Embayment, western Canada. *In:* Geology of the Peace River Arch. S.C. O' Connell and J.S. Bell (eds.). Bulletin of Canadian Petroleum Geology, v. 38, p. 115-145.

Beranek, L.P. and Mortensen, J.K. 2006. A Triassic link between Yukon-Tanana and North America; new detrital zircon age, geochemical, and biostrati- graphic data. Geological Society of America, Cordilleran Section, Abstracts with Program, v. 38, p. 5–6.

Beranek, L.P. and Mortensen, J.K. 2007. Latest Permian to Middle Triassic accretions of the Yukon-Tanana, Stikine and Quesnel terranes to North America; new detrital zircon age data from Triassic rocks in Yukon. Geological Society of America, Cordilleran Section, Abstracts with Program, v. 39, p. 69.

Bond, D.P.G., Wignall, P.B. 2010. Pyrite framboid study of marine Permian–Triassic boundary sections: a complex anoxic event and its relationship to contemporaneous mass extinction. Geolical Society of America Bulletin, v. 122, p. 1265–1279.

Botes, A., Henderson, J., Nakale, T., Nantanga, K., Schachtschneider, K., & Seely, M. 2003. Ephemeral rivers and their development: testing an approach to basin management committees on the Kuiseb River, Namibia. Physics and Chemistry of the Earth, v. 28, p. 853-858.

Bottjer, D.J. and Droser, M.L. 1991. Ichnofabric and siliciclastic depositional systems:

integration for sequence stratigraphic analysis. American Association of Petroleum Geology Bulletin v. 75, p. 545.

Bracciali, L., Marroni, M., Luca, P.,Sergio, R. 2007. Geochemistry and petrography of Western Tethys Cretaceous sedimentary covers (Corsica and Northern Apennines): from source areas to configuration of margins. Geological Society of America Special Papers, v. 420, p.73-93.

Chatellier J.D., Moslow, T.F., Haverslew, B. 2014. The Use of X-Ray Fluorescence for Sequence Stratigraphy and Geomechanics of Shale. GeoConvention 2014: May 12 – 16 2014, Calgary, AB. Available from http://www.geoconvention.com/archives/2014/418_GC2014_The_use_of_X-Ray_Fluorescence.pdf

Davies, G.R. 1997. The Triassic of the Western Canada Sedimentary Basin: tectonic and stratigraphic framework, Palaeogeography, Paleoclimate and biota. In: Triassic of the Western Canada Sedimentary Basin. T.F. Moslow and J. Wittenberg (eds.). Bulletin of Canadian Petroleum Geology, v. 45, p. 434–460.

Davies, G.R., Hume, D. 2016. Lowstand / Slope-Onlap Wedges In The Montney: Stratigraphic And Sequence Framework, Reservoir Significance (Oral Presentation). GeoConvention 2016: May 7 – 11 2016, Calgary, AB. Available from http://www.geoconvention.com/uploads/2016abstracts/224_ GC2016_Lowstand_Slope_Onlap_Wedges_in_the_Montney.pdf

Davies, G.R., Moslow, T.F. and Sherwin, M.D. 1997. The lower Triassic Montney Formation, west-central Alberta. In: Triassic of the Western Canada Sedimentary Basin. T.F. Moslow and J. Wittenberg (eds.). Bulletin of Canadian Petroleum Geology, v. 45, p. 474–505.

Dixon, J. 2000. Regional lithostratigraphic units in the Triassic Montney Formation of Western Canada. Bulletin of Canadian Petroleum Geology, v. 48, p. 80–83.

Drzewiecki, P.A. and Simo, J.A.T. 1997. Carbonate platform drowning and oceanic anoxic events on a mid-Cretaceous carbonate platform, south-central Pyrenees, Spain. Journal of Sedimentary Research, v. 67, p. 698-714.

Dzulynski, S. and Kotlarczyk, J. 1962. On load-casted ripples. Ann. Soc. Géol. Pologne v. 32, p. 148–159.

Ekdale, A. A. 1985. Paleoecology of the marine endobenthos. Palaeogeography, Palaeoclimatology, Palaeoecology, v. 50, p. 63-81.

Ekdale, A. A., & Mason, T. R. 1988. Characteristic trace-fossil associations in oxygen-poor sedimentary environments. Geology, v. 16, p. 720-723.

Erwin, D.H. 2006. Extinction: How life on earth nearly ended 250 million years ago. Princeton University Press, Princeton, New Jersey, 296 p.

Faraj, B., Harold, W., Addison, G., McKinstry, B., Donaleshen, R., Sloan, G., Lee, J., Anderson, T., Leal, R., Anderson, C., Lafleur, C., Ahlstrom, A. 2002. Shale gas potential of selected Upper Cretaceous, Jurassic, Triassic and Devonian shale formations in the WCSB of Western Canada: Implications for shale gas production. *Gas Technology Institute.* Des Plaines, Illinois. 103 pages

Ferri, F. and Zonneveld, J-P. 2008. Were Triassic rocks of the Western Canada Sedimentary Basin deposited in a foreland? Canadian Society of Petroleum Geologists Reservoir, v. 35, p. 12–14.

Föllmi, K. B., & Grimm, K. A. 1990. Doomed pioneers: Gravity-flow deposition and bioturbation in marine oxygen-deficient environments. Geology, v. 18, p. 1069-1072.

Hayes, L.E., Beatty, T.W., Henderson, C.M., Love, G.D., and Summons, R.E. 2007. Evidence For Photic Zone Euxinia Through The End-Permian Mass Extinction In The Panthalassic Ocean (Peace River Basin, Western Canada). Palaeoworld, v. 16, p. 39-50.

Hildred, G.V., Ratcliffe, K.T., Wright, A.M., Zaitlin, B.A., Wray, D.S. 2010. Chemostratigraphic applications to low-accomodation fluvial incised-valley settings: an example from the lower Mannville Formation of Alberta, Canada. Journal of Sedimentary Research, v. 80, p. 1032-1045.

Jahnert, R., De Paula, O., Collins, L., Strobach, E., & Pevzner, R. 2012. Evolution of a coquina barrier in Shark Bay, Australia by GPR imaging: Architecture of a Holocene reservoir analog. Sedimentary Geology, v.281, p. 59-74.

Jarvis, I., and Jarvis, K. 1992. Plasma spectrometry in the earth sciences: techniques, applications and future trends. Chemical Geology, v. 95, p.1-33.

Jenkyns, H.C., 2010. Geochemistry of oceanic anoxic events. Geochemistry, Geophysics, Geosystems 11, Q03004. doi:10.1029/2009GC002788.

Kelts, K., and Mckenzie, J.A., 1984, A Comparison Of Anoxic Dolomite From Deep-Sea Sediments: Quaternary Gulf Of California And Messinian Tripoli Formation Of Sicily, in Garrison, R.E., Kastner, M., and Zenger, D.H., eds., Dolomites of the Monterey Formation and Other OrganicRich Units: SEPM, Pacific Section, p. 19–28

Kendall, D.R. 1999. Sedimentology and stratigraphy of the Lower Triassic Montney Formation, Peace River Basin, subsurface of northwestern Alberta. . Unpublished M.Sc. Thesis, University of Calgary, Calgary, Alberta, 394 p.

Krapf, C. B., Stollhofen, H., & Stanistreet, I. G. 2003. Contrasting Styles Of Ephemeral River Systems And Their Interaction With Dunes Of The Skeleton Coast Erg (Namibia). Quaternary International, v. 104, p. 41-52.

Lumsden, D. N. 2003. Organodiagenetic Dolomite On A Deep Subtidal Shelf, Fort Payne Formation (Mississippian), Tennessee, U.S.A. In Ahr, W. M.; Harris, P. M.; Morgan, W.

A.; and Somerville, I. D., eds. SEPM Special Publication 78: Permo-Carboniferous Carbonate Platforms and Reefs, p. 323–332.

MacEachern, J.A., Bann, K.L., Pemberton, S.G., And Gingras, M.K. 2007. The Ichnofacies Paradigm: High-Resolution Paleoenvironmental Interpretation Of The Rock Record, In MacEachern, J.A., Bann, K.L., Gingras, M.K., and Pemberton, S.G., eds., Applied Ichnology: SEPM, Short Course Notes 52, p. 27–64.

Martinsen, O. J., Lien, T. & Jackson, C. 2005. Turbidite systems offshore Norway. In: Dore, A. G. & Vining, B. A. (eds) Petroleum Geology: North-West Europe and Global Perspectives—Proceedings of the 6th Petroleum Geology Conference, 1147–1164. q Petroleum Geology Conferences Ltd. Published by the Geological Society, London.

Mazzullo, S.J., 2000, Organogenic Dolomitization In Peritidal To Deep-Sea Sediments: Journal of Sedimentary Research, v. 70, p. 10–23.

Mei, S. 2009. New insights on faults in the Peace River arch region, northwest Alberta, based on existing well-log data and refined trend surface analysis, Can. J. Earth Sci. 46, no. 1, 41–65, doi: 10.1139/ E09-006

Moslow, T.F. 2000. Reservoir architecture of a fine-grained turbidite system: Lower Triassic Montney Formation, Western Canada Sedimentary Basin. In: Deep-water Reservoirs of the World, Conference Proceedings, Gulf Coast SEPM. P. Weimer, R.M. Slatt, J. Coleman, N.C. Rosen, H. Nelson, A.H. Bouma, M.J. Styzen, and D.T. Lawrence (eds.). p. 686–713.

Moslow, T.F. and Davies, G.R. 1997. Turbidite reservoir facies in the Lower Montney Formation, west-central Alberta. *In:* Triassic of the Western Canada Sedimentary Basin. T.F. Moslow and J. Wittenberg (eds.), Bulletin of Canadian Petroleum Geology v. 45, p. 507-536.

Myrow, P. M., Fischer, W., & Goodge, J. W. (2002). Wave-modified turbidites: combined-flow shoreline and shelf deposits, Cambrian, Antarctica. Journal of Sedimentary research, v. *72*, p. 641-656.

Mulder, T., and Alexander, J. 2001. The physical character of subaqueous sedimentary density currents and their deposits. Sedimentology, v. 48, p. 269–299.

Mutter, R.J. and Neuman, A.G. 2006. An enigmatic chondrichthyan with Paleozoic affinities from the Lower Triassic of Western Canada. Acta Palaeontologica Polonica, v. 51, p. 271–282.

Mutti, E. 1977. Distinctive thin-bedded turbidite facies and related depositional environments in the Eocene Hecho Group (South central Pyrenees, Spain). Sedimentology, v. 24, p. 107-131.

Nakajima, T. 2006. Hyperpycnites deposited 700 km away from river mouths in the Central Japan Sea. Journal of Sedimentary Research, v. 76, p. 60–73.

Nance, H. S. and Rowe, H. 2015. Eustatic controls on stratigraphy, chemostratigraphy, and water mass evolution preserved in a Lower Permian mudrock succession, Delaware Basin, west Texas, USA. Interpretation, v. 3, p. SH11-SH25.

National Energy Board, BC Oil and Gas Commission, Alberta Energy Regulator and BC Ministry of Natural Gas Development. 2013. Energy briefing note: the ultimate potential for unconventional petroleum from the Montney Formation of British Columbia and Alberta; National Energy Board, BC Oil and Gas Commission, Alberta Energy Regulator and BC Ministry of Natural Gas Development, 17 p.

NASA. 2008. Phytoplankton Bloom off Namibia. Retrieved from: https://www.nasa.gov/multimedia/imagegallery/image_feature_975.html

Nickling, W. G., & Neuman, C. M. 2009. Aeolian sediment transport. In Geomorphology of desert environments. p. 517-555. Springer Netherlands.

Pearce,T.J., Wray, D. S., Ratcliffe, K. T., Wright, D. K., Moscariello, A. 2005. Chemostratigraphy of the Upper Carboniferous Schooner Formation, southern North Sea. In: Carboniferous Hydrocarbon Geology: The Southern North Sea and Surrounding Onshore Areas. J.D. Collinson, D.J. Evans, D.W. Holliday and N.S. Jones (eds.). Yorkshire Geological Society, Occasional Publications series, v. 7, p. 147–164.

Pearce, T. J., Besly, B. M., Wray, D. S., Wright, D. K. 1999. Chemostratigraphy: a method to improve interwell correlation in barren sequences—a case study using onshore Duckmantian/Stephanian sequences (West Midlands, UK). Sedimentary Geology, v. 124, p.197-220.

Plank, T., & Langmuir, C. H. 1998. The chemical composition of subducting sediment and its consequences for the crust and mantle. Chemical geology, v. 145, p. 325-394.

Pemberton, S. G., and MacEachern, J. A. 1997. The ichnological signature of storm deposits: the use of trace fossils in event stratigraphy. Paleontological Events: Columbia University Press, New York, 73-109.

Pemberton, S.G., Mac Eachern, J.A., Ranger, M.J., 1992. Ichnology and event stratigraphy: the use of trace fossils in recognizing tempestites. In: Pemberton, S.G. (Ed.), Applications of Ichnology to Petroleum Exploration, a Core Workshop. Soc. Econ. Paleontol. Mineral., Core Workshop 17, p. 85–117.

Pisciotto, K.A., 1981, Review of secondary carbonates in the Monterey Formation, California, in Garrison, R.E., Kastner, M., and Zenger, D.H., eds., Dolomites of the Monterey Formation and Other OrganicRich Units: SEPM, Pacific Section, p. 119–140.

Plank, T., & Langmuir, C. H. 1998. The chemical composition of subducting sediment and its consequences for the crust and mantle. Chemical geology, v. 145, p. 325-394.

Playter, T. L. 2013. Petrographic and X-ray Microtomographic Analysis of the Upper Montney Formation, Northeastern British Columbia, Canada. Unpublished M.Sc. Thesis, University of Alberta, Canada. 113 p.

Playter T, Corlett H, Konhauser K, Robbins L, Zonneveld J.P. In Review. New Evidence for Global Volcanism Following the End-Permian Mass Extinction.

Playter T, Corlett H, Konhauser K, Robbins L., Rohais, S., Crombez, V., MacCormack, K., Rokosh, D., Prenoslo, D., Furlong, C.M., Pawlowicz, J., Gingras, M.K., Lalonde, S., Lyster, S., Zonneveld, J.P. In Review. Clinoform identification and correlation in fine-grained sediments: case study using the Triassic Montney Formation

Posamentier, H. W., & Allen, G. P. 1993. Variability of the sequence stratigraphic model: effects of local basin factors. Sedimentary geology, v. 86, p. 91-109.

Ratcliffe, K.T., Wright, A.M., Montgomery, P., Palfrey, A., Vonk, A., Vermeulen, J., Barrett, M., 2010. Application of chemostratigraphy to the Mungaroo Formation, the Gorgon field, offshore northwest Australia. APPEA Journal, 50th Anniversary Issue, p. 371–388.

Ratcliffe, K. T., Wright, A. M., Schmidt, K. 2012. Application of inorganic whole-rock geochemistry to shale resource plays: an example from the Eagle Ford Shale Formation, Texas. The Sedimentary Record, v. 10, p. 4-9.

Ratcliffe, K., Wright, M., 2012. Unconventional methods for unconventional plays: using elemental data to understand shale resource plays. PESA News Resour. 2012, p. 55-60.

Raup, D.M. 1979. Size of the Permo-Triassic bottleneck and its evolutionary implications.

Science, v. 206, p. 217-218.

Reading, H.G., and Richards, M. 1994. Turbidite systems in deep-water basin margins classified by grain size and feeder system. American Association of Petroleum Geologists Bulletin, v. 78, p. 792–822.

Reineck, H. E. and Singh, I. B. 1972. Genesis Of Laminated Sand And Graded Rhythmites In Storm-Sand Layers Of Shelf Mud. Sedimentology, v. 18, p.123-128.

Richards, B.C., Barclay, J.E., Bryan, D., Hartling, A., Henderson, C.M. and Hinds, R.C.,1994, Carboniferous strata of the Western Canada Sedimentary Basin; in Geological Atlas of the Western Canada Sedimentary Basin, G.D. Mossop and I. Shetsen (comp.), Canadian Society of Petroleum Geologists and Alberta Research Council, Special Report 4, 221–250

Rowe, H., Hughes, N., Robinson, K. 2012. The quantification and application of handheld energy-dispersive x-ray fluorescence (ED-XRF) in mudrock chemostratigraphy and geochemistry. Chemical Geology, v. 324, p. 122-131.

Sano J.L., Ratcliffe K. T., D.R. Spain, 2013, Chemostratigraphy of the Haynesville Shale, *in* U. Hammes and J. Gale, eds., Geology of the Haynesville Gas Shale in East Texas and West Louisiana, U.S.A. AAPG Memoir 105, p. 137–154.

Seilacher, A. 1969. Fault-graded beds interpreted as seismites. Sedimentology, v. 13, p.155-159.

Seilacher, A. and Hemleben, C. 1966. Beiträge zur sedimentation und fossil-fürung des Hunsrückschiefers 14. Spurenfauna und Bildungstiefe der Hunsrückschiefer (Unterdevon). Notizblatt des Hessichen Landesamtes fur Bodenforschung zür Wiesbaden, v. 94, p. 40–53.

Sellwood, B. W. and Valdes, P.J. 2006. Mesozoic climates: General circulation models and the rock record. Sedimentary Geology, v. 190, p. 269-287.

Shaw, P. J. (2003). Multivariate statistics for the environmental sciences. 1st ed. Hodder-Arnold. P. 233.

Sholkovitz, E.R. and Soutar, A., 1975. Changes in the composition of the bottom water of Santa Barbara basin: effect of turbidity currents. Deep-Sea Research, v. 22, p. 13-22.

Smith, R.M,H., Mason, T.R. and Ward, J.D., 1993. Flash-flood sediments and ichnofacies of the Late Pleistocene Homeb Silts, Kuiseb River, Namibia. In: C.R. Fielding (Editor), Current Research in Fluvial Sedimentology. Sedimentary Geology, v. 85, p. 579-599.

Stollhofen, H., Stanistreet, I. G., von Hagke, C. and Nguno, A. 2014. Pliocene–Pleistocene climate change, sea level and uplift history recorded by the Horingbaai fan-delta, NW Namibia. Sedimentary Geology, v. 309, p. 15-32.

Svendsen, J., Stollhofen, H., Krapf, C. B., & Stanistreet, I. G. 2003. Mass and hyperconcentrated flow deposits record dune damming and catastrophic breakthrough of ephemeral rivers, Skeleton Coast Erg, Namibia. Sedimentary Geology, v. 160, p. 7-31.

Totten, M. W., Hanan, M. A., Weaver, B. L. 2000. Beyond whole-rock geochemistry of shales: The importance of assessing mineralogic controls for revealing tectonic discriminants of multiple sediment sources for the Ouachita Mountain flysch deposits. Geological Society of America Bulletin, v. 112, p. 1012-1022.

Tribovillard, N., Algeo, T., Lyons, T.W., Riboulleau, A., 2006. Trace metals as paleoredox and paleoproductivity proxies: an update. Chemical Geology, v. 232, p. 12–32.

Van Loon, A.J. and Wiggers, A.J. 1976. Primary and secondary synsedimentary structures in the lagoonal Almere Member (Groningen Formation, the Netherlands). Sedimentary Geology, v. 16, p. 89–97.

Velbel, M.A. 1990. Influence of temperature and mineral surface characteristics on feldspar weathering rates in natural and artificial systems: a first approximation. Water resources research 26: 3049-3053

Walker, R.G. 1967. Turbidite sedimentary structures and their relationship to proximal and distal depositional environments. Journal of Sedimentary Research, v. 37, p. 25-43.

Walker, R.G. 1985. Mudstones and thin-bedded turbidites associated with the Upper Cretaceous Wheeler Gorge conglomerates, California: a possible channel–levee complex. Journal of Sedimentary Research, v. 55, p. 279–290.

Wentworth, C.K. 1922. A scale of grade and class terms for clastic sediments: Journal of Geology, v. 30, p. 377–392.

Wetzel A. 2002. Modern Nereites in the South China Sea – Ecological association with redox conditions in the sediment. Palaios v. 17, p.507–515.

Wetzel, A., and Uchman, A. 1998. Deep-sea benthic food content recorded by ichnofabrics: A conceptual model based on observations from Paleogene flysch, Carpathians, Poland. Palaios, v. 13, p. 533–546.

Wilkin, R.T., Barnes, H.L., and Brantley, S.L. 1996. The size distribution of framboidal pyrite in modern sediments: An indicator of redox conditions: Geochimica et Cosmochimica Acta, v. 60, p. 3897–3912.

Windom, H.L. and Chamberlain, C.F. 1978. Dust-storm transport of sediments to the north Atlantic Ocean. Journal of Sedimentary Petrology, v. 48, p. 385–388.

Wood, J. M., Sanei, H., Curtis, M. E., & Clarkson, C. R. 2015. Solid bitumen as a determinant of reservoir quality in an unconventional tight gas siltstone play. International Journal of Coal Geology, v. 150, p. 287-295.

Woods, A.D., Bottjer, D.J. and Corsetti, F.A. 2007. Calcium carbonate seafloor precipitates from

the outer shelf to slope facies of the Lower Triassic (Smithian-Spathian) Union Wash Formation, California, USA; sedimentology and palaeobiological significance. Palaeogeography, Palaeoclimatology, Palaeoecology, v. 252, p. 281-290.

Wright, A.M., Ratcliffe, K.T., Zaitlin, B.A., Wray, D.S., 2010. The application of chemostratigraphic techniques to distinguish compound incised valleys in lowaccommodation incised-valley systems in a foreland-basin setting: an example from the Lower Cretaceous Mannville Group and Basal Colorado Sandstone (Colorado Group), Western Canadian Sedimentary Basin. In: Ratcliffe, K.T., Zaitlin, B.A. (Eds.), Application of Modern Stratigraphic Techniques: Theory and Case Histories: SEPM Special Publication, 94, p. 93–107.

Udden, J.A., 1914, Mechanical composition of clastic sediments: Geological Society of America, Bulletin, v. 25, p. 655–744.

Zaragosi, S., Le Suave, R., Bourillet, J. F., Auffret, G., Faugeres, J. C., Pujol, C., & Garlan, T. 2001. The deep-sea Armorican depositional system (Bay of Biscay), a multiple source, ramp model. Geo-Marine Letters, v. 20, p. 219-232.

Zonneveld, J. P., Gingras, M. K., & Beatty, T. W. 2010a. Diverse ichnofossil assemblages following the PT mass extinction, Lower Triassic, Alberta and British Columbia, Canada: evidence for shallow marine refugia on the northwestern coast of Pangaea. Palaios, v. 25, p. 368-392.

Zonneveld, J. P., MacNaughton, R. B., Utting, J., Beatty, T. W., Pemberton, S. G., & Henderson, C. M. 2010b. Sedimentology and ichnology of the Lower Triassic Montney Formation in the Pedigree-Ring/Border-Kahntah River area, northwestern Alberta and northeastern British Columbia. Bulletin of Canadian Petroleum Geology, v. 58, p. 115-140.

Zonneveld, J.P., Golding, M., Moslow, T.F., Orchard, M.J., Playter, T. and Wilson, N. 2011. Depositional framework of the Lower Triassic Montney Formation, west-central Alberta and northeastern British Columbia; *in* recovery – 2011 CSPG CSEG CWLS Convention, p. 1–4.

Zonneveld, J. P., Moslow, T.F. 2014. Perennial River Deltas of the Montney Formation: Alberta and British Columbia Subcrop Edge (Oral Presentation). GeoConvention 2014: May 12 – 16 2014, Calgary, AB. Available from http://cseg.ca/assets/files/resources/abstracts/2014/core/490_GC2014_Perennial_River_Deltas_of_the_Montney_Fm.pdf

Zonneveld, J. P., Moslow, T.F. 2017. Depositional history and Palaeogeographic evolution of the Montney in the Western Canada Sedimentary Basin (Oral Presentation). GeoConvention 2017: May 15 – 19, 2017, Calgary, AB. Available from http://www.geoconvention.com/uploads/2017abstracts/312_GC2017_Depositional_history_and_Palaeogeographic_evolution_Montney_WCSB.pdf